University of Alberta

SCALE TESTING HARD ROCK WASTE DUMP STABILITY UNDER HAULER MOTION

by

Niousha Rahmani

A thesis submitted to the Faculty of Graduate Studies and Research
in partial fulfillment of the requirements for the degree of

Master of Science

in

Mining Engineering

Department of Civil and Environmental Engineering

Spring 2014
Edmonton, Alberta

Dedication

This thesis is dedicated to my family who has supported me all the way since beginning of my studies, as well as my husband who has been a great source of motivation and inspiration, and has helped me throughout my study.

Abstract

Mining methods have changed and grown to fulfill extractive demands. Heavy machinery is used to extract overburden in open pit and open cast mines and to create waste dumps prone to slope stability issues. As the heaviest equipment operating on dump locations, mine haul trucks require a safe, stable surface to work on, so the stability of waste dumps is hugely important. Slope failures frequently occur on mine cut slopes, embankments, dumps, and road cut surfaces, so an improved understanding, monitoring, and support of such slopes is important to prevent failure, loss of equipment and fatalities. One of the most important differences between waste dump slopes and other slopes such as embankments or road cuts is not only that waste dumps are made up of loose face dumped material but also goes that trucks impact cyclic loads which affect stability. For example, significant weight at hundreds of tonnes has a huge impact on slope stability. This cyclic loading scenario on mine waste dumps has yet to be investigated fully.

This study looks at the stability of waste dumps under the impact of mining equipment based on physical modeling (laboratory scale tests), numerical modeling and “Slide” slope stability software. During the study on the stability of waste dumps by physical modeling, data related to rolling resistance was also recorded.

It has been concluded that the results from both the physical and numerical modeling determined acceptable states for truck path by both truck location for

the chosen test material, Dolomitic limestone (1/3 and 1/2 truck width from crest), and constructing a safety berm along the crest of slope, and for wet conditions.

Acknowledgments

I would like to express my deepest appreciation to my supervisor, Dr. Tim Grain Joseph, for his guidance, enthusiasm, and continual encouragement through this endeavor. Also, his support throughout the research and writing of this thesis is gratefully appreciated. Without his persistence and support this M.Sc. research project would have not been possible.

Also, I am grateful to Lucas Duerksen for helping with laboratory tests and providing the laboratory research facilities, and to Christine Hereygers for helping with some of the laboratory tests.

I am thankful to the Hammerstone Corporation for providing Dolomitic limestone chips for my laboratory tests.

I acknowledge the financial support provided by NSERC and the University of Alberta. I am grateful to the University of Alberta and the Department of Civil and Environmental Engineering for providing me with research and teaching assistance during my graduate studies.

Finally I am grateful to my husband, Babak Nikbakhtan, who has been a great source of encouragement and help during my graduate studies.

Contents

List of Figure

List of Tables

List of Equations

List of Symbols and Abbreviation

#	Number of events
o	Degree
Mya	Millions years ago
GVW	Gross Vehicle Weight
RR	Rolling Resistance
S.F	Safety factor
ASTM	American Society for Testing and Materials
d_{50}	Particle diameter at 50% in the cumulative distribution
g	Ground bearing level
E	Elastic modules
E_{ps}	Plastic modules
δ	Deformation
δ_{ps}	Total deformation
δ_s	Elastic deformation
δ_{ps}	Plastic deformation

τ	Shear stress
σ	Normal stress
c	Cohesion
$\emptyset$	Friction angle
M	Moment
F	Force
P	Pressure
R	Tire Radial
φ	Tire Diameter
A_{tire}	Tire footprint
m	Meter
cm	Centimeter
mm	Millimeter
V	Voltage
Hz	Hertz, Frequency unit
Kg	Kilogram

N	Newton
kph	Kilometer per hour
kPa	Kilopascal
Mpa	Mega Pascal

Chapter 1: Introduction

The importance of waste dump stability under mining equipment operations has become a greater concern with changes in the equipment size and extraction method changes. Huge haul trucks and mine equipment are used to extract and transport economic materials and dump uneconomic materials as waste piles have over taken the competency of road and waste dump surface to support operations.

During the past decade, more waste dump failures and truck damage have been reported due to increases in the size of heavy machinery used at mine sites and transport waste materials. Waste dump stability and preventing both truck and dump failures has become an important focus for mine planning, to create a safe place for equipment and operators.

The most important waste haul tool used is the mine truck. The effect of increased capacity haul trucks on stability of waste dumps is considerable. The aim of this research is to investigate the impact of truck movement on waste dump stability. With hard rock mining waste dumps in mind, the material selected for waste material modeling was broken dolomitic limestone chip (hereafter referred to as "limestone"). Dolomite is commonly located in the heart of the oil sand region manifest as the Devonian basement (360 to 420 Mya).

An offshoot focus of this research was to compare rolling resistance for different operating conditions, to prevent adverse increases in rolling resistance, considering a potentially impact on waste dump stability.

The goals of this research were to:

- Develop an understanding of hard rock waste dump failures and parameters affecting dump stability.
- Design a scale waste dump haul truck test to determine the behavior of broken rock under truck movement for varying states of broken rock.
- Model actual dump stability and truck loading interactions in “Slide” software to establish minimum safety factors for the dolomite waste dump.
- Link safety factors for a waste dump slope to the g-level activity of trucks.

Chapter 2: Literature review

2-1. Introduction

Mining methods have changed and grown over time to fulfill the changing demand of operations and economy. However, rarely do these changes include a consideration of increasing safe management at waste dump. Heavy machinery continues to be used to extract overburden and ore in open pit and open cast mines. Uneconomic waste materials should be placed back "in-pit" but are still predominantly stacked at different places around the mine termed waste dumps. With an increase in hauler fleet sizes as the demand for production continues to increases, mines are becoming increasing unstable and unsafe which it will increase by working cycles on these dump area. As a result, the stability of waste dumps is becoming a major concern and is attracting greater attention worldwide (Das, 2011)**.** Many slope failures have occurred during the past decade on high walls, embankments, dumps, and road cuts. This is a function of increasing the size of equipment to accommodate the operation and volume of materials placed in dumps. An improved understanding, of monitoring and slope stability is important to prevent landslides and unexpected failure.

There are different mine extraction techniques, but the majority involve drilling and blasting. These methods create loose overburden or waste rock that must be moved to waste dumps to create a possibility of exploration of the valuable ore. Thus the stability of dumps has become more important (FLORA, 2009). A good knowledge of waste rock materials' properties, particle good interfacial strength, foundation conditions, and an understanding of groundwater or seepage is

essential to design and plan a waste dump. This knowledge may be obtained from field studies which include geological and geotechnical mapping of on-site soils and rock, sampling boreholes, on-site monitoring wells, excavation test pits, sampling waste rock, ore, and foundation materials (Orman, Peevers, & Sample, n.d.).

Failure and instability of waste dumps are among the most important consideration in safe mine management for both operators and regulators. Failure of dumps is considered a dangerous occurrence which disturbed operations due to vicinity of dumps to haul roads, increasing the opportunities for equipment burial. All dump failures increase costs to a mine. Appropriate plans for mine and designs for dumps and stockpiles, reduces such cost and safety concern.

All parameters that affect dump stability should be considered and evaluated through the design life of waste dumps.

2-2. Different kinds of waste dump failures

Different types of failure that can occur in dumps are described below, with typical failure modes shown in Figure 1.

2-2.1. Surface or edge slumping

In this kind of failure, a thin wedge of material moves parallel to the dump face, moving down slope. The reason for soil shallow failure is over-steeping of the dump-face angle, which initiates from the crest of the dump. The reasons for developing over-steeping are placement of cohesive or low permeability waste materials, in thick lifts or pushing material over a dump crest.

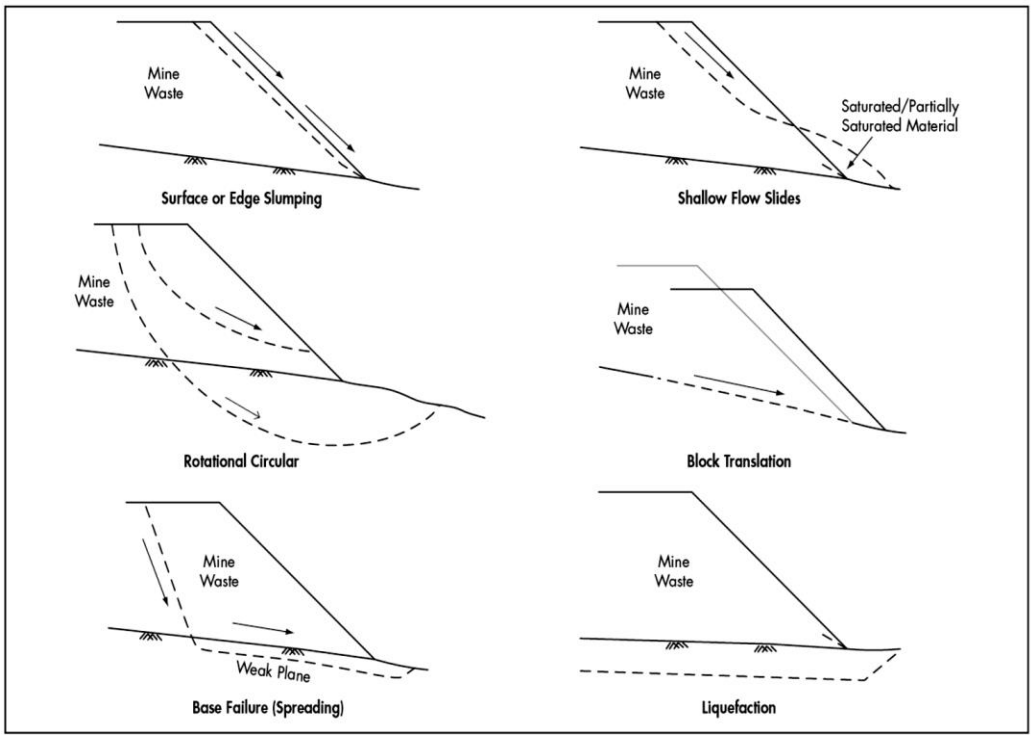

Figure 1: Failure modes in dumps (Orman et al., n.d.)

Heavy precipitation then leads edge-slumping, which is compounded by an increase in pore-pressure in low-permeability waste. Over-steeping of a crest may extend to the initial interlocking of blocks in a coarse, rock-fill dumps (A. M. G. Robertson, Robertson, & Kristen, n.d.).

2-2.2. Plane failure

This type of failure occurs along a single plane of weakness within the dump. The reason for this type of failure is the existence of either a bedding plane weakness or a poor quality waste band, or where primary dumps are on top of snow or ice. The plane causing failure is plane of weakness parallel to a dump slope or daylights in the dump face (Orman et al., n.d.).

2-2.3. Shallow flow slides

This type of failure occurs in saturated dumps. Rain or snowmelt cause material to flow down slopes leading to shear failure or collapse of soil structure, thus create of shallow flow slides (A. M. G. Robertson et al., n.d.).

2-2.4. Rotational circular arc failures

These are mass failures along a curved failure surface within the dump. These occur because of excessive dump height, excessive loading, caused by earthquake, weak or fine grained materials, a reduction in toe support, or high pore-water pressures. This type of failure may also be induced by the motion caused by heavy equipment operating near the crest of dump face angle. When a soil or rock mass is weak strength or contains high pore pressure, as is found in a deep fine-grained rock or soil deposits, rotational circular arc failure may also develop in the foundation (A. M. Robertson, 1970).

2-2.5. Creep failure

This is a variation of rotation circular arc failure with widespread rotational shearing, characterized by bulging at the dump toe (Orman et al., n.d.).

2-2.6. Base failure

Base failure, often called spreading, may occur when a thin, weak base layer is placed over a foundation. This weak layer is usually inclined toward the foundation. Foundation spreading by definition occurs when a slope wedge moves laterally(Orman et al., n.d.).

2-2.7. Block translation

Block translation, also called plane sliding, occurs in weak, and thin soil and steep foundation slopes. A bulk mass of the dump slides similar to a rigid block along a weakness plane, where the weak plane may be located within the foundation soil, along the interface between the foundation and the dump mass, or along a defined interface. This kind of failure may result from high water tables in embankments, earthquakes, and the decay of organic materials beneath a dump (A. M. Robertson, 1970).

2-2.8. Other variation

Other classifications of the failure in rock fill and waste dumps may be termed: (1) circular; (2) non-circular semi-infinite slope; (3) multiple block plane wedge; (4) log spiral (bearing capacity of foundations); (5) flow slides and mud flow; (6) cracking; (7) gulling; (8) erosion; (9) slide or slump (Sankar, n.d.). All of these are merely extended variations of the failure mode described above (Figure 2).

2-2.9. Cracking

Cracking is predominately a surface failure that mostly happens in mine waste dumps due to differential settlement of waste material and affective surface tensile strength, through wetting and drying mechanisms (Sankar, n.d.) (Figure 3).

2-2.10. Gulling

Gulling failure has been observed in dumps and is a dominant erosion mechanism (Sankar, n.d.). Heavy rains cause this failure mechanics through washing out of fines, resulting in collapse of the coarse matrix of waste material. (Figure 4)

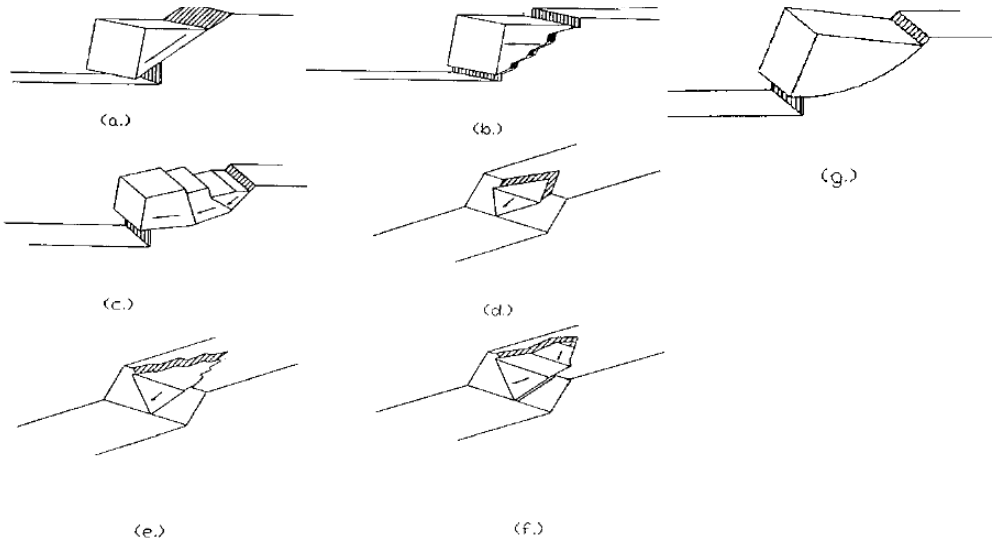

Figure 2: Failure types in rock fills and dumps (after Brown, 1994): a) single blocks with slope plane; b) single block with stepped planes; c) multiple blocks with multiple planes; d) single wedge with two intersecting planes; e) single wedge with multiple intersecting planes; f) multiple wedge with multiple intersecting planes; g) single block with circular slip path (Sankar, n.d.)

Figure 3: Cracking (Sankar, n.d.)

2-2.11. Slide and Slump failures

This type of failure occurs in fully or partially saturated dump materials. Erosion at the base of a slope is the main cause of the slide, which may have rotational or transitional movements (Sankar, n.d.). (Figure 5)

Figure 4: Gulling failures in dumps (Sankar, n.d.)

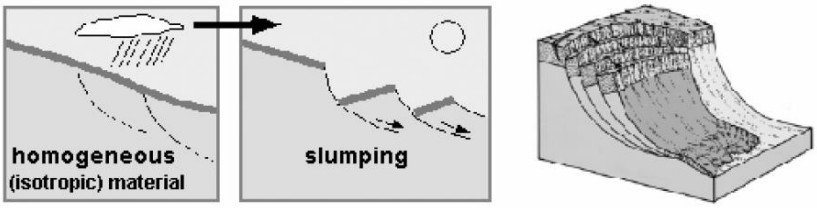

Figure 5: Slump failures in slope (Sankar, n.d.)

2-3. Factors affecting dump stability

For designing and analyzing the stability of the dumps, there should be a systematic and appropriate collection of data and parameters, which affect the dump's stability. Data should include, the size and complexity of the project, as well as the consequence of a potential failure (Orman et al., n.d.). Factors that affect the stability of a dump are:

2-3-1. Site topography

Site topography provides a historical view of the target region area and parameters that may affect slope stability, where these features may have been presumed to provide lateral support or toe buttressing to improve the dump

stability. Topographic information should include data on zones which may lead to failure in dumps which should include information on the entire drainage area to reflective the unsafe zones because of waste movement (Orman et al., n.d.).

2-3-2. Dump geometry and stacking method

The geometry of a dump is related to the mode of dumping including boundaries, height and design slopes. These factors have a major impact on slope stability. Increasing each may cause a decrease in the stability of the dump (Omari & Boddula, 2012).

2-3-3. Geotechnical and mechanical properties of mine waste and foundation

Mine waste and back foundation materials' geotechnical properties such as density, saturation, and shear-strength have an effect on dump stability. Most data collected are based on laboratory tests and site investigation. These indicate particle size distribution, specific gravity, permeability, compression index, soil classification, and the relative degradation behavior of waste materials. Soil tests are conducted for shear strength, permeability, hydraulic conductivity and consolidation, permitting stable depth determination for any loose or incompetent soils. These factors are critical for designing a dump and to avoid failure. Due to geotechnical instrument measurement tool limits, time and budget restraints, it is impossible to impose actual field conditions, in laboratory tests, so verification tests are necessary during dump construction, to ensure that all parameters used during design are reasonable, accurate, and appropriate.

It should be mentioned that the size and configuration of waste piles are strongly related to the stability of a dump. In particular, the height of the pile, the volume (from weight and density of loose to steadily consolidated materials) and the slope angle should be considered.

Shear strength and friction angle are common geotechnical properties of waste dump material that have a significant effect on the stability of dumps. Increasing the shear strength of waste materials increases the stability for waste dumps. Material strength is changed with increasing dump height, time and higher dump loading and become as a nonlinear strength(U.S.E.P.A., 1995).

The friction angle is mentioned as one geotechnical parameter. In a direct reflection of dump material strength and independent of the applied stress, the friction angle will be lower for materials located higher in the dump because of overall lower applied stress. The friction angle of rock fill increases between 4° and 8° for every 10-fold decrease in effective normal stress (Barton & Kjaernsli, 1981).

Another aspect that should be considered is the effect of weathering on geotechnical properties. The weathering of dump materials may lead to a decrease in dump stability as it can also reduce the effective friction angle (Orman et al., n.d.).

2-3-4. Groundwater and phreatic surface

Water in mines whether ground water or surface water, is an important consideration which may result in problems in the mine such as failure and the

erosion of waste piles. The degree of saturation has a direct impact on the effective strength of the material, lowering the ability to resist failure. Therefore this matter should be considered as critical in evaluating the design of waste piles. Seepage analysis is a good way to assess the stability of the dump, as it reflects the level of free flowing water drastically reducing the slope strength. This establishes flow through the dump and the height of the phreatic surface.

As dump materials are essentially anisotropic, the stress-strain behaviour is erratic. “The visco-elastic behaviour due to the presence of water poses a serious threat during the rainy season.” Failure may occur with rising pore water pressure which leads to a reduced shear strength of the dump material (Kainthola, Verma, Gupte, & N.Singh, 2011).

2-3-5. Seismic forces

A natural seismic load is a set of a dynamic load which is important in evaluating stability of dump slopes. The seismic response a slope is related to the characteristics of input ground motions and the dynamic properties of the waste materials. There are four methods to analysis the seismic stability of slopes, which are the pseudo-static method, the Newmark sliding block analysis method, the numerical analysis methods, and the physical measurement techniques. In the pseudo-static method, seismic forces are assumed constant and equal to a vertical and horizontal force. The center of gravity of a potential sliding body is taken as acting point of an equivalent force; and the unstable direction of slope is considered as a direction of equivalent force. Earthquake acceleration coefficients

are determined from practical experience based on the degree of seismic damage and slope design.

The Newmark sliding block analysis was derived from the pseudo-static method, and the difference between these two methods is that the Newmark method depends on the displacement of sliding blocks, and not a minimum factor of safety. These two methods both exhibit the deficiency of being unable to reflect dynamic characteristics and the failure mechanism of a sliding body under seismic load.

Physical measurement techniques use single frequency input ground motion, for a simple surface and at small scale. It can reflect weak geological features, damage mechanisms and the stability state of the slopes, and may be employed for seismic stability analysis.

Numerical analysis method which is based on simulating different Physical measurement techniques, reflect the dynamic response and damage characteristics of slopes under seismic load, via finite element and finite different methods (Guo, Ge, & Wang, 2011).

2-3-6. Liquefaction

Liquefaction is another parameter that can affect the stability of a dump. This is prevalent in low-lying topography with the shallow foundations including fine grained zones through which pore water cannot readily dissipate. Seismic activity and rapid loading also cause liquefaction (Srour, 2011).

In addition, liquefaction of foundation materials can occur in a susceptible waste material and pose the greatest risk by earthquake. Liquefaction due to seismic events is typically limited to 20 m in depth or shallower, due to the beneficial effects of confining pressure against liquefaction susceptibility (Orman et al., n.d.). High variation in temperature can influence on the dump failure. Water freezing in voids or repeated freeze/thaw cycles may result in gradual loss of strength which finally affects the stability of the dump (Kainthola et al., 2011).

2-3-7. Key drives for this research

In considering motion of a heavy hauler moving on a dump; carrying waste material to a dump location near the crest of the dump; the motion of the hauler creates a pseudo seismic loading that reduce the effective strength of the dump materials and a property for failure creative unsafe working condition. It is this premise that is driver for this research work.

2-4. Modeling of waste dump

The modeling of the fragmented loose waste rock, generated and dumped in opencast mines may be modeled via discontinuous based particle-particle interaction mechanics. The elements of such a model are the distinct nature of geo-materials represented in a bonded and un-bonded matrix assembly. The characteristics of over-burden dump material could be previously determined via laboratory tests of synthetic materials akin to the behaviour of the field materials (Koner & Chakravarty, 2010).

In the structural stability, fragmented rock and loose soil creates difficulty and establishes the degree of interaction. Waste material composed of lumps and grains, evaluated via inter-particle deformations and failures will be widely disturbed due to differential loading. Sophisticated constitutive models, high order continua, and varying numerical techniques have been used in continuum mechanics for simulating a structural change of such particulate materials. When the disturbance of a structure is enhanced, more complicated theory may be necessary to simulate an appropriate model; and the phenomena of discontinuous nature should be described via continuum mechanics. The model which is appropriate for modeling mechanical behaviour of a geological material is the Distinct Element Method (DEM). This method provides a simile to discontinuum mechanics. By using such modeling, soils and rocks may be recognized as an assembly of un-bonded or bonded particles and their macroscopic behaviour realized from the properties and interactions of their microscopic constituents. The behaviour of materials can be simulated at the macro scale (dilation, strain localization, slip, strain softening) by using simple laws and parameters on the micro scales. Appropriate observation and visualization of particle interaction permit linking the responses at macroscopic and microscopic levels.

In this research reliance has been made on using visually recorded deformation characteristics of the macro and micro level using strain cameras.

Broken rock in the open pit mines frequently occupied dump space in a few square kilometres. From the behaviour of the on compacted rock and waste, stability and settlement may be determined. Stability is related to two parameters,

1) the quality of the fragments (size, internal porosity, degree of weathering, angularity, roughness, uniaxial strength); 2) method of dumping. Both influenced the loading conditions due to immediate (vehicle movement but also more distant, blasting, earthquake, rainfall, etc.) and time (Koner & Chakravarty, 2010).

Finite element methods represent powerful alternative approaches to study slope and dump stability. Slope failure in finite element study however is only recognized through inter-element zones in which the shear strength of material is less than shear stresses and also shear strength is unable to resist (Kainthola et al., 2011).

To analyse the effect of seismic load on dump stability, the Discrete Element Methods (DEM) is seen as more appropriate. As such boundaries allow energy to radiate and not reflect outward where the time of the model is dependent on the time in which surface waves propagate and loosen or compacted material and hence change surface stiffness and ability to resist load. The most complicated part of modeling dynamic response of over burden (OB) dumps under earthquake is the determination of input dynamic loads. Field measurement can yield a velocity history near surface, where the velocity changes as a function of the input load. Another important component in the dynamic behaviour is time history. Distinct elements and data are impacted by time history; the fragmented and loose soil behaviour of over-burden materials in dump may be simulated, with sliding, failure surface; and failure initiation point may be determined. Field engineers can thus predict and take reinforcing and/or remedial measures to stop failure at prior to initiation (Koner & Chakravarty, 2010).

The Mohr-Coulomb failure criterion is frequently in numerical analysis of dump material behaviour and stability. Generally, soft and loose mine dumps contain poorly segregated soil and rock. Failure effects via combinations of adverse normal stress, generating shear failure in the dump occur through by slippage of particles; "So dumps will fail when the shear stress on the failure plane at failure is an exclusive function of the normal stress acting on that plane." (Kainthola et al., 2011).

The failure criterion is simply defined as the Mohr-Coulomb linear approximation of the normal and shear stress.

Equation 1

$$\tau = c + \tan \varphi$$

Where τ is the shear strength, σ is the normal stress, φ is the angle of internal friction and c is the cohesive strength of the material, which may not be present if the dump is made up of frictional particle zones.

The shear potential of dump material has major influence on stability. Loose and broken material usually has low shear strength which may increase with time, as material becomes buried and compacted. So evaluation of shear strength of material in the laboratory versus in situ testing methods is an important consideration in studying dump stability (Kainthola et al., 2011).

"The strength of the material depends on the grain size, as well as the interlocking of the material; the deformability has been found to be associated

with arrangement of the granular material as well its compaction." (Kainthola et al., 2011).

Placing waste dumps on mine slopes raises another important issue related to both dump and mine slope stability. Figure 6 and Figure 7 shows a typical example of such a problem which by constructing waste dump on the active mine slope, the factor of safety for slope reduce from 1.25 to 1.1. So this reality shows that adding waste dump can decrease the safety and enhance the possibility of the failure (Das, 2011).

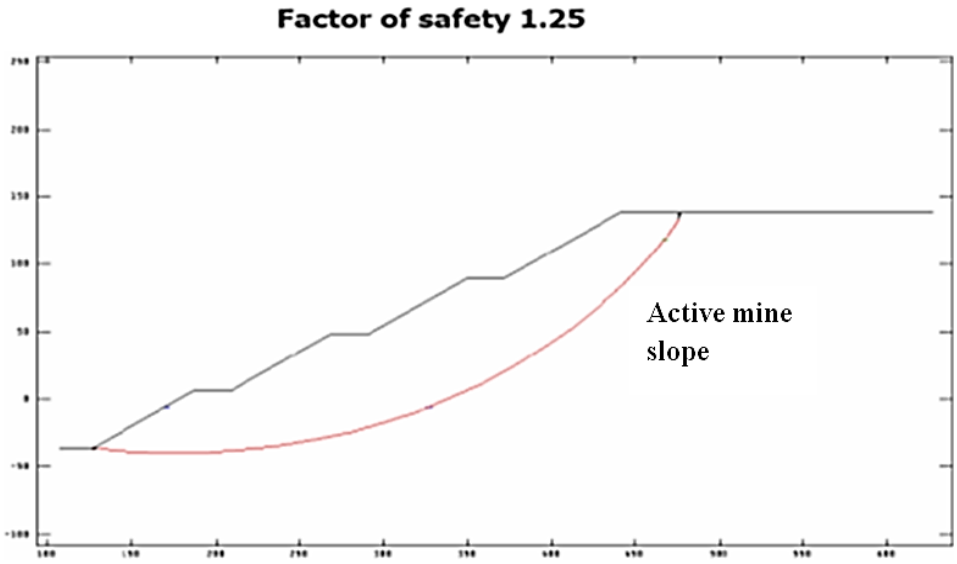

Figure 6: Stability analysis of active mine slope without overlying dump (Das, 2011)

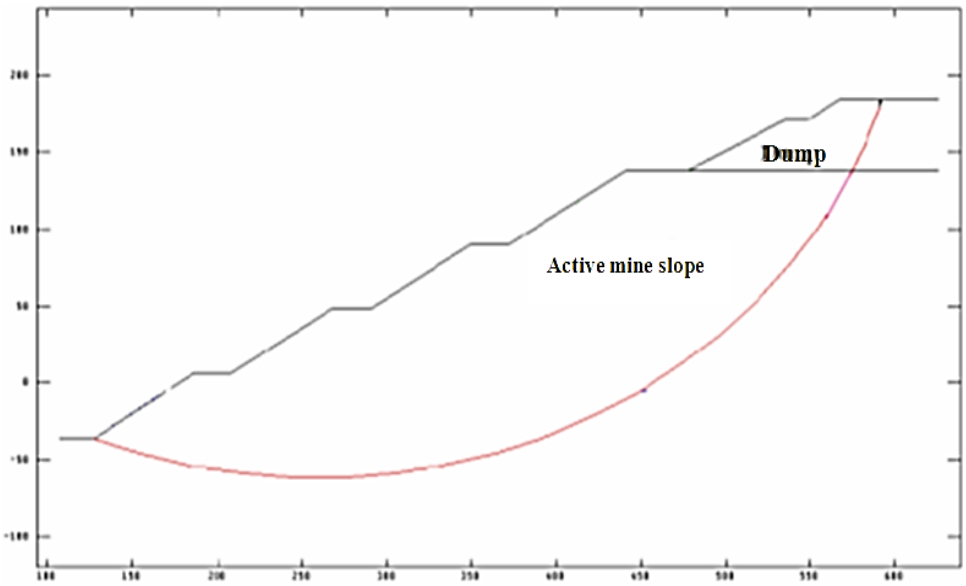

Figure 7: Stability analysis of active mine slope with overlying dump (Das, 2011)

2-5. Dump stability assessment procedure

Slope stability performance should be frequently reviewed and remedial measures taking when necessary, during the mining operation. This applies further for the future mine extensions or when the pit is extended deeper**.**

A typical geotechnical assessment of slope stability contains:

1. "Prepare a conceptual mine layout and select concept design for open pit and spoil slopes;
2. Collect geotechnical data;
3. Define design parameters;
4. Define factors of safety;
5. Analyse geotechnical slope stability;
6. Refine slope geometries to conform the factor of safety" (Orman et al., n.d.).

In assessing the dump stability, data should first be collected. The collected data should be reflective of the slope design required, where the data should also be a function of the factors affecting geotechnical stability. Typical data collected from dumps provide information such as: 1) bearing capacity of underlying foundation materials; 2) stability of slopes formed by the dumped material; and 3) permeability and drainage characteristics of the dump. The data should provide: 1) a description of the soil below the dump, inclusive soil type, particle size distribution, plasticity, moisture content, density, shear strength (total and effective stress, angle of friction, and cohesion), compressibility, thickness and depth of rock; 2) hydrological conditions below the dump site inclusive groundwater level and permeability; 3) geotechnical properties of dump materials inclusive particle size distribution, density, anticipated compacted density, plasticity, dispersion index, mineralogy, shear strength, permeability, and any variation created by weathering or deterioration; and 4) other data identified as having relationship to the dump, such as earthquake loading and surcharge (Orman et al., n.d.).

Beyond collecting and evaluating data, a geotechnical dump analysis and design dumps may be completed. Typical analysis of dump or stockpiles includes methods of slices, circular or non-circular, and multiple wedges or sliding block analysis. Designs of dumps include: 1) reference to a similar group of stock piles or dumps that have similar properties; 2) those with similar cross sections, whereby as a guide permits selecting and appropriate structure for a dumps; and 3) knowledge of material parameters and groundwater. These kinds of properties

will be necessary for determining slope angle for an acceptable factor of safety (Orman et al., n.d.).

Evaluating the potential circular arc stability of a dump or stockpile is important, especially when there are weak layers in the structure. There are key parameters to determine short and long term stability of dumps or stockpiles. Parameters for short term stability are cohesion for the undrained, total stress conditions (C_u), internal angle of friction for the undrained, total stress conditions ($\emptyset_u$). For long term stability are cohesion for effective stress (c'), and internal angle of friction for effective stress (c'). The overall costs of poor slope design can be mitigated over the long term, by using short term properties in slope design. If the design of the slope is poor, it may result in:

1. "lost production and resources;
2. Reduced personal safety;
3. Increased risk of equipment damage;
4. Damage to rehabilitated areas;
5. Unnecessary re-handling of materials during slope reshaping" (Orman et al., n.d.).

2-6. Slope monitoring

Slope monitoring is done to detect early stages of failure, which may give indication of required stabilization before the catastrophic failure, or if no changes are be made to prevent failure; a predicted time to failure is a key to abandon a failure area, to reduce damage costs.

There are several techniques employed to monitor slopes such as: 1) instrumentation; 2) photo-gramammetry; 3) GPS; 4) satellite imagers as common survey methods. Some other slope monitoring instruments are extensometers, time domain reflectometry, inclinometers, piezometers, and crack meters (Sankar, n.d.).

2-6.1. Extensometer

Extensometers are placed in boreholes and consist of tensioned rods which provide displacement information for the rock (Sankar, n.d.).

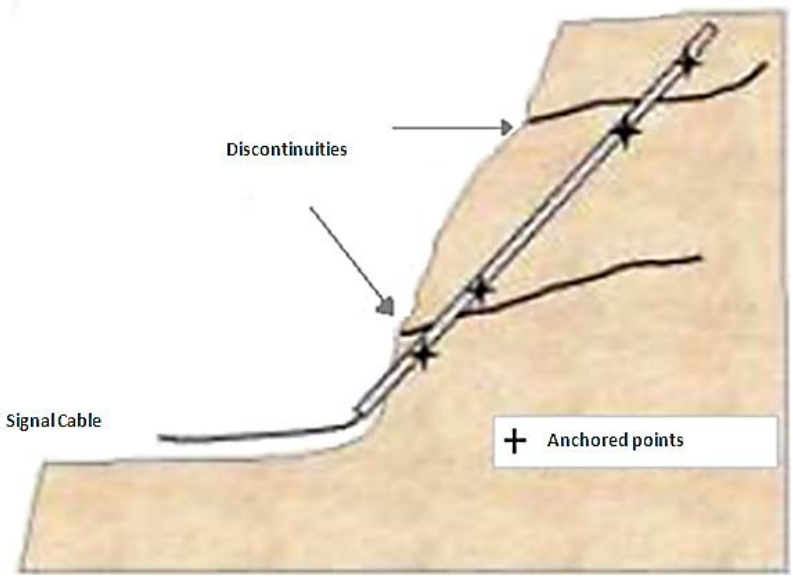

Figure 8: Slope with extensometer (Sankar, n.d.)

2-6.2. TDR

"In a pulse waveform is generated down a cable grouted in a borehole. If the pulse encounters a change in the characteristic impedance of the cable, it is reflected." Comparing the returned and emitted pulses, the reflection coefficient of the cable at that point and the change in impedance with time corresponds qualitatively to

the rate of ground movement can be determined. TDRs have low installation costs, no limits on hole depth, immediate determination of movement, and remote data acquisition capability (Sankar, n.d.). (Figure 9)

2-6.3. Inclinometers

Inclinometers enable: 1) shear zones to be located; 2) the type of shear along the zone may be determined, whether planner or rotational; 3) the shear zone movement can be measured and determined for, accelerating, or decelerating movement. They can be used to monitor slopes and landslides to recognize the movement zone (Sankar, n.d.). (Figure 10)

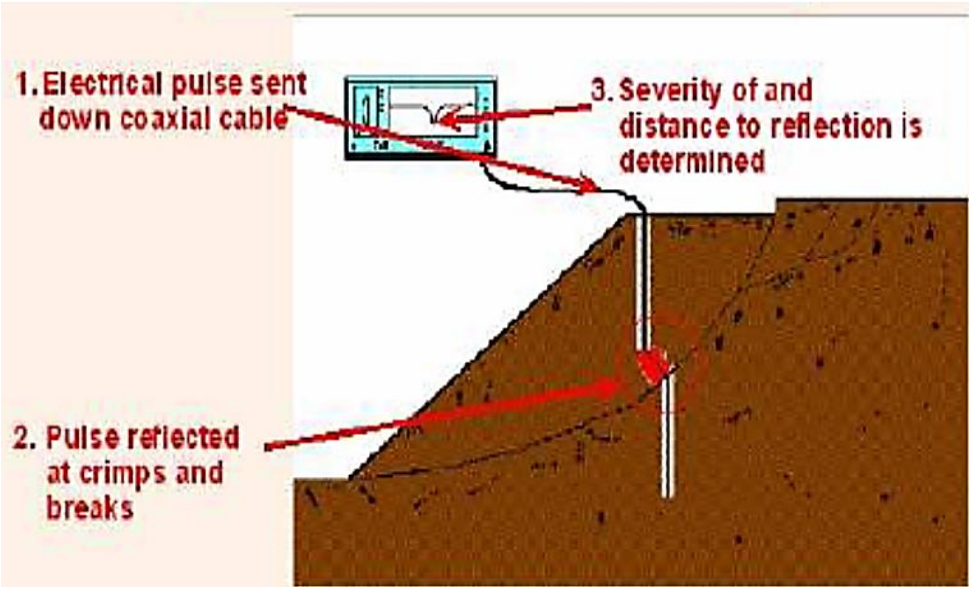

Figure 9: Principle of TDR (Sankar, n.d.)

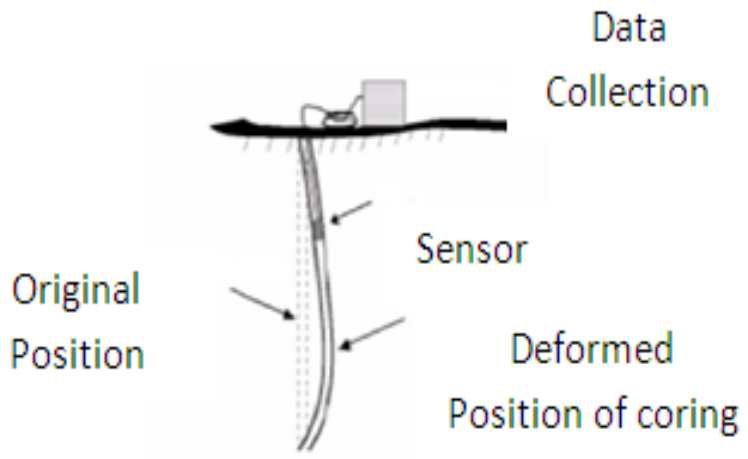

Figure 10: Inclinometers (Sankar, n.d.)

2-6.4. Piezometers

Piezometers can be used to monitor poor water pressure, to determine safe rates of water inflow in to an excavation. Slope stability, dewatering performance, ground improvement systems, pore pressures and containment systems for landfills and tailing dams can be monitored by the pizometers (Sankar, n.d.).

2-6.5. Laser Monitoring

Laser monitoring can be used to scan entire slope walls. In this method a camera paired with the laser and takes photographs all through the scan, then the data collected by both the laser and camera is transferred to a computer and analysed using specific software (Sankar, n.d.).

2-6.6. Seismic Monitoring

This method measures and predicts slope and dump deformation by measuring micro seismic events caused by brittle movements within a rock slope (Sankar, n.d.).

2-7. Effect of mining equipment operation on ground during cyclic loads

Waste dumps created with broken rock effectively behave as a soil or loose material, where failure in these waste dumps is frequently semi parallel to the surface in a circular shape is named a circular arc failure .The Circular arc failure in the waste dump occurred when individual particles of broken rock are small compared with the size of the waste dump and as such they don't have any interlocking nature because of the size and shape (Hoek & Bray, 1977). The safety factor of such a slope which is:

Equation 2

$$S.F = \frac{Shear\ Strength\ \ available\ to\ resist\ sliding}{Shear\ stress\ \ mobilised\ along\ failure\ surface}$$

Failure happens when the shear stress which causes movement along a surface is greater than the shear strength which resists failure. The shear stress is dependent on the normal stress that is applied along the surface, which in this study is the weight of slope plus the operation of a truck, which create an additional normal stresses, along the surface.

There are two different types of mining equipment in surface mining. The first relies essentially on tracks, roller paths, rollers and side frames; the second relies on tires for movement. In both cases the footprint created is variable; creating different ground loading and different normal stresses. This ground loading is the function of kinematics of the machine and the ground performance properties (T.G Joseph & Sharif-Abadi, 2006). In general, tire equipment and surface mine create much higher normal stress and are hence the focus in this research work.

The reaction of different ground materials is complicated by the cyclic loading events generate by mobile equipment. Cyclic load tests in general suggest all material loses stiffness with in increasing the cyclic loads. Parameters like load magnitude, material structure and climate have an effect on the degree of softening during cyclic loading.

Most research performed on oil sand to recognize the behavior of oil sand as a soft ground under cyclic loading. Work which wass done on laboratory triaxial and field tests used plate load cells by Joseph (2002). Oil sand is generally a broken, unlocked and loose material, whose geotechnical properties vary with the climate. In summer the stiffness decreases and the ground deformation increases such that it behaves as weak clay, whereas in winter, it behaves as sandstone (T.G Joseph & Sharif-Abadi, 2006). Cyclic loading soft ground, causes stability of equipment on surface to decrease when shovels works in cycles, they sink in to the ground due to cyclic track pressures, causing rack and roll motion in the frame of the equipment body (T.G Joseph & Sharif-Abadi, 2006; Sharif-Abadi & Joseph, 2005).

There is no clear indication of the peak stress for oil sand with increasing strain particular for oil sand of high bitumen content. The material has a considerable post-peak behavior before reaching a residual value. The pseudo-elastic stiffness of the post peak reduces by increasing the number of cycles (Figure 11 and Figure 12) where the total deformation is the sum of the elastic and plastic deformation as shown in Figure 12 (T.G Joseph & Sharif-Abadi, 2006; Sharif-Abadi & Joseph, 2005).

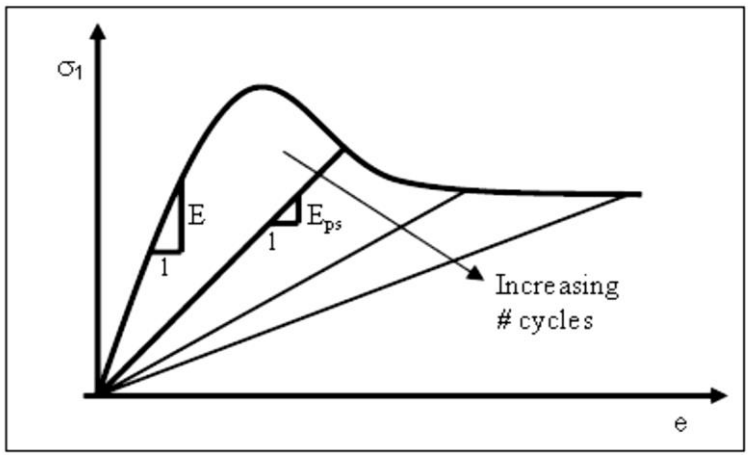

Figure 11: Modules with number of cycle (Sharif-Abadi & Joseph, 2005)

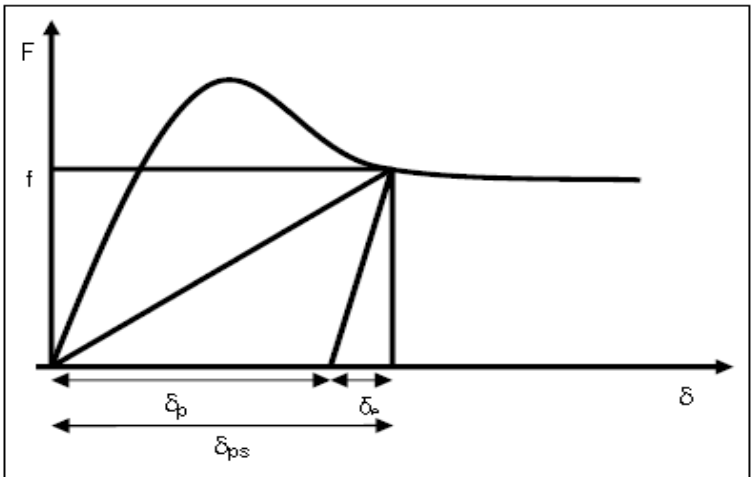

Figure 12: Total deformations (Sharif-Abadi & Joseph, 2005)

Based on filed and laboratory tests for oil sand test, confining pressure is a function of applied load, where this induced confining pressure is an effective horizontal stress. Figure 13 shows the comparison between field and laboratory tests. Based on tests for determining the deformation of the ground (soft ground) under mining equipment, it can be realized that induced horizontal stresses can be predicted from the loading condition of mining equipment in the static or dynamic duty (Sharif-Abadi & Joseph, 2005).

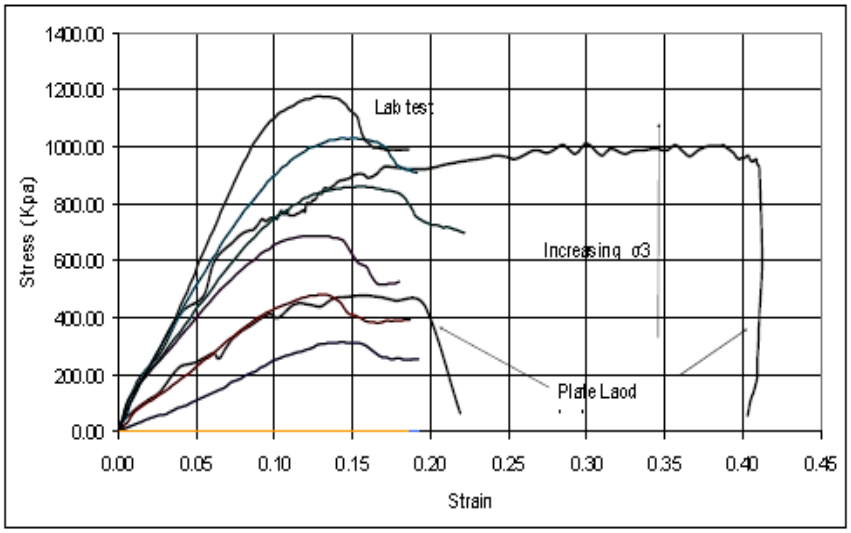

Figure 13: Comparing field and laboratory test (Sharif-Abadi & Joseph, 2005)

2-8. Rolling Resistance

Rolling Resistance is a material property of the ground. It is defined via the driving pull forces required to overcome resistance between the tire and the ground.

Studies on rolling resistance go back to the 19th century. Morin started investigating rolling resistance by study in the resistance to motion for horse-drawn wagons (Komandi, 1999). He studied rolling resistance by changing rear and front axle loads and speed. This study was continued by Gerstner and Bernstein in beginning of the 20th century. They studied rolling resistance for deformable soils. The believed that the most important parameter affecting rolling resistance is the force needed to deform the soil (Komandi, 1999). There have been two interpretations for rolling resistance in the classical approach, the first defines the rolling resistance as the force to pull the wheel regardless of driving or towing the wheel, and the second is the result of a torque or moment, not force.

This confusion was resolved by Heyde (1957). He realized that rolling resistance is effectively the moment, where the driving moment has to merely overcome rolling resistance, where only the balanced moment has an effect on the wheel-soil contact area (Anand, 2012).

In 1999, Komandi found that rolling resistance is a function of both rotation and forward motion under driving and towing conditions. As rolling resistance is introduced as a function of moment, it causes the wheel to rotate in place, when a driving moment is greater than the rolling resistance (Anand, 2012).

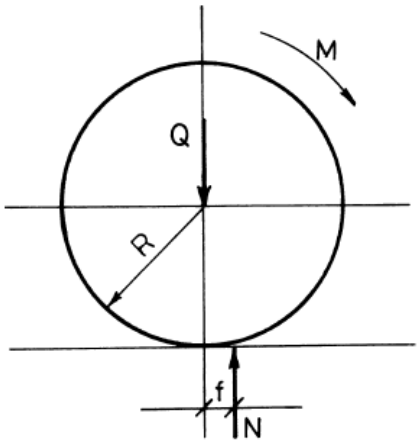

Figure 14: Force and moments on tire (based on the classical approach)

Interpretations of rolling resistance are somewhat focused on the interest focus of people who performed the studies. Basically all studies on rolling resistance, yield common parameters that affect rolling resistance via (Anand, 2012):

- Soil characteristics
- Tire pressure, temperature and flexure
- Condition of mining surface (roughness)

- Wheel loading relative to activity on a smooth surface
- Internal friction between wheel and axle
- Speed (although this has subsequently been shown to not be a factor)

The prime objective of this study focuses on rolling resistance on a waste dump running surface; so the definition of rolling resistance during truck movement on a waste dump will be the prime focus for this study. Most mine waste dumps are unpaved, and the condition of a waste dump surface is recognized to have an important effect on the immediate and long-term performance of waste dump running surface and haulage operation costs.

Rolling resistance on any waste dump, surface or haul road, is defined as the tractive effort that a vehicle must overcome between the tire and ground (Tannant & Regensburg, 2001).

Road traction or friction has an effect on rolling resistance. Based on the performance (resistance to deformation) of a waste dump or haul road, increasing the traction between tire and ground, the RR can potentially be decreased. Based on such as interpretation, it is suggested that , rolling resistance depends on the tire type and operating conditions, wheel load, number of tires in contact with the ground, and road conditions (Tannant & Regensburg, 2001). For example operations have documented that by increasing 0.6% in rolling resistance per centimeter of tire penetration causes an increase in resistance to movement of 1.5 to 2%.A ramp slope, with a base rolling resistance of 2% will see a drop in truck speed by 10 to13% for an additional rolling resistance increase of 1% (Thompson, 1999).

Such parameters reflectively these observations can be specified below via the parameters of:

- Internal power train friction
- Tire flexure under load
- Tire penetration
- Road deflection
- (Air resistance)- a minor consideration relative to the other consideration (Tannant & Regensburg, 2001).

An increase in rolling resistance can cause to impacts on wear and tear for a truck. This indicates increase in cost of operations, such as fuel cost, and reduction in availability. Referring to Figure 15, increasing rolling resistance causes fuel cost to increase and production to decrease, as more energy in required to overcome the resistance between the ground and the tire (Tannant & Regensburg, 2001).

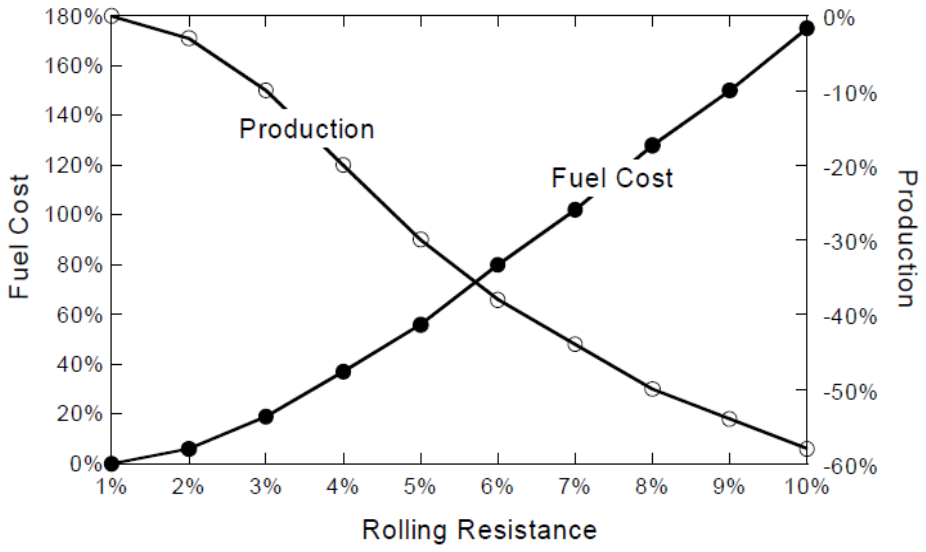

Figure 15: Rolling resistance- performances (Tannant & Regensburg, 2001).

Considering rolling resistance in related to the performance of a truck, it is obvious that parameters which increase the rolling resistance should be kept low, and measures should be taken to prevent increases. Conditions impacting ground properties or tire characteristics attributable to rolling resistance should be monitored and judicially improved to reduce rolling resistance and associated impacts.

Different ground materials cause different rolling resistance between tires and ground. Here some commonly case of materials have been tested to compare rolling resistance performance. These materials were sand, oil sand, pit run and limestone. Rolling resistance tests were performed for different slope gradients and speeds. The results of these tests showed that sand has the highest rolling resistance and followed by oil sand. Pit run and limestone had lower rolling resistance than the sand. Of all four materials evaluated limestone showed the lowest rolling resistance for the same tire operating condition. Similar tests were done with capping oil sand surface with other materials, as capping or application of a "wearing coarse " with different materials is routine in haul road construction, where for oil sands mining operation; sand, pit run and limestone are the most commonly available road building material. Capping oil sand with these materials allowed a comparison of the effect of composite of materials with individual materials road design.

The results showed that no composite materials gave a rolling resistance less than an individual material performance (Figure 16 to Figure 18). Of all the composites; limestone capping on oil sand showed the least rolling resistance but

a rolling resistance was higher than just using limestone (Anand, 2012). This is also a function of the compactive effect used to prepare a limestone running surface. The ranges of rolling resistance values extracted from the tests are shown in the Table 1.

The impact of speed on rolling resistance was also examined in the tests. The result of such measurement confirmed a theory of Pope (1971) considering speed on rolling resistance. The test was done with two wheels; the first with a rigid plate and a second with cut away at the rim, that showed increasing speed cause a decrease in rolling resistance (Pope, 1971)**.** The same observation of speed was shown for sand, pit run, limestone and sand cap, although other composited did not yield relationships between speed and rolling resistance (Anand, 2012).

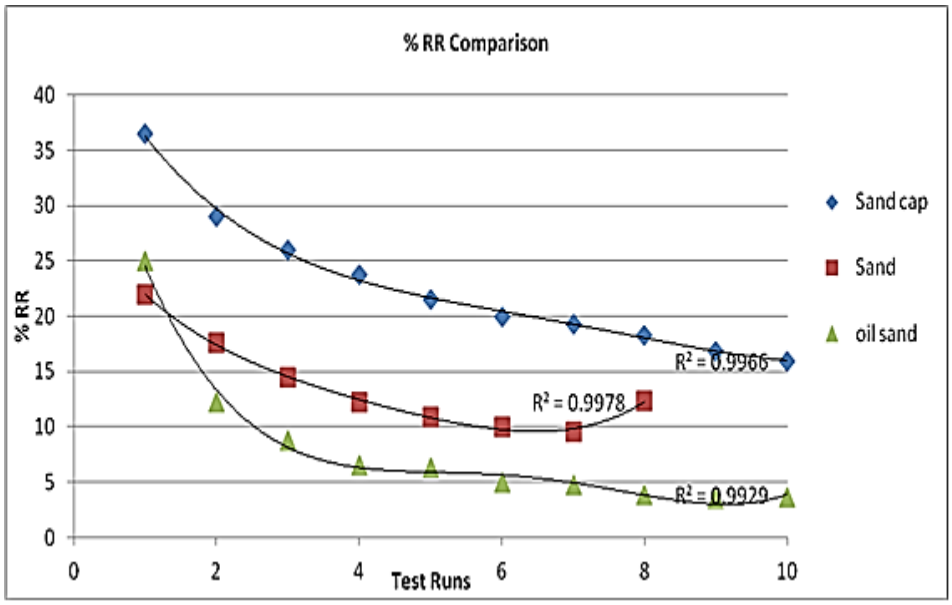

Figure 16: Average % RR vs. test runs for sand, sand cap and oil sand (Anand, 2012)

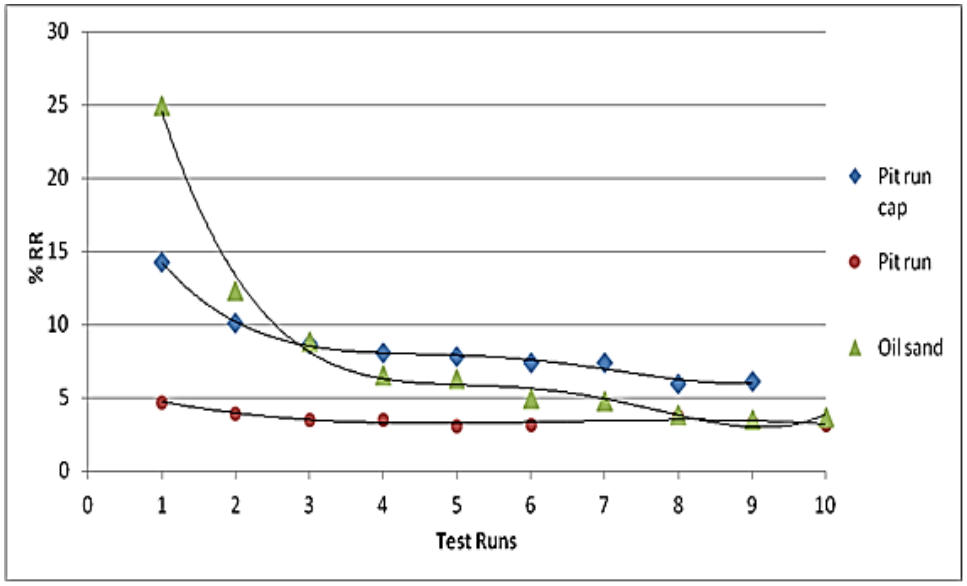

Figure 17: Average % RR vs. test runs for pit run, pit run cap and oil sand (Anand, 2012)

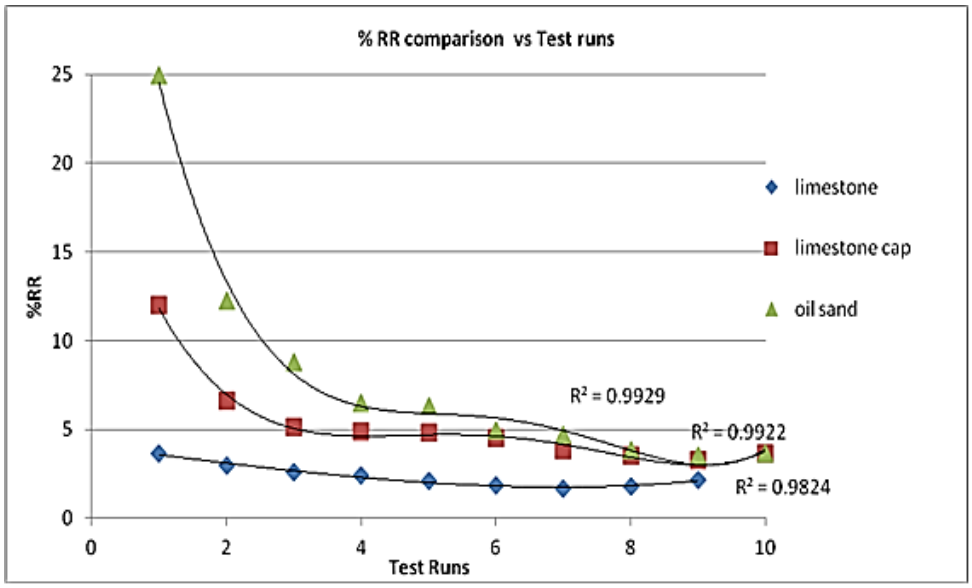

Figure 18: Average % RR vs. test runs for limestone, limestone cap and oil sand (Anand, 2012)

Table 1: Rolling resistance of different materials and composites (Anand, 2012)

Material	Converged % RR	Range
Sand	12 %	10 to 15%
Oil sand	5.5 %	4 to 7%
Pit run	4 %	3 to 5%
Limestone	3 %	2 to 4 %
Sand cap	17 %	14 to 26 %
Pit run cap	7 %	6 to 8 %
Limestone cap	4.5 %	3 to 5 %

Chapter 3: Scaling

3-1. Truck Scaling

For the past 40 years the most versatile choice in mining equipment for transporting waste materials has been the haul truck. The size and model of hauler selected for this investigation was the Caterpillar, 793D. The Characteristics of this truck are showed in Table 2.

Table 2: Properties of Truck (CAT, n.d.)

Nominal payload capacity (tonnes)	Gross Machine Operating mass (tonnes)	Chassis mass (tonnes)	Tire Size	Tire Diameter (m)
218	384	117	40.00R57	3.3

In this test the dimensions of this size of truck and dumping requirement would be impossible and impractical in lab. Thus scale model which is a miniature version of a larger physical system, such as an approach for testing simplifies logistics and for such testing in an economical and realistic manner was used.

The tire size selected for scale truck was 15.25 cm tire which is 22.83 times smaller than the actual class hauler. Base on the linearity relationship which is existed between footprint area of the tire and vertical deformation (Figure 19) and scalable equal slope, it is obvious that the behavior of all size of the tire will be the same for the all range of footprint area vs. vertical deformation. Thus by performing test on the 15.24 cm tire the behavior of actual tire in 3.3 m diameter can be predicted (Sharma, 2009). Six tires in 15.25 cm diameter, properties shown

in Table 3, were attached to the hauler truck structure in similarly to actual tires. The conventional rear dump hauler arrangement of four tires in rear and two tires in front is having a balance load distribution (33% to front and 67% to rear axle). To construct the structure of the scaled truck, the same scale factor was used for the dimensions of the truck frame at 22.83× smaller. The dimensions of the truck in scale are shown in Figure 20.

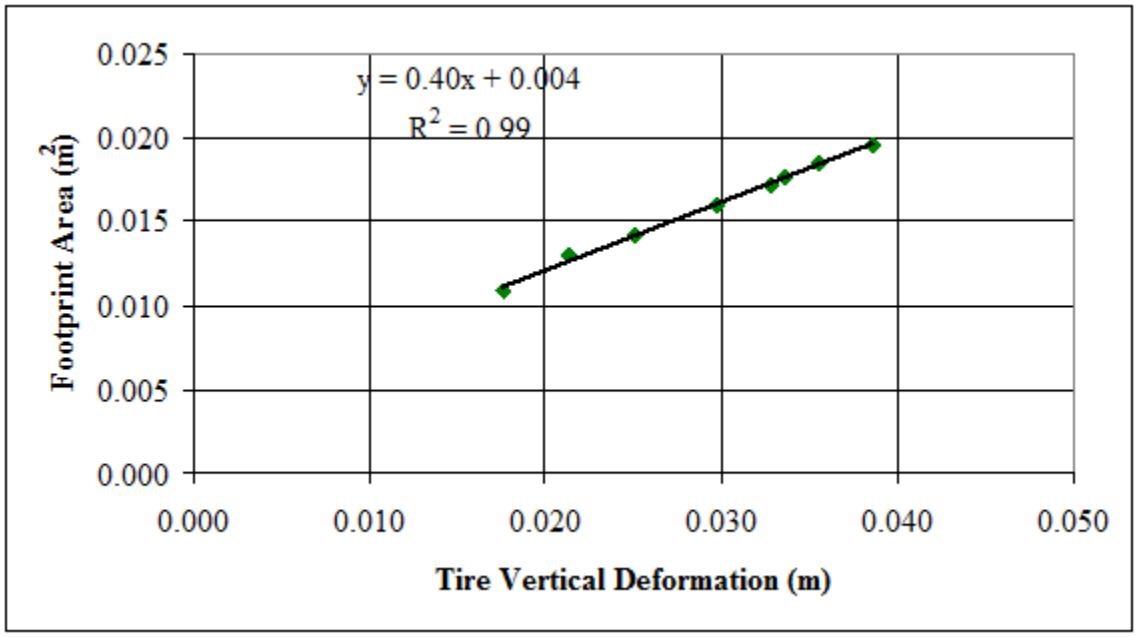

Figure 19 : Variation of footprint area with tire vertical deformation

Table 3: Properties of Tire 2.00×6

Size (cm)	Type	Diameter (cm)	Load Rating (kg)	Pressure rating (kPa)	Mass (kg)
2.00×15.25	Tube	15.25	90.7	206.8	0.73

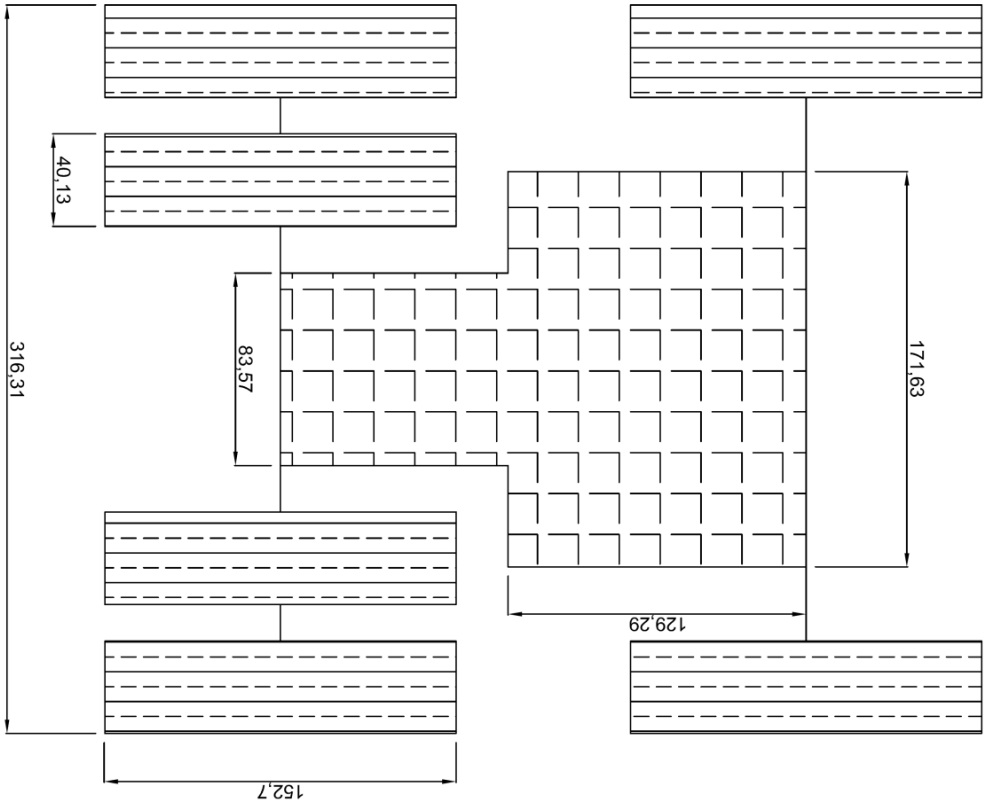

Figure 20: Scaled truck sketch (mm)

3-1.1. Tire flexure test

To account for the properties of the scale tire include internal pressure and load per tire, tire flexure test was done to find these characteristics at scale. These tests were done by applying different loads on the tire at different internal pressure and measuring the vertical deformation of tire by applied load. The apparatus used for the test is shown in Figure 21.

1. Hydraulic pump applies load
2. Pressure regulator
3. Steel frame attached to bench
4. Actuating piston
5. Piston extension rod (rigid)

6. Tire mount
7. LVDT, linear vertical displacement transducer
8. Digital acquisition recording amount of LVDT displacement

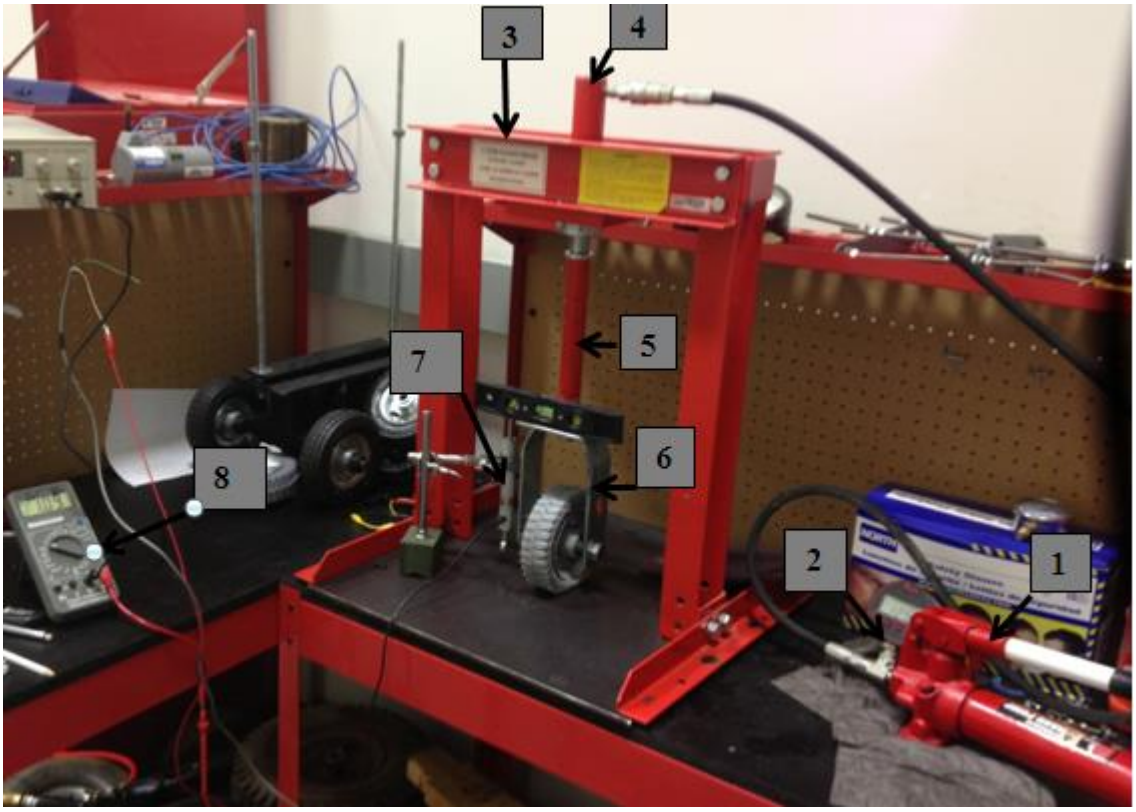

Figure 21: Tire Flexure Test

To measure the vertical deformation of the tire, the tire was held in a vertical position connected to a piston. By actuating a hydraulic pump, oil was moved in-to the cylinder that transferred loading to the tire. The tire was loaded and the LVDT deformed by an amount that the acquisition system recorded as a degree of deflection. By recording a voltage proportional to displacement in cm (10 V=5cm), the vertical deformation and strain for the tire was calculated reacting against a plane surface for varying applied loads. This test was performed for a range of internal tire pressures from 13.8 to 68.9 kPa and for applied loads

proportional to hydraulic pump pressures between 689 to 1379 kPa. The vertical deformation for the tire was recorded in 138 kPa steps of applied load proportional to the hydraulic pressures. From the deformation recorded, the tire strain by applied load was calculated and used to develop a graph of load vs. strain, Figure 23.

The weight of vehicle was calculated by using cube root scaling which indicates:

Equation 3

$$Gross\ vehicle\ weight = 384\ tonnes$$

Equation 4

$$Weight\ per\ tire = \frac{384}{6} = 64\ tonnes$$

Equation 5

$$cube\ root\ \ 22.83\ scale = \frac{\sqrt[3]{64}}{22.83} = 0.175\ tonnes$$

Equation 6

$$cubed\ of\ cube\ root\ scale = 0.175^3\ = 5.37\frac{kg}{tire}$$

So the total weight of the scale truck was designed as 32.22 kg.

Evaluating actual truck data collected over 14 cycles, it was seen that loads per tire was equivalent to a 1g static reference condition, but when truck was moving, overloading events occurred, that caused failure of waste dump running surface. Critical higher g-levels for truck run cycles can cause roll and pitch motions for

the truck, which cause deformation of dump surface and slope failure. Preventing slope failure should be considered for the high critical g events for truck cycles not only 1g events, as slope failure studies. The maximum critical events found for actual truck data ranged from 1.5g to 1.84g such that a midpoint of 1.67g was selected as the critical g-level for the study (Figure 22).

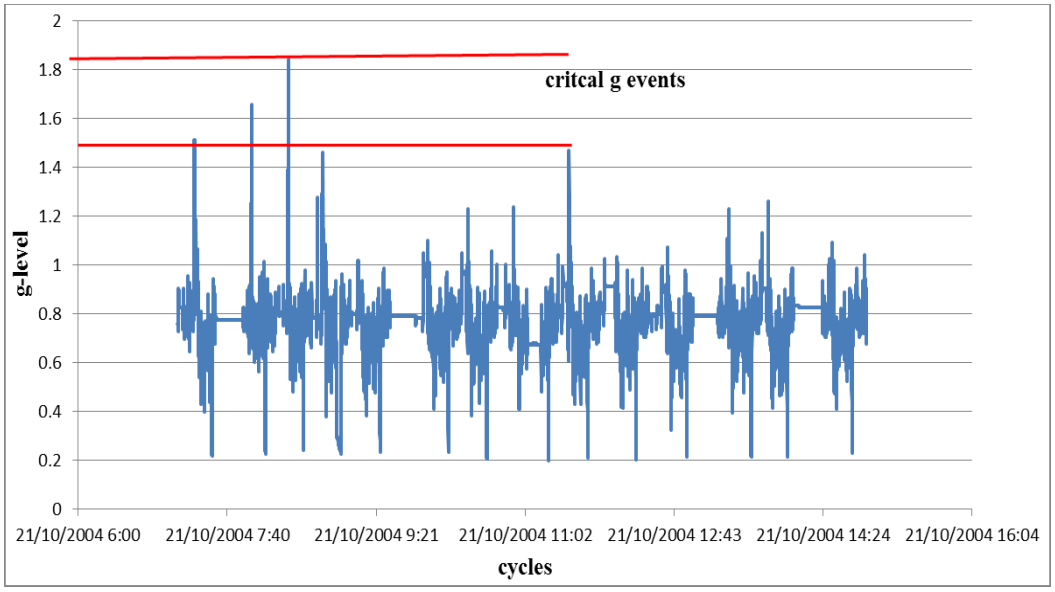

Figure 22: Total g-level of actual truck data

The total loading for the scale truck, at 32.22 kg, is the 1g reference condition load, but the load selected for the scale truck was based on a 1.67 g (critical g events) at 54.4 kg, 9 kg per tire.

Figure 23 indicates that the load is linearity related to strain regardless of internal tire pressure (27.5-68.9 kPa), with a high correlation which is seen at 27.5 kPa internal tire pressure. To scale the load on a tire, a common constant scaling diametral strain rule of 7% strain at loading measured in the field was used. Consequently 35 kg was established as the 1g base load for each tire.

The load versus strain graph showed a "scalable" equal slope, whereby the behavior was the same for all load vs. strain. By decreasing strain and load 4×less, the load per tire was established at 9 kg load at 1.8% strain for a 27.5 kPa internal pressure, equivalent to the 1.67g condition.

Pressure and load in a 27.5 kPa tire is shown in Table 4 and specified for 7% strain plotted in figure 22. Based on the flexure test and equal slope of relationship, the 27.5 kPa internal pressure with a 9 kg load per tire for a total weight of 54.4 kg was selected for truck in 1.67g.

The foot print area of a tire on the ground is directly proportional to the stiffness, internal pressure, strain and diameter of tire. The footprint area of a scale tire is calculated using square root scaling. The footprint area of an actual truck tire, 40.00R57, is 1.15 m^2.

Equation 7

$$Square\ root\ \ 22.83\ scale = \frac{\sqrt[2]{1.15}}{22.83} = 0.047\ m^2$$

Equation 8

$$Squared\ \ 22.83\ scale = 0.047^2 = 0.00219\ m^2$$

The footprint area of the small tire was measured in lab at 21.94 cm^2, confirming the geometric relationship, which was established by Dr. Joseph for any size of tire, footprint area at 7% strain is equal to Equation 9.

Equation 9

$$A = 1.35 \emptyset \delta = 0.00219\ m^2$$

$A = Footprint\ area$

$\emptyset = Tire\ diameter$

$\delta = Tire\ deformation$

This relationship also indicated that the ground pressure in the lab and field will be directly related to the scale factor selected, measure the ground pressure of the scaled tire would also be correlated to the equal slope for each range of load-strain as shown in Equation 10 and Equation 11 (the experiment error is less than 5.5%).

Equation 10

$$P_{grount\ at\ 7\%\ starin} = \frac{33.11(kg) * g}{1.35 * 0.07 * 0.1524^2} = 148\ kPa$$

Equation 11

$$P_{ground\ at\ 1.8\%\ starin} = \frac{9(kg) * g}{1.35 * 0.018 * 0.1524^2} = 156\ kPa$$

Table 4: Load flexure test data in 27.5 kPa

Internal tire pressure at 27.5 kPa						
pump pressure (kPa)	stable pressure pump(kPa)	Diff (Stab P, Initial Pressure) (kPa)	Voltage	Load (kg)	Deformation (mm)	strain
689	679	472	0.81	15.1	4.05	2.66
827	822.5	616	1.14	19.7	5.7	3.74
965	969	762	1.44	24.4	7.2	4.72
1103	1127	920	1.82	29.4	9.1	5.97
1241	1249	1045	2.12	33.3	10.6	6.96
1379	1430	1224	2.37	39	11.85	7.77

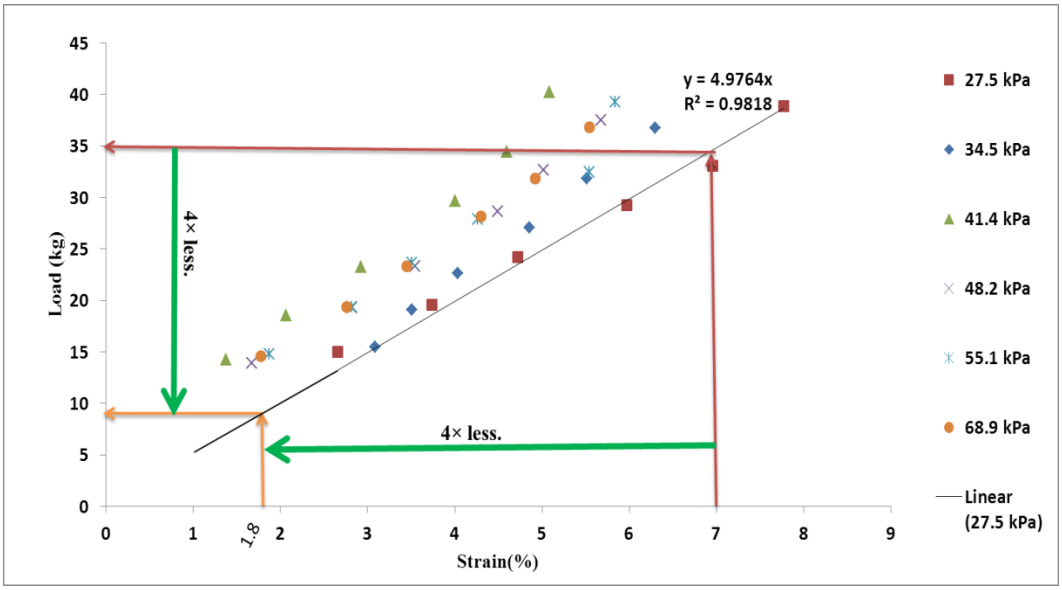

Figure 23: Load vs. Strain graph of 15.24cm tire

3-2. Rolling Resistance calibration test

Parameters affecting tire performance including rolling resistance, may be normalized by evaluating tire performance as a calibrated base set of conditions. By understanding the base rolling resistance of the scale tire, the rolling resistance between the waste dump material and the tire during truck movement on the waste dump can be determined.

This calibration test was completed on an empty steel test bed of dimension 2 m length, 0.8 m width, and 0.1 m depth. The length of the test bed was selected as 2 m so that the tire can have at least 4 complete rotations, and 0.8 m in width that any interference from sidewalls was negated. The depth of the test bed was maintained based on the rule that a zone influence by depth for 3 × half tire widths as shown in Figure 25 (Perloff, 1975) commensurate with Boussinesq

analysis. The depth of test bed was selected to be greater than the critical depth to account for any effects from the test bed base.

The test bed has a perfect plane adjustable ramp, varied by grade from 0, 2.85, 5.1, 7.7, to 12.8% incline.

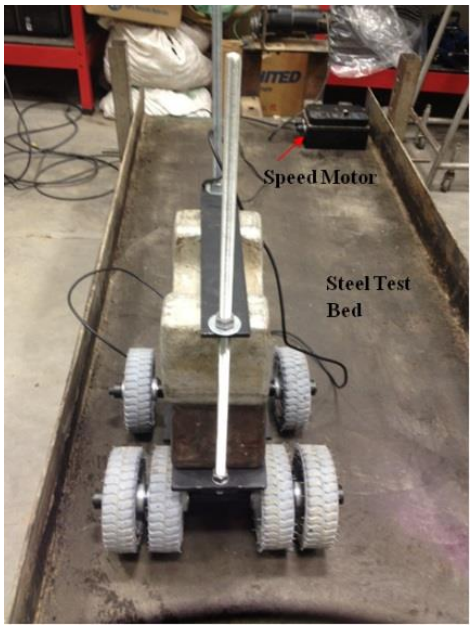

Figure 24: Truck on empty test bed

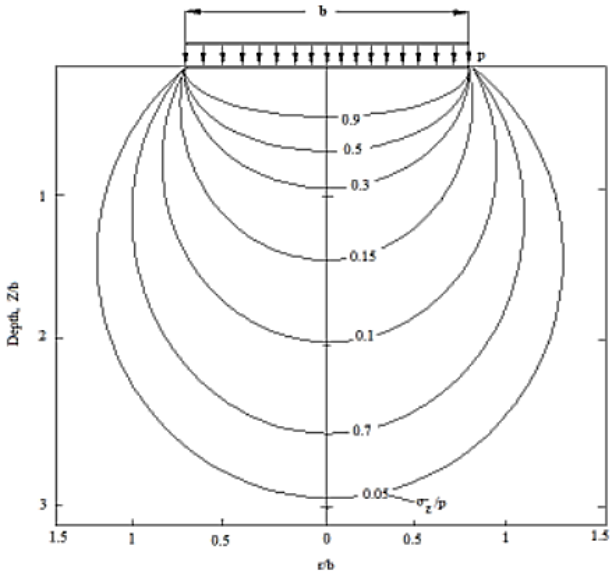

Figure 25: Contours of constant vertical stress beneath a uniform loaded circular area (Perloff, 1975)

9 kg tare weight scaled truck was loaded with 45.4 kg weight at 27.5 kPa internal tire pressures. The truck gross vehicle weight was the 54.5 kg, which was connected to the pull motor, via a load cell attached to the truck. As the truck was pulled by the motor, a load cell collected all load forces via an EDAQ data acquisition system which recorded the data.

Pulling the truck in an empty test bed was performed for all test bed grades at speeds ranging from scale equivalence to 17 to 30 kph in the field. The weighted mean of pull forces in each test bed grade are shown in Table 5 plotted in Figure 26 through Figure 31. From these plots, total weighted mean of each grade was determined.

Table 5: Weighted mean pull forces

Test bed Inclines	Speed	Weighted mean of pull force(N)					Total Weighted Mean of pull forces(N)
		17 kph	21 kph	24 kph	28 kph	30 kph	
0		12.1	11.94	12.29	12.12	12.12	12.16
2.85		26.33	25.67	26.25	25.58	24.41	25.91
5.1		39.1	39.32	39.34	39.21	39.42	39.27
7.7		51.9	51.8	52.0	52.46	52.94	52.28
10.3		67.12	66.54	65.74	67.02	65.04	66.39
12.8		78.32	79.53	78.35	78.88	76.57	78.42

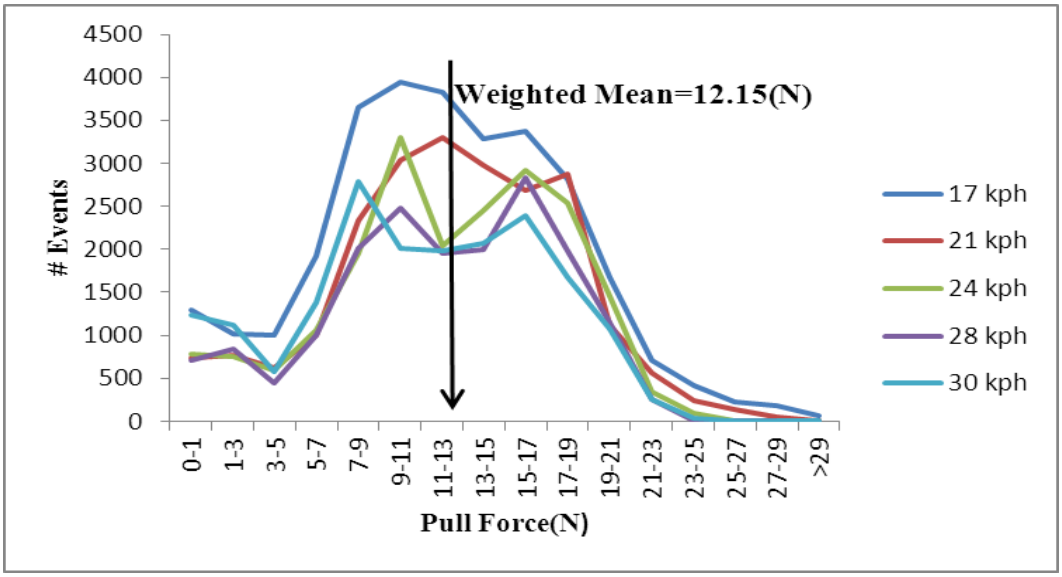

Figure 26: Pull force vs. # event in 0' plane bed slope

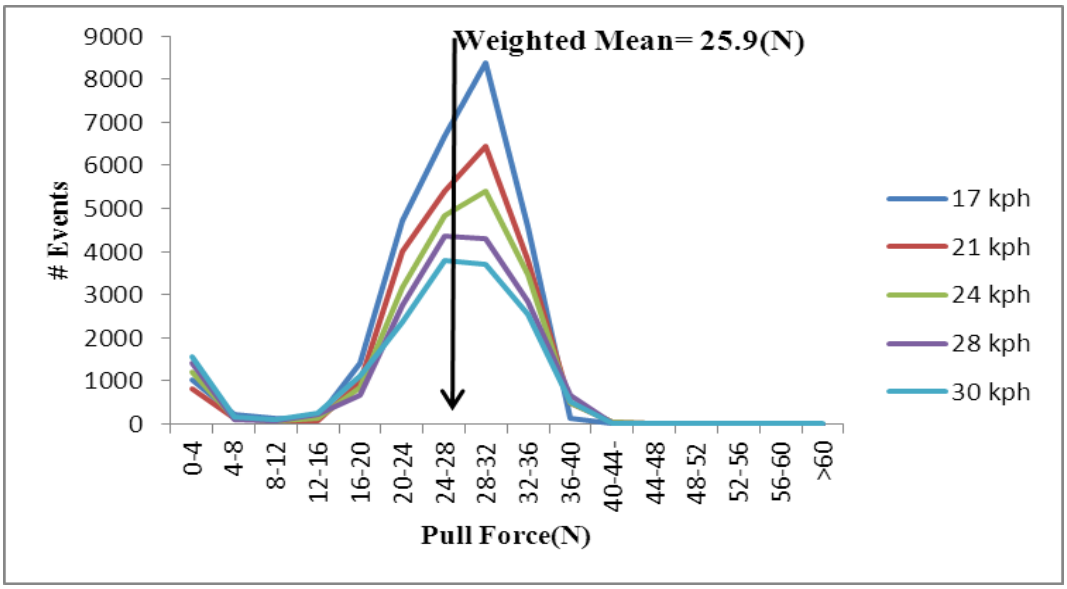

Figure 27: Pull force vs. # event in 2.85' plane bed slope

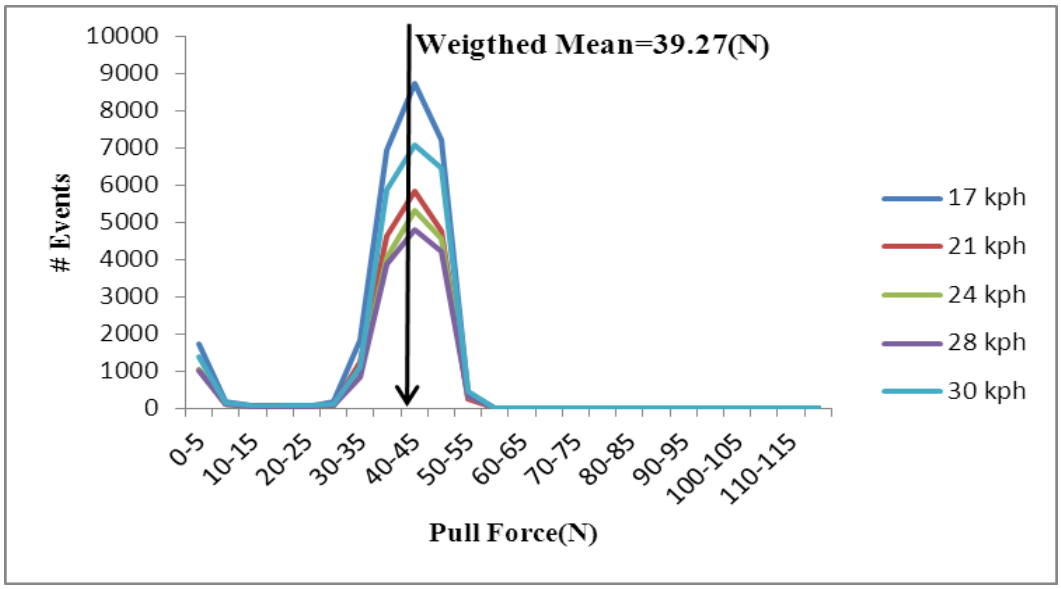

Figure 28: Pull force vs. # event in 5.1' plane bed slope

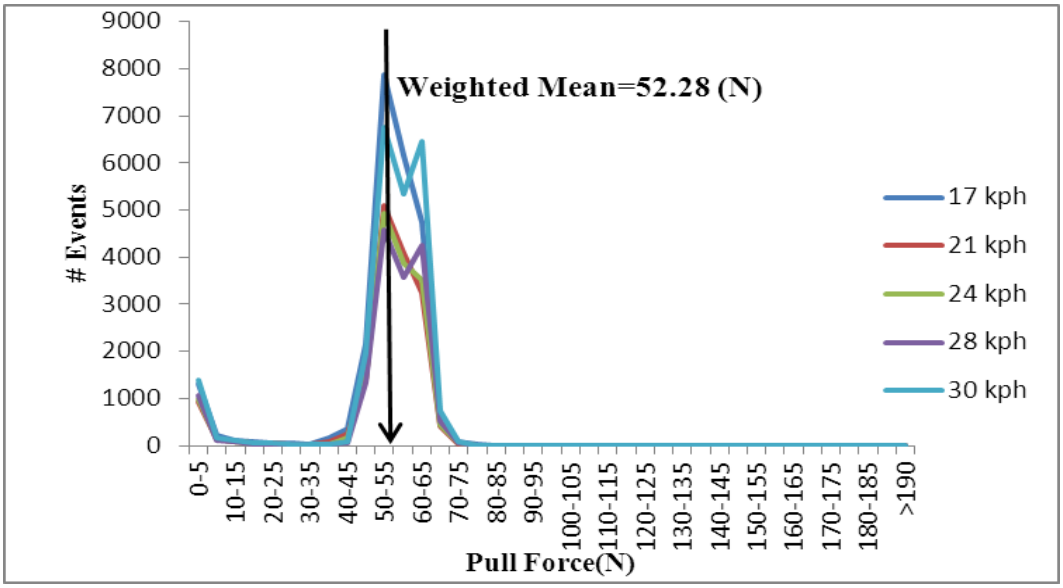

Figure 29: Pull force vs. # event in 7.7' plane bed slope

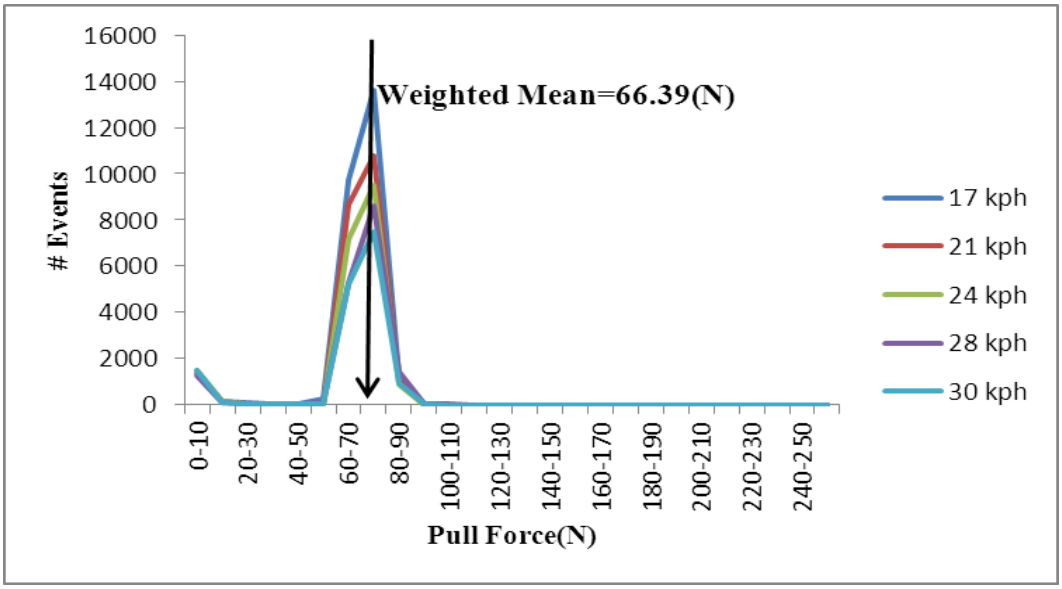

Figure 30: Pull force vs. # event in 10.3' plane bed slope

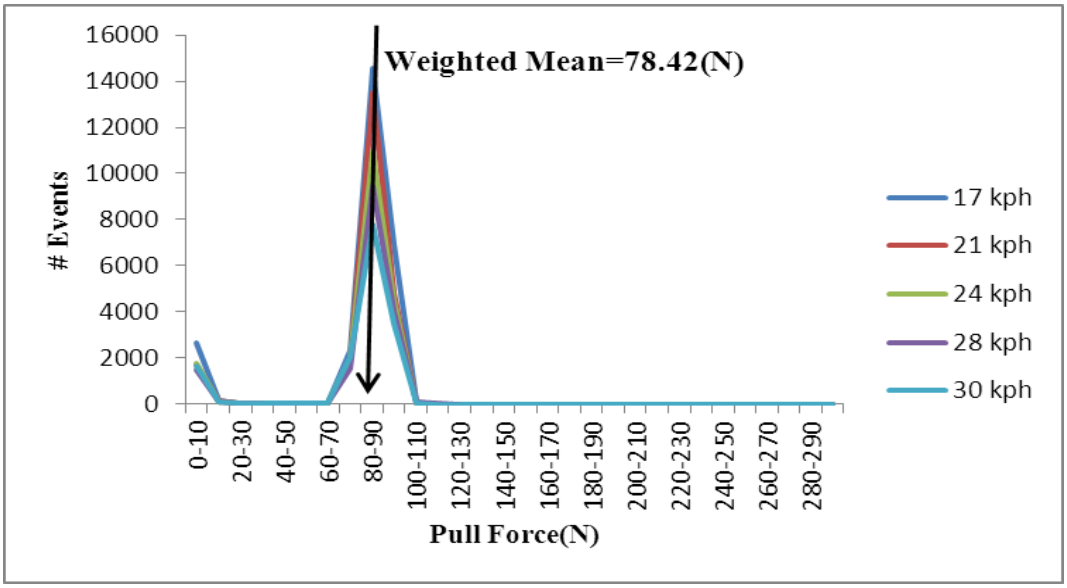

Figure 31: Pull force vs. # event in 12.8' plane bed slope

Rolling resistance is usually expressed as a resistance force proportion to the gross vehicle weight, and equivalent to a percent road grade. As an example, this means that the amount of force that a truck needs to overcome a 20% rolling resistance on a horizontal surface is the same as force required to move a truck

uphill at a grade of 20% with no surface rolling resistance (Tannant & Regensburg, 2001).

Hence the slope of the weighted mean pull force by ramp grade can be used to calculate the rolling resistance of the scale tired vehicle. In Figure 32, the slope of the graph which shows rolling resistance for the 15.24 cm tire truck model will be:

Equation 12

$$RR = \frac{F - 0.027}{0.012}$$

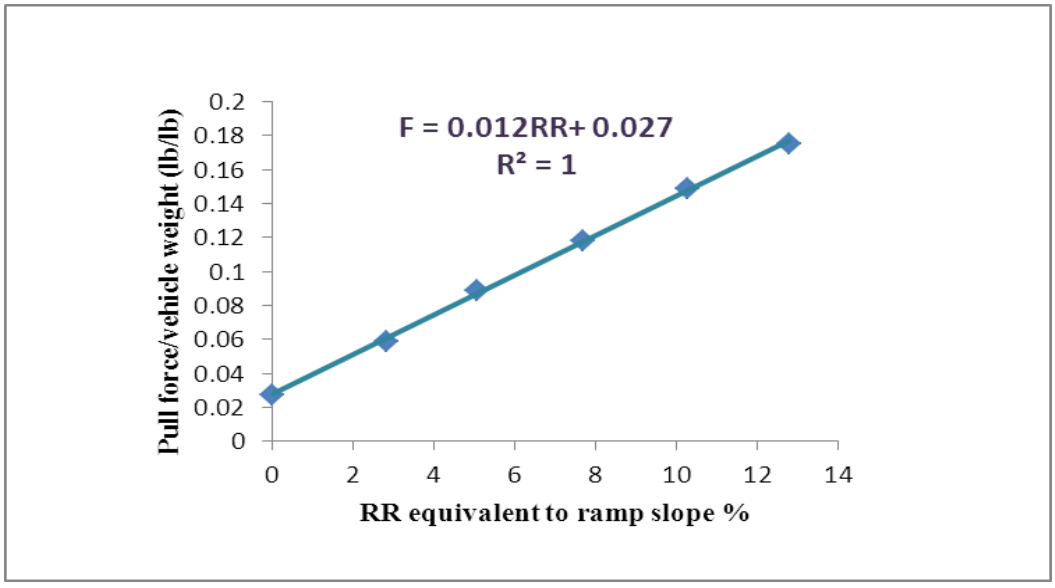

Figure 32: Pull force/vehicle weight vs. RR equivalent to ramp slope%

3-3. Dump Scaling

The size, height and slope angle of the waste pile was modeled to match the dimensions of a typical hard rock waste dump.

The material selected to build the dump was the dolomitic limestone chip. Dolomitic limestone is a sedimentary rock that contains carbonates of calcium and magnesium, or a combination of these two minerals. The density of the broken dolomite chip was determined as 1550 $^{kg}/_{m^3}$ and a natural slope angle of 37 degrees when free dumped.

The aeromechanics of the material was proportional to the tire-material contact relationship in the field and the scale factor to the dimension of the broken material in the lab tests. The maximum size of broken rock in the field was 101 cm, using scaling with the 22.83, the maximum size of broken limestone chip in the lab was determined as 4 cm.

Considering the tire properties, the width and footprint area of the tire were 4 cm and 0.0022 m^2, the d_{50} dimension of the broken scale materials was 0.6 cm that allowed the tire to be in contacted with 6 to 8 particles of crushed limestone in the contact area. Based on scale size and tire properties, the size of broken limestone was set at the d_{50} of 0.6 cm.

The dimension of the broken material varied from very fine to 0.025m passing. Based on the size distribution the minimum, maximum and d_{50} dimensions are given in Table 6 and shown in Figure 33.

The height of the dump was defined as the vertical distance from the toe to the crest of the dump. Actual field dimensions are from dump range from 20 m to 400 m (Piteau, 1991). Using the scale factor of 22.83, the range of waste dump height

in the lab was from 0.9 to 18 meter; here a 1 meter was selected for the dump height as a practical on a laboratory scale.

Table 6: Size distribution of Limestone

Dimension of limestone chip(cm)		
Range	Scaled size	Actual size
Minimum	0.06	1.37
Maximum	1.6	36.53
d_{50}	0.58	13.24

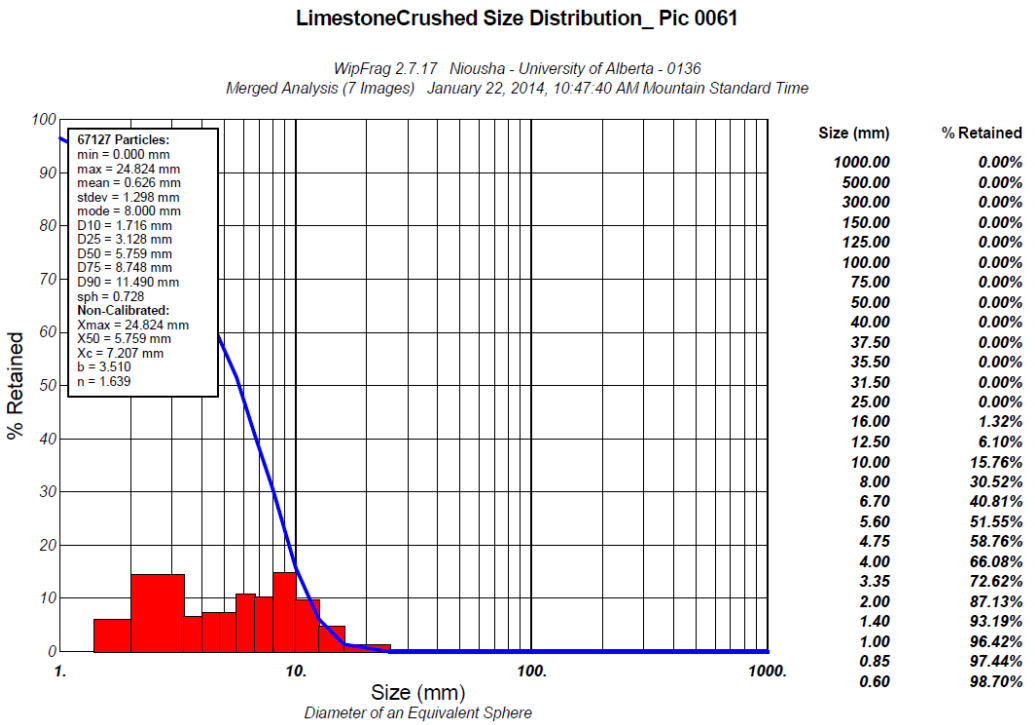

Figure 33: Size distribution of limestone

The size of the dump was designed to avoid the impact of truck loading on boundary conditions, so the width of top of the dump was set as 3 times of the truck width, at 1.89m. The length of the dump was set at 4 m, so that the truck tires would have at least 3 full rotations.

The slope face angle of the dump, from the crest to toe was purely defined by material used to build the dump. This angle was 37 degrees, within typical range for limestone and hard well blasted rock from 26 to 37degree (BSI (BSI PROPRIETARY INFORMATION), 2011).

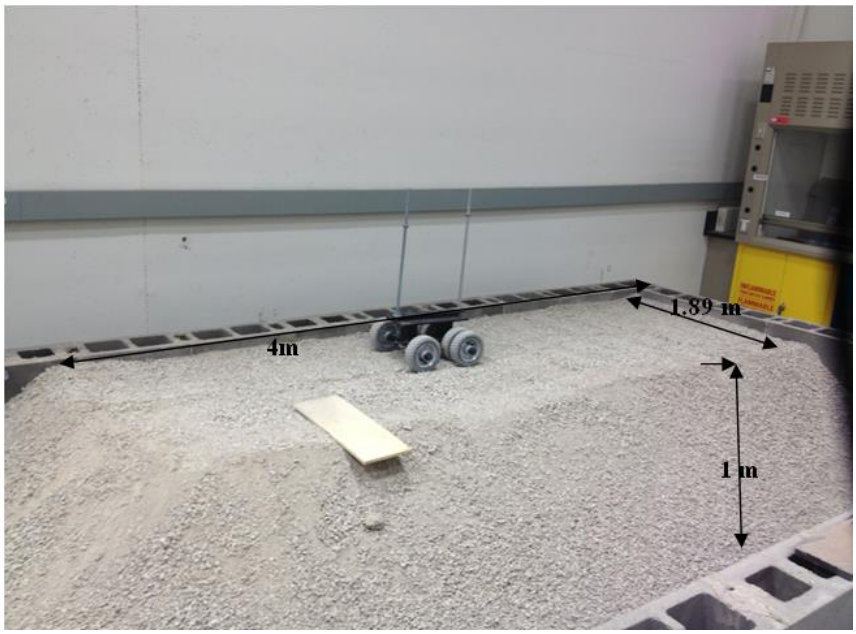

Figure 34: Dimension of waste dump

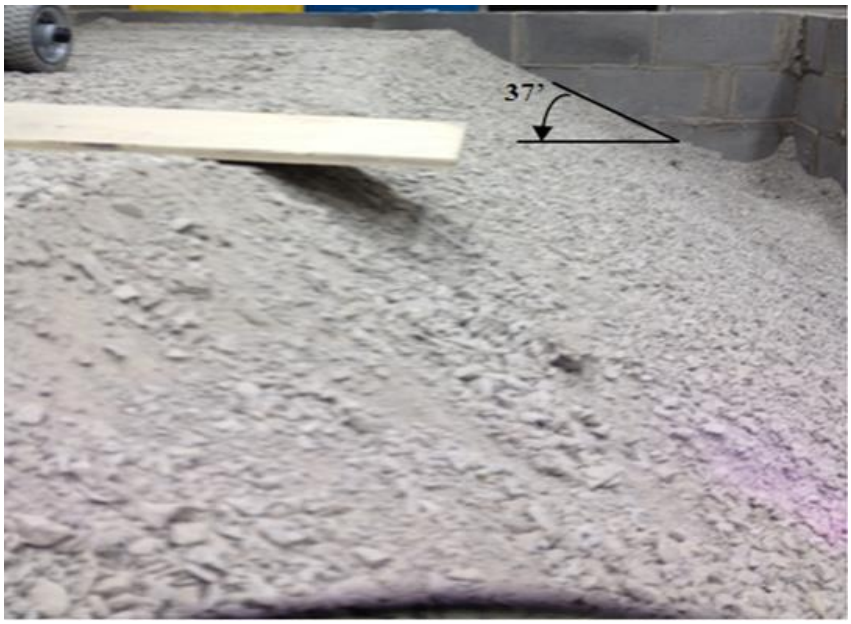

Figure 35: Crushed limestone slope angle

Chapter 4: Laboratory Tests

4-1. Introduction

Studies and researches on dump stability have traditionally been based on the geotechnical properties and external influences such as ground water or solely seismic load. The effect of dynamic loading has been studied on oil sand but very little exists for other waste materials. This study focuses on the effect of mining equipment movement as dynamic loads on loose and broken rock via laboratory scale tests to study the stability of a broken rock waste dump.

Rolling resistance between tires and the broken rock has been analyzed during truck movement for different conditions to consider how rolling resistance may change during the truck motion including stable to the failure modes of adjacent dump faces.

In order to gain a comprehensive understanding of the effect of mining equipment operation on waste rock surface, stability of waste dump structures, experiments were performed to measure movement and displacement of the broken rock surface under dynamic load as applied by active mining equipment. These experiments utilized by taking snapshots of the surface and slope of the dump during such surface loading activity.

4-2. Preparation Dump

The dump of broken limestone was constructed in rectangular area regarding to dump scale dimension. Procedure of construction was the free dumped, without any additional compaction during dumping.

Area of $1m^2$ was selected in middle of dump face zone. This area was coloured in layers of 2 cm. Two locations were selected for studying the impact of truck movement. The first was set as the one third of the truck width (11 cm) and the second at half of the truck width (17 cm) from the crest edge of the dump, shown in Figure 36.

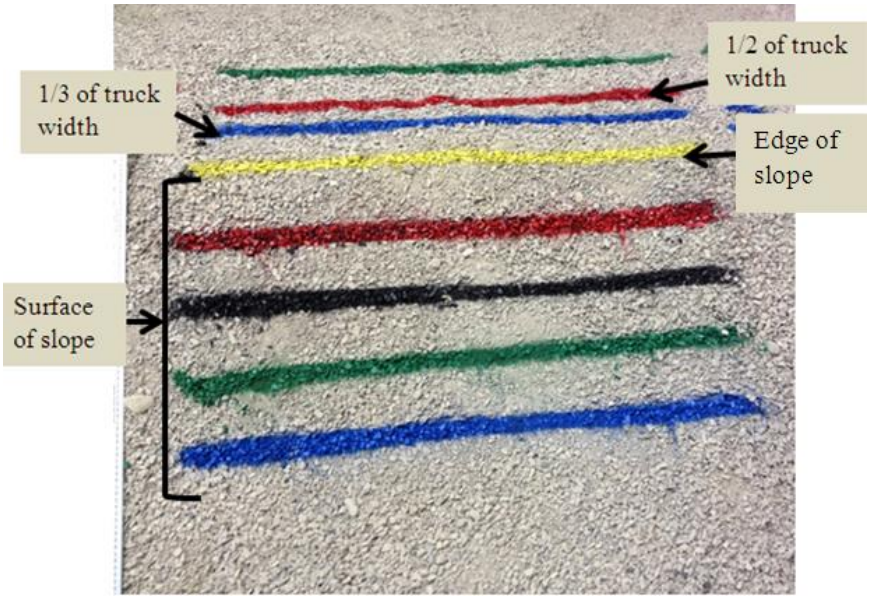

Figure 36: Scaled size dump

The scale truck was loaded to nominal payload with 22.6 kg and connected to the pull motor by a steel wire; via a load cell connected to the truck chassis. These parts are shown in Figure 37.

1. Pull motor
2. Wire
3. Load cell

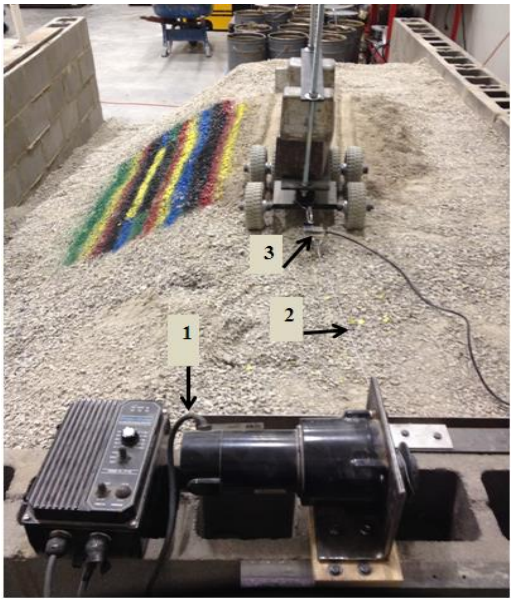

Figure 37: Truck which is connected to speed motor via load cell

4-3. Test Introduction

The procedure of test commend with taking photos of the surface of the slope during truck movement focusing on the movement of the colored layers to visually measure the displacement of the dump layers.

The first test series used the free dumped condition of the broken limestone, with no compaction or surface improvement. The truck was initially run at 17 kph speed on the dump at half the width of the truck from the crest and the one third width of truck from the crest. During the movement the camera took pictures at 5 seconds intervals to build a dynamic picture of the displacement and movement of the color layers at the surface of the slope. The load cell recorded all pull forces during the movement of the truck at 10 Hz collection. These pull forces were used to study and analyse the rolling resistance between the tires and broken limestone.

The second set of test followed pre-compaction of the surface to simulate the applied packing of a dozer, grader or other trucks on the dump. Here data recorded, provided a comparison to the uncompacted state.

The third condition tested, considered a safety berm; similar to actual conditions where dozer would create a safety berm to keep haulers from accessing to close to the dump crest. The height of the safety berm was set by the diameter of tires, 2.0 m for a 240 truck and 2.9 m for a 360 truck. It was recommended base on field practice that the ratio of safety berm height to tire diameter was 3/4; and all berms should be greater than 1 m regardless of tire diameter (Tannant & Regensburg, 2001).

Wet conditions were tested as the fourth consideration. In actual practice, trucks run on waste dump sprayed surface with water to dampen dust. This action also causes greater compaction and broken rock crushed cohesion.

4-4. Test results for displacement of broken rock surface

4-4-1. Test Run for half truck width from edge of slope (17 cm)

4-4-1-1. Free dumped of crushed limestone:

This condition was dry limestone with no compaction. The test was done at 17 cm from the crest for 10 test runs and 20 truck movements (backward and forward). During each test run photos were taken at 0.2 Hz of the surface of the dump to monitor movement of layers indicating slope displacement. It was seen that no changes in surface displacement occurred during truck movement from the first to the last visual record. There was also no rolling of crushed limestone down slope.

However the truck movement dedicate the ground profile to change. This was due to the weight of the truck on uncompact limestone. The total weight of the truck during movement caused compaction of the crushed limestone along the truck path. From Figure 42, it was obvious that the ground underneath the tires deformed 2.5 cm on both sides of the truck, which as correlation in field, it will be 10 cm.

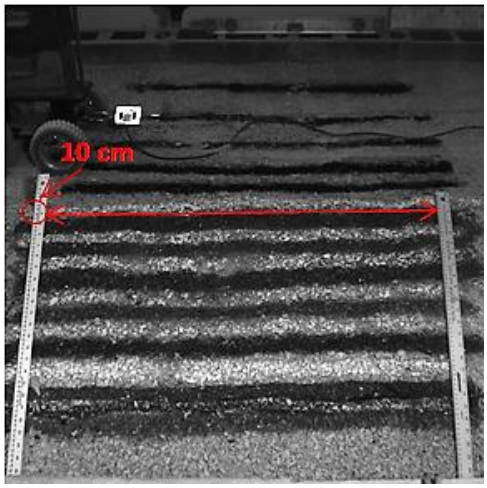

Figure 38: first second, test run 1

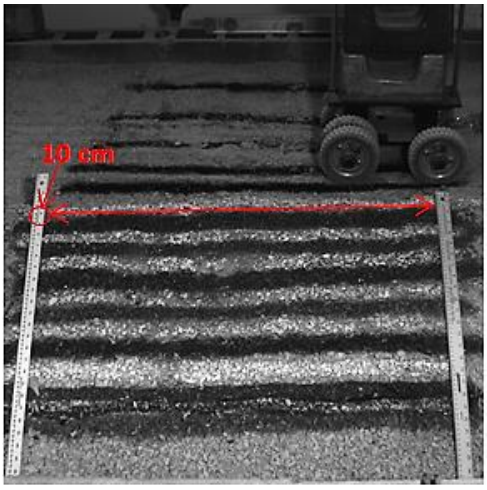

Figure 39: last second, test run 1

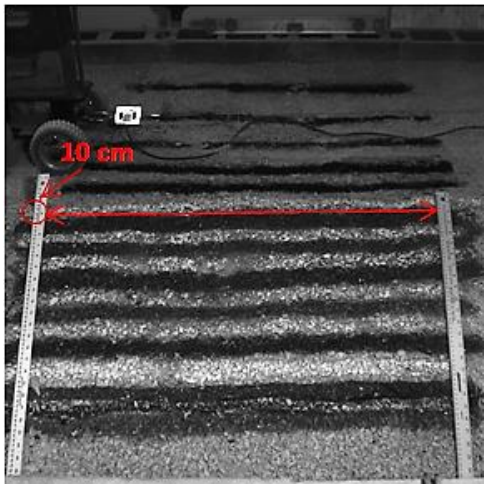

Figure 40: first second, test run 10

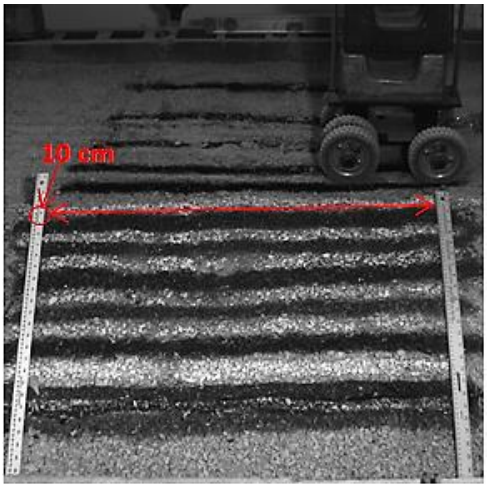

Figure 41: last second, test run 10

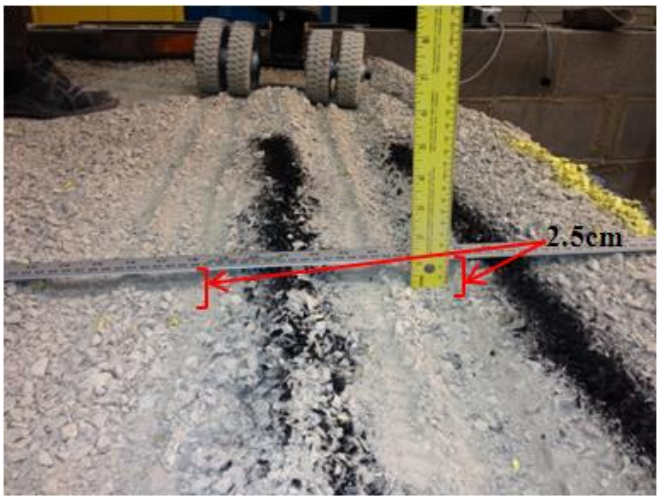

Figure 42: Ground profile of truck movement in 17 cm from edge

4-4-1-2. Post 22.6 kg compaction on crushed limestone + safety berm

This test studied the effect of the safety berm on the stability of a dump. The height of the safety berm was determined based on the field relation between height and tire diameter. The scale tire diameter is 15.24 cm so the height of safety berm was calculated as 11.5 cm.

Equation 13

$$\frac{\text{Height of Safety Berm}}{Tire\ Diameter} = \frac{3}{4}$$

Equation 14

$$Height\ of\ Safety\ berm\ = \frac{3}{4} \times\ 15.24\ =\ 11.5$$

Where a dozer builds a safety berm, the ground beneath is compacted due to the weight of the machine by pressure of 158.6 kPa. Broken limestone in the lab should be compacted by pressure 6.9 kPa, calculated from scaling factor. This

work was done by using a steel weight in 22.6 kg with dimension of 12.7*25.4 cm during building safety berm in lab, to simulate the same scale dozer pressure.

Figure 43: Dump with Safety berm

From the pictures which were taken of the surface of the slope, the truck weight during the runs had little to no effect on the stability of the dump, as the distance of the truck from the crest was large. The ground profile of the road under the truck path changed a minor amount and yielded footprint area during movement of 0.5 cm and by the scaling up; it will be equivalent to the actual depth, in 11.4 cm, which is shown in Figure 48. The tire penetrate due to pre-compaction of the surface was less than the previous un-compacted surface test.

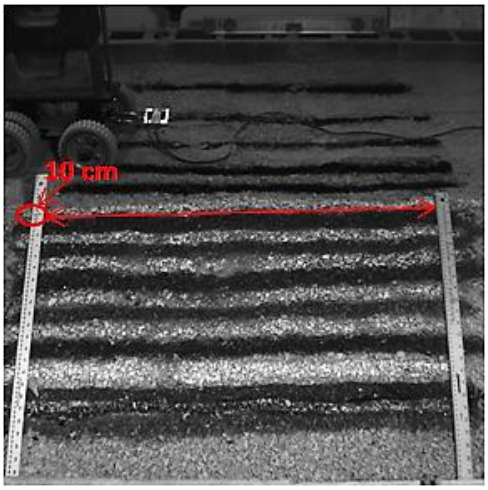

Figure 44: 10th second, test run 1

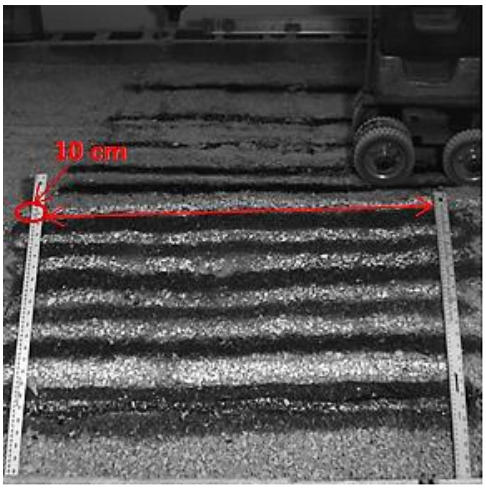

Figure 45: 55th second, test run 1

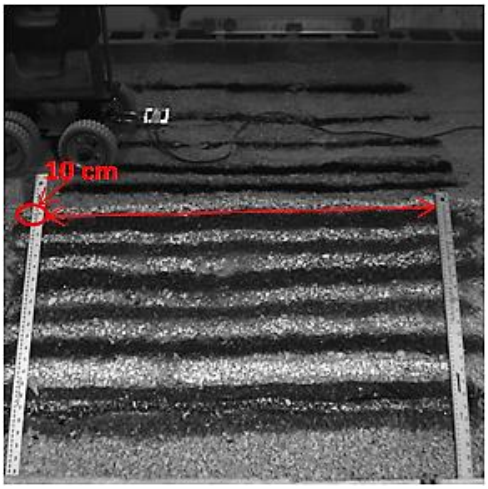

Figure 46: 10th second, test run 5

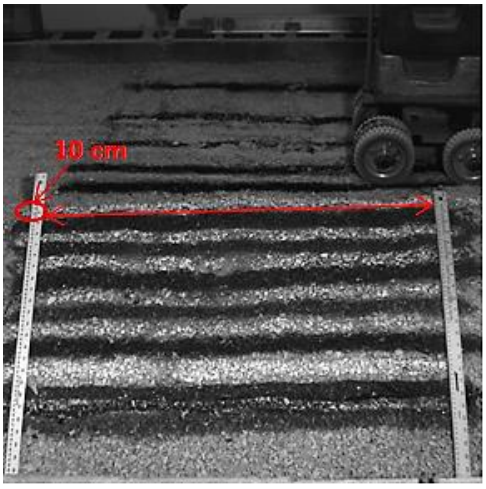

Figure 47: 70th second, test run 5

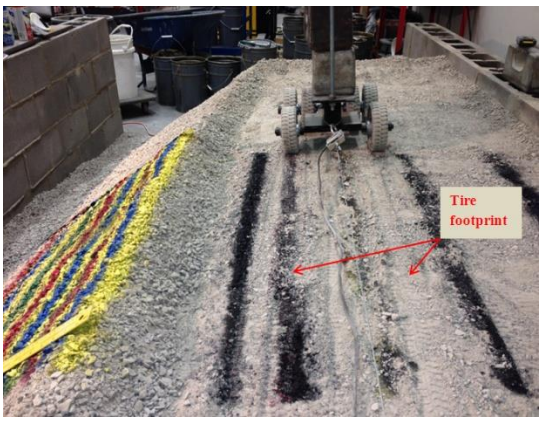

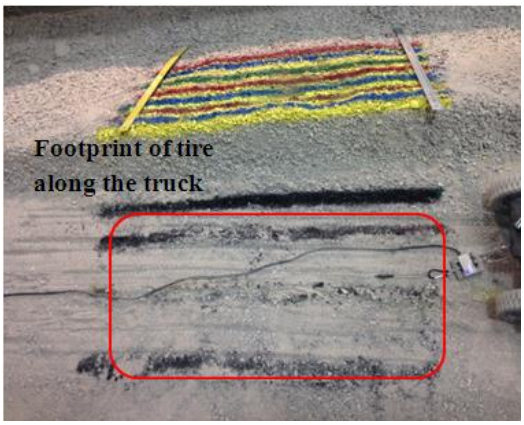

Figure 48: Ground profile changing

4-4-1-3. Wet Condition at 6% resistance increase by volume

This test was performed for a dump surface with water added to improve the surface bonding and decrease the impact of truck movement on the dump. The specific depth of limestone beneath a tire which was mixed with the water is a function of the depth of influence below the tire. This depth was calculated via equation 15. The depth of a 15.24 cm scale tire with a footprint area of 22 cm^2 was 14 cm.

Equation 15

$$D = 3 \times \sqrt{A_{tire}}$$

In a mine haul road construction three to four layers are used. The lower layer is the sub-grade which is the natural surface of the base ground. In some mines this may be leveled to create a better surface on which to build the haul road. The three others layers include:

1) The sub-base is the first layer adjacent to the sub-grade. It has different thickness for different road loading conditions, which are directly related to the material performance of that layer. Common materials found on site in a mine are used to form this layer.

2) The Sub-course is the second layer of the haul road; usually formed from mine waste or other load materials.

3) The last layer in direct connection with the truck tires is called the surface-course, for which gravel is usually used (Tannant & Regensburg, 2001).

The depth of tire influence should be considered in deciding thickness and compaction of these three layers. One third of the specific depth which was calculated from the equation 15 was selected as the depth that was mixed with water in lab, due to construction of surface course in lab. This depth was determined as 4.6 cm.

The proportion of water for the mix was set as 6% with 94% by volume broken limestone. By density of limestone at 1550 kg/m^3, 50 kg of limestone was mixed with 2 kg of water. The mix was spread on the surface of the dump compacted with the 22.6 kg to simulate a scale of actual conditions of operating by dozer at 158.6 kPa.

Figure 49: Waste dump in wet condition

After preparing the surface of the dump, the same test was run and analyzed for the truck running in wet conditions. The test was started at 17cm from the crest with pictures taken of 0.2 Hz for 10 test runs. During each test run it was observed that truck movement had no effect on the stability of the dump and no failure or

rolling broken rock was seen. Figure 51 to Figure 56 show the first and last second of test runs 1, 2 and 10.

Only the ground profile has changed during truck movement. In the first test the ground deformed along the tire route by 0.5 cm and this deformation compounded to the last test run for a total of 1.5 cm.

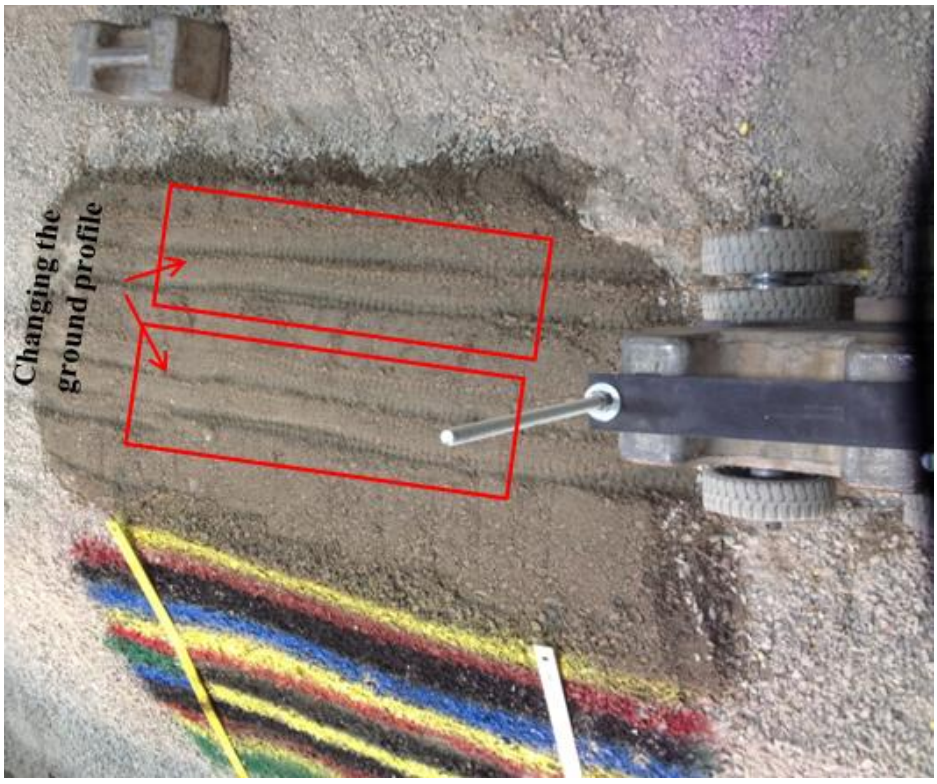

Figure 50: Ground profile changing during the test runs

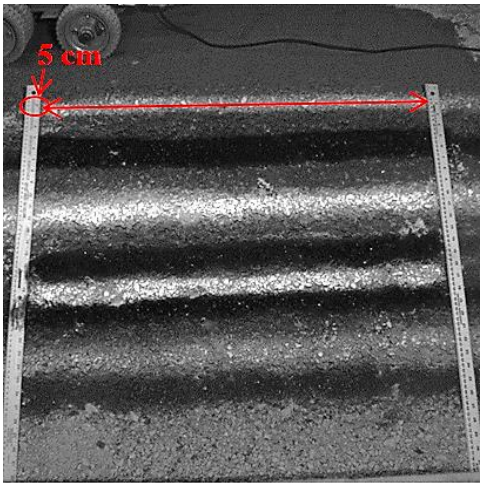

Figure 51: first second, test run 1

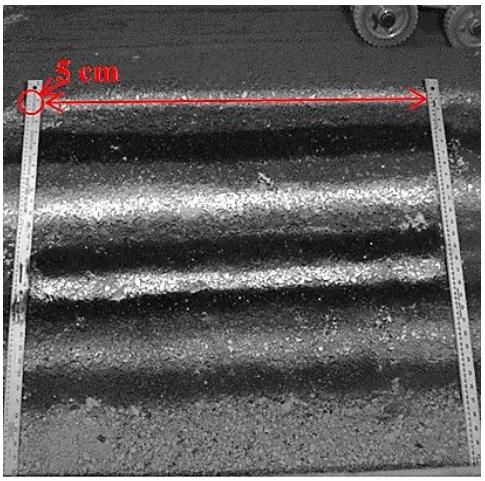

Figure 52: 65th second, test run 1

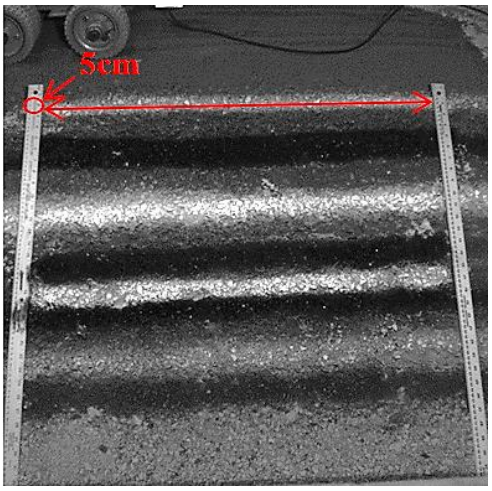

Figure 53: first second, test test run 2

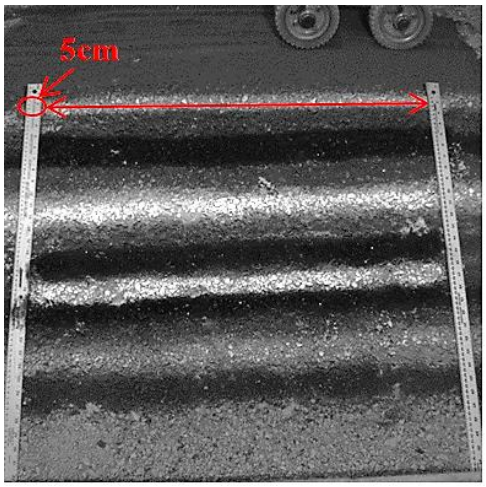

Figure 54: 60th second, test run 2

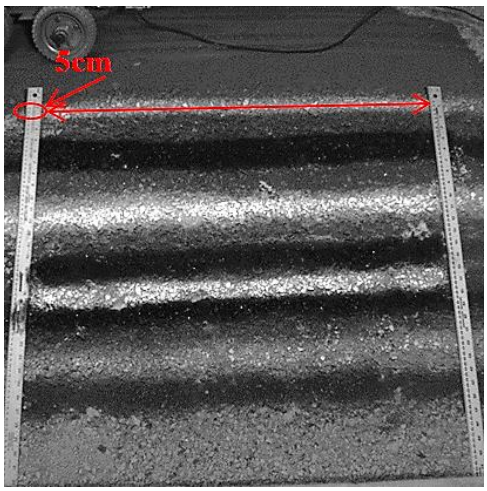

Figure 55 first second, test run 10

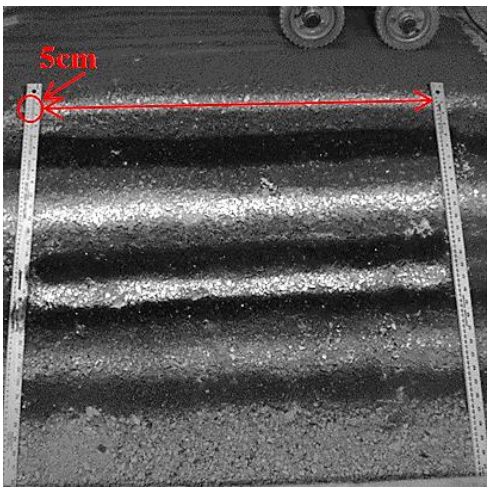

Figure 56 60th second, test run 10

4-4-2. Test Run for one third of truck width from dump crest (11 cm)

4-4-2-1. Free dumped of crushed limestone

These tests were illustrated at 11 cm from the edge of the crest, representing one third of the truck width. Tests were performed by truck running at 17 kph speed on a fresh constructed dump to eliminate any previous effects of truck movement from previous tests.

1. For the first test run, based on pictures taken at 0.2 Hz, it was observed that the top colored layer, near the crest moved with truck movement. When the truck started to move a small volume of broken limestone accumulated in front of the tire and pushed by the truck, causing the edge of the slope to move and broken rock move down slope. This movement ahead of the truck is a "bow wave" effect shown in Figure 58, Figure 59, Figure 60 with a red ellipse. The upper band of material in the tuck route deformed by 2 cm (from 1.5 to 3.5 cm).

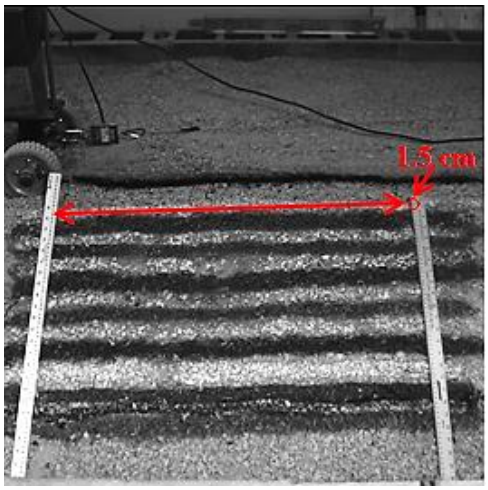

Figure 57: first second, test run 1

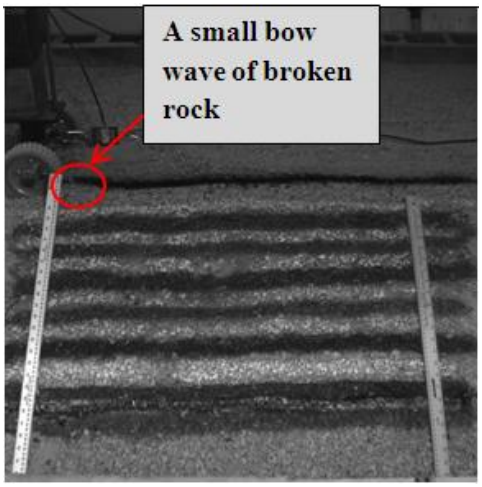

Figure 58: 5th second, test run 1

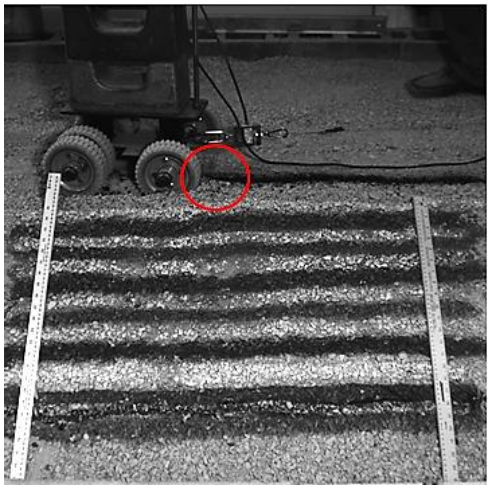

Figure 59: 25th second, test run 1

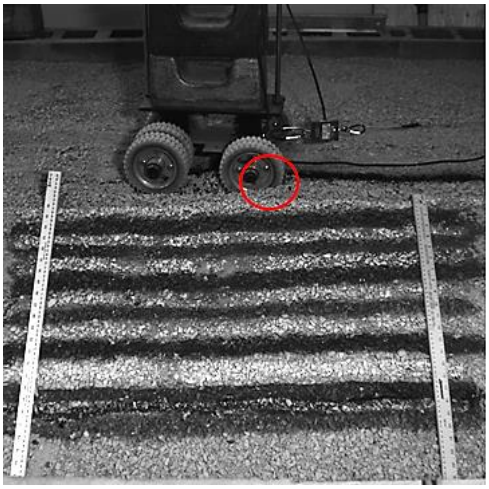

Figure 60: 35th second, test run 1

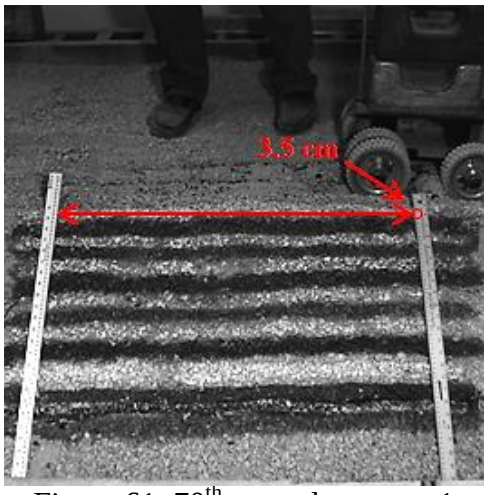

Figure 61: 70th second, test run 1

2. The second test run was started immediately following the previous one, some of the crushed limestone rolling down from the top layers and which comparison of the images for the first and last, it was obvious that the colored layers of limestone chip had moved 3.5 cm to 4 cm, for a deformation of 0.5 cm.

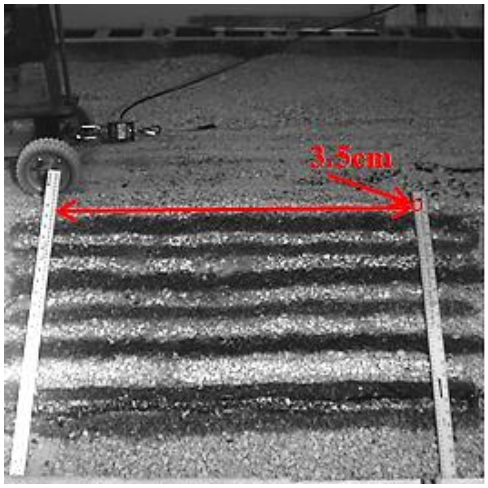

Figure 62: 5th second, test run 2

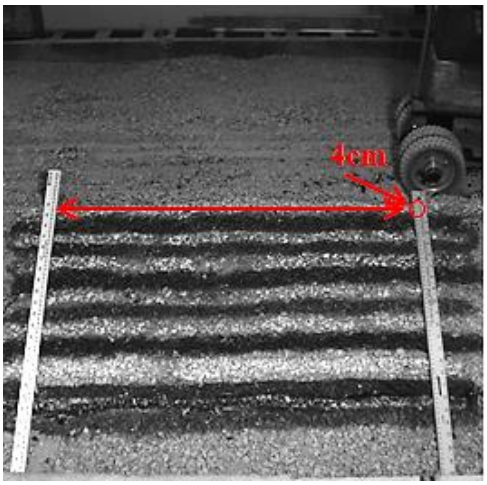

Figure 63: last second, test run 2

3. The third test run was completed by pulling the truck at 17 kph over the dump surface. The ground beneath the tires moved, pushing the crest down slope in the first to 25 second interval, Figure 64 and Figure 65 showed a very small movement of the layers at1cm.

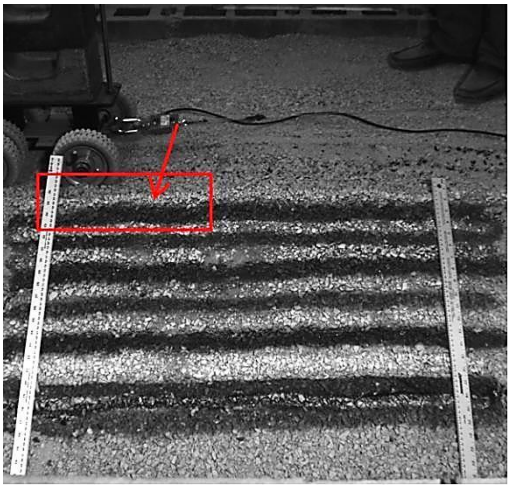

Figure 64: first second, test run 3

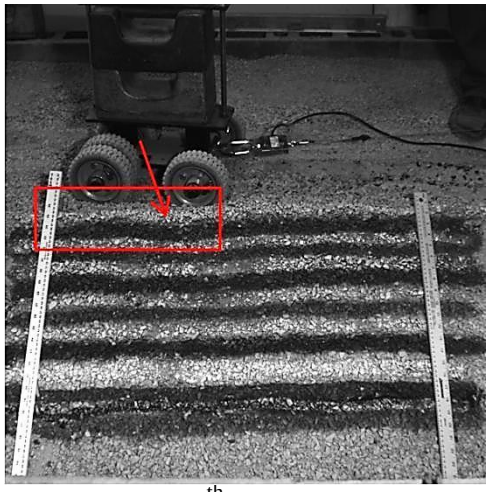

Figure 65: 25th second, test run 3

In the next ten seconds the two top layers of broken deformed by another 1 cm, which was shown in Figure 66 and Figure 67. As the tire penetration increased, the direction of the right front tire veered toward the edge of the crest. Continuing

the truck run caused a circular arc failure at 37.5 cm from the start of truck running, and continuing for 60 cm along the route. In this 23.5 cm zone the broken limestone failed and rolled down slope for 18 cm, as illustrated in Figure 68.

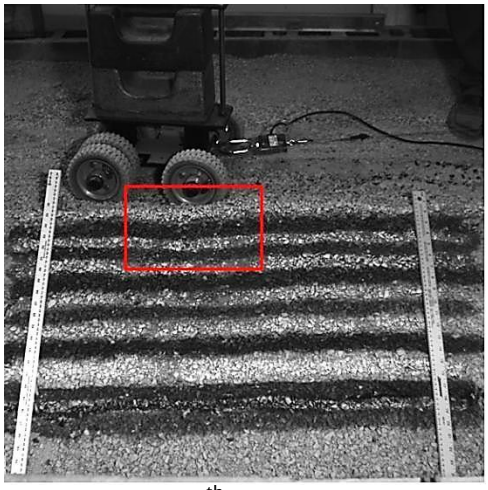

Figure 66: 25th second, test run 3

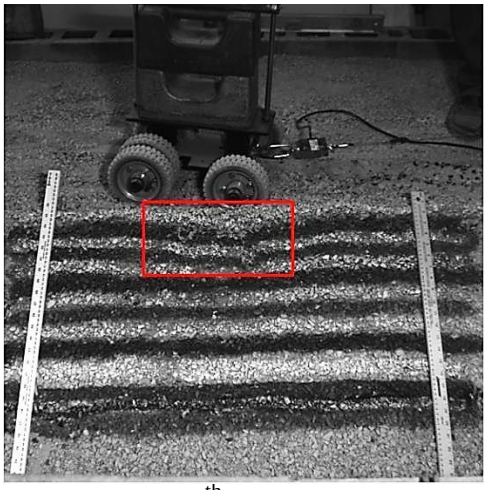

Figure 67: 35th second, test run 3

Figure 68: 40th second, test run 3

In an interval 5 seconds failure extended with broken materials moving down slope and failure extending to 28 cm from the top of the slope (Figure 69). With truck motion the failure extended horizontally for 15cm (with a total length of failure at 37.5 cm) and crushed limestone rolling 2 cm more than in the previous

photo. From 50 to 55 seconds the front right tire of the truck sank in to the ground more than half the tire diameter (7 cm) and caused it to veer toward the edge of slope as seen in Figure 71, highlighted by red ellipse. During these 5 second period a portion of broken limestone rolled down, with failure extending horizontally towards the end of the truck path for 7.5 cm. A circular arc failure expanded for 8 cm down slope (Figure 71).

Figure 69: 45th second, test run 3

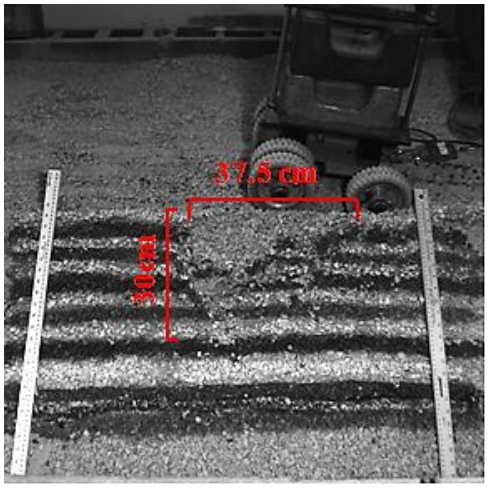

Figure 70: 50th second, test run 3

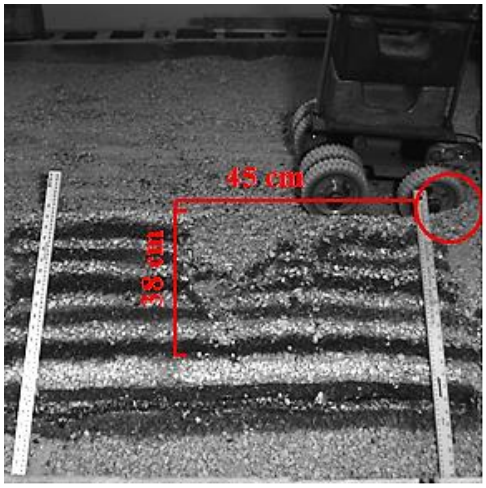

Figure 71: 55th second, test run 3

4. The forth test run started in conditions over a previous circular arc failure from previous test run, where upon most of the top layers of broken limestone

flowed down slope in extended failure. In the first 15 seconds of the test, material rolled down slope and progression to failure thereafter increased. This condition was amplified by truck movement, with greater broken material rolling down slope, causing tire penetration nearer the crest and changing the direction of the truck to veer over the crest.

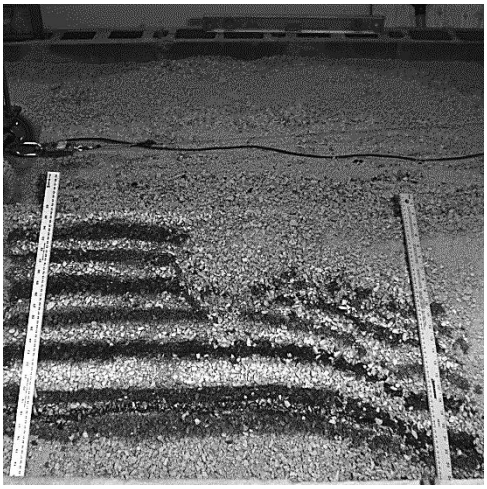

Figure 72: first second, test run 4

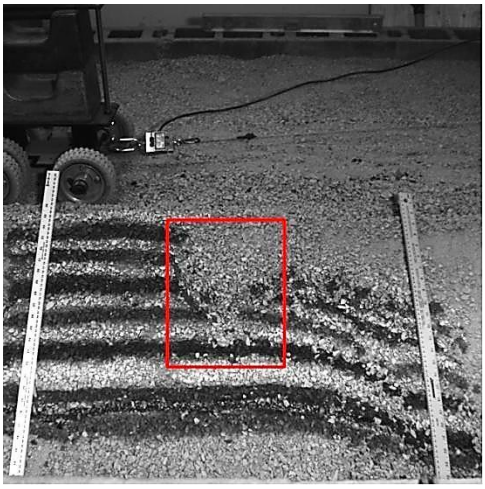

Figure 73: 15th second, test run 4

Figure 74: 20th second, test run 4

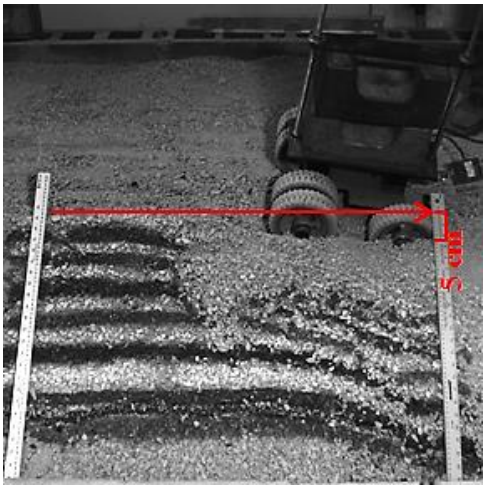

Figure 75: 65th second, test run 4

5. In the fifth test run, a greater merging of layers occurred and adding to the failure from the previous steps. Further broken limestone move down slope during truck movement, similar to the previous step, and the direction of the truck

changed with failure towards down slope. The ground profile beneath the front right tire deformed with penetration to 4 cm. (Figure 83, Figure 84).

Figure 76: 10thsecond, test run 5

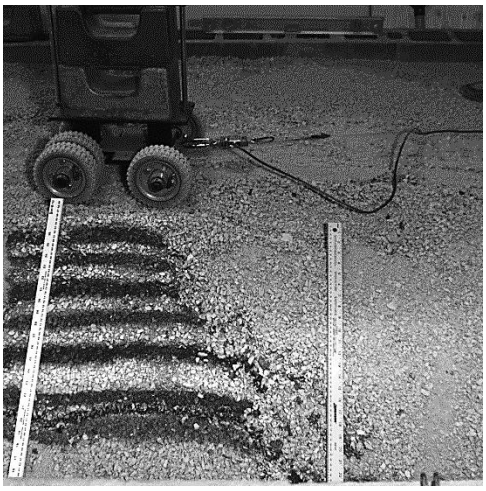

Figure 77: 15th second, test run 5

Figure 78: 10th second, test run 5

Figure 79: 30th second, test run 5

Figure 80: 35th second, test run 5

Figure 81: 40th second, test run 5

Figure 82: Truck failure

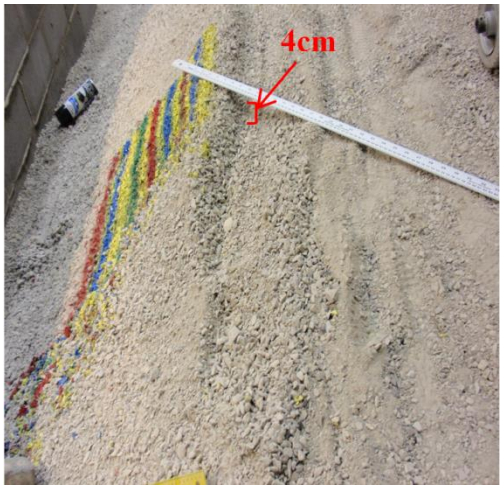

Figure 83: Changing Ground profile

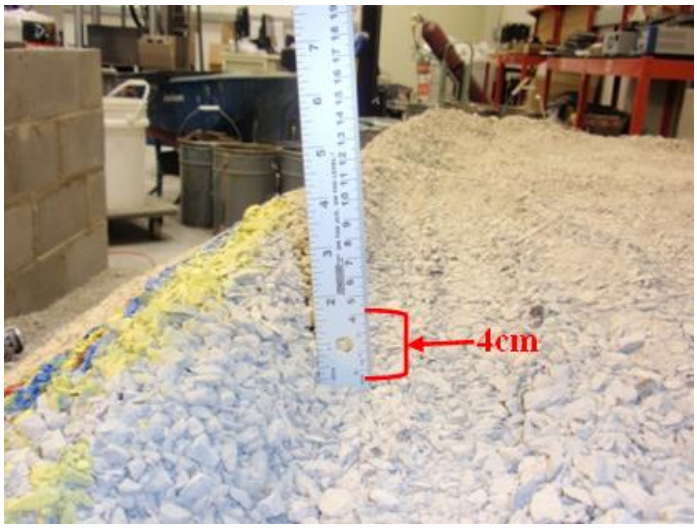

Figure 84: Ground profile

6. In the last test run in the sequence, when the truck started to run a huge circular arc failure occurred with in material from the first point of truck run moving down slope and causing the truck to roll over the crest and down slope.

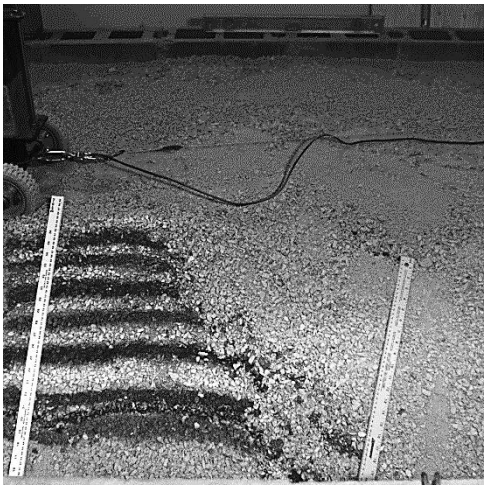

Figure 85: 5th second, test run 6

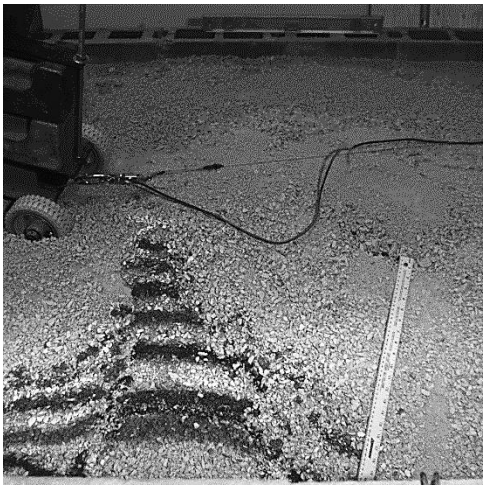

Figure 86: 10th second, test run 6

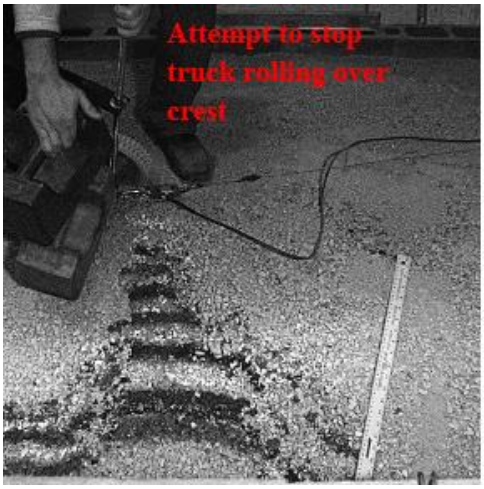

Figure 87: 15th second, test run 6

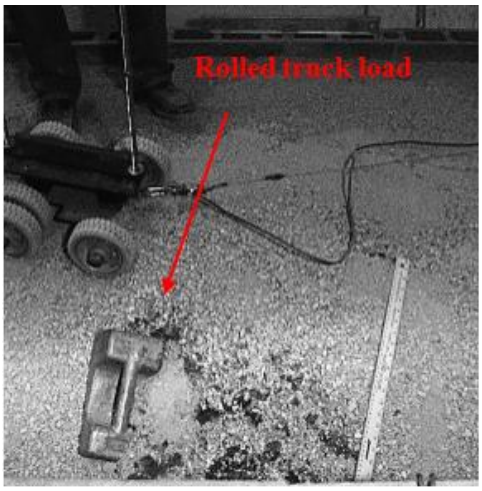

Figure 88: 20th second, test run 6

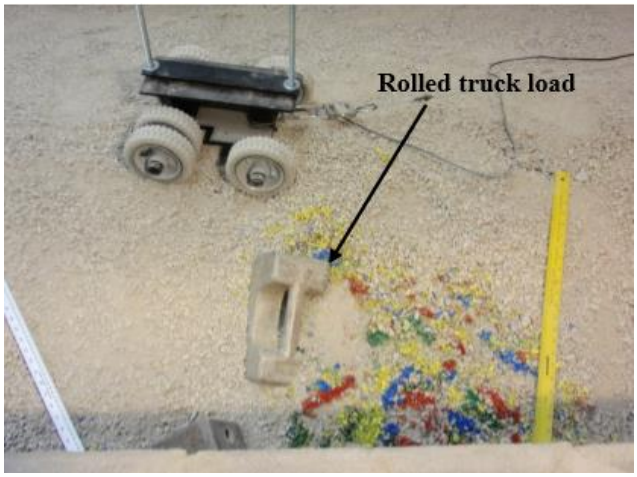

Figure 89: Failure of Truck

4-4-2-2. Post 22.6kg compaction on crushed limestone:

Compaction was added beyond free dumped materials by using the 22.6 kg mass generating 6.9 kPa equivalents to a dozer compacting at 158.5 kPa to simulate the actual dozer preparation. This allowed a study of the effect of compaction on dump stability with truck runs at one third of the truck width from the crest.

Test run 1 to 4: During the first four test runs there was no visual impact on stability, however the second test run, a few crushed limestone particles did roll down slope, shown in Figure 93.

Figure 90: 10th second, test run 1

Figure 91: 70th second, test run 1

Figure 92: 10th second, test run 2

Figure 93: 55th second, test run 2

Figure 94: 10th second, test run 3

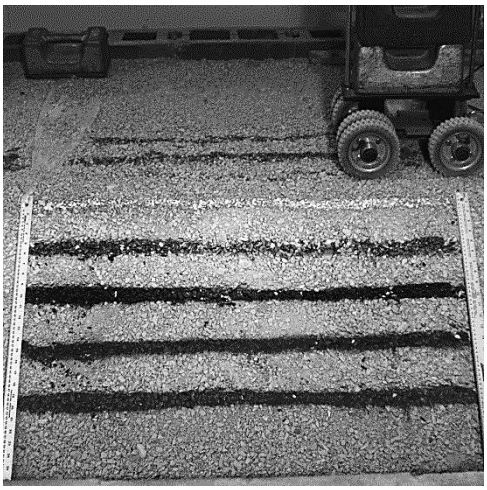

Figure 95: 65th second, test run 3

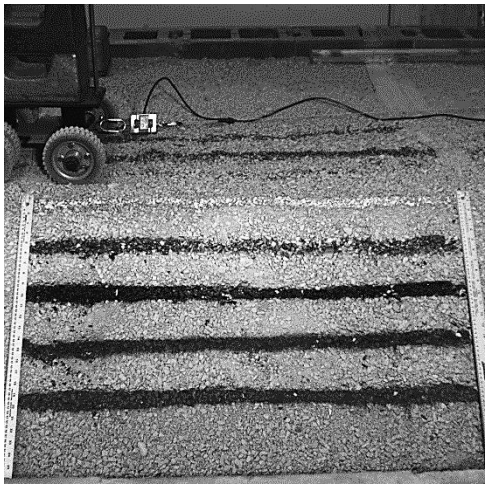

Figure 96: 20th second, test run 4

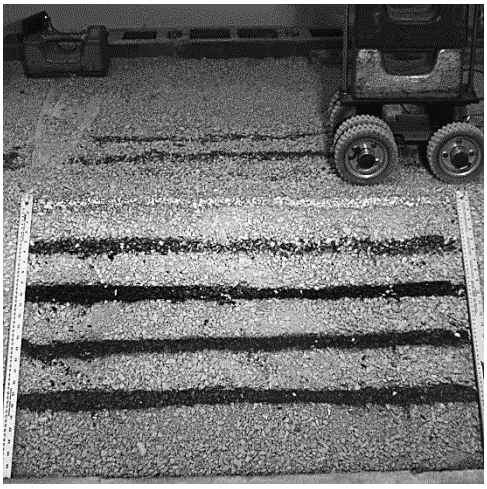

Figure 97: 65th second, test run 4

Test Run 5: In the fifth test run more broken rock rolled down slope in the first 20 seconds and at 30 seconds, the region beneath the tires on moved down slope by 1cm showing that the crushed limestone was affected by truck movement (Figure 99). This movement also caused the truck to change route and the tire further to penetrate to the ground (Figure 101 and Figure 102). This behaviour continued with the truck veering towards edge of the crest, causing the failure from the crest of the dump (Figure 103).

Figure 98: 15th second, test run 5

Figure 99: 30th second, test run 5

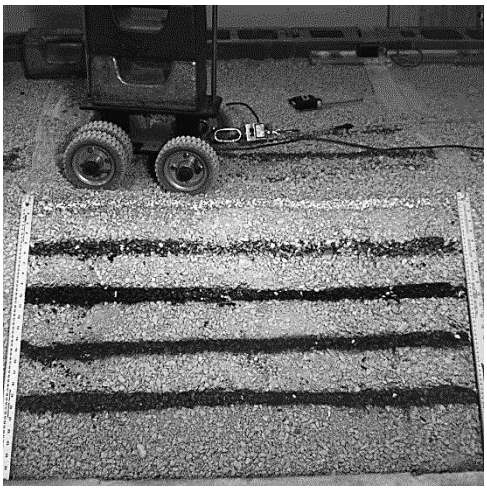

Figure 100: 35th second, test run 5

Figure 101: 40th second, test run 5

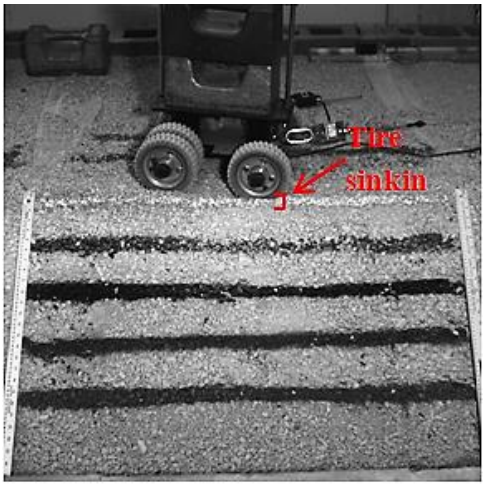

Figure 102: 45th second, test run 5

Figure 103: 50th second, test run 5

Test Run 6 to 9: In the next four test runs nothing happened. Moving the truck back and forward 20 times generate greater compaction that effectively decreased the impact of the truck weight and movement compared to the initial test performed.

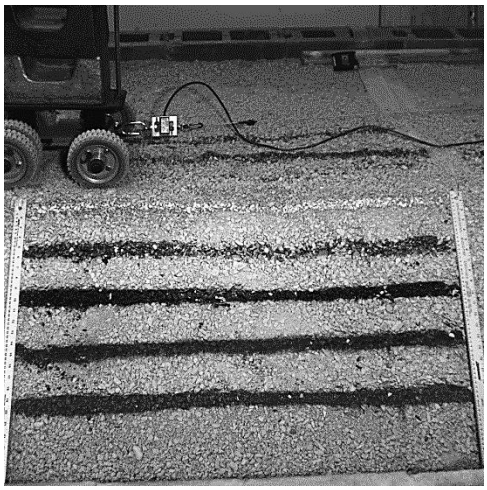

Figure 104: 15th second, test run 6

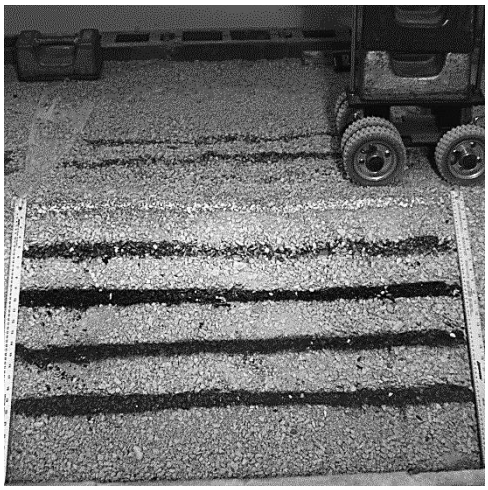

Figure 105: 65th second, test run 6

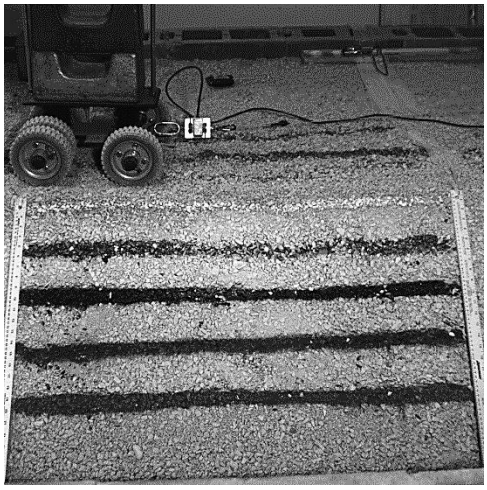

Figure 106: 15th second, test run 7

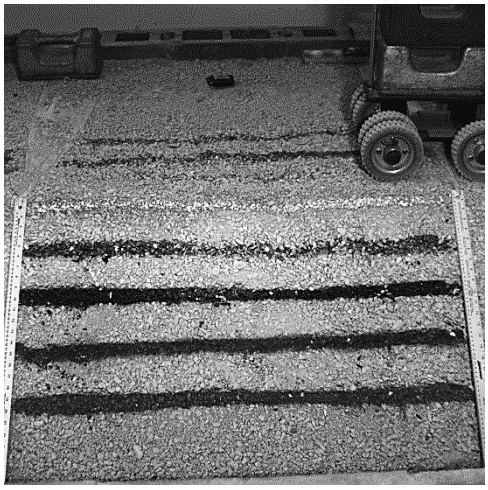

Figure 107: 65th second, test run 7

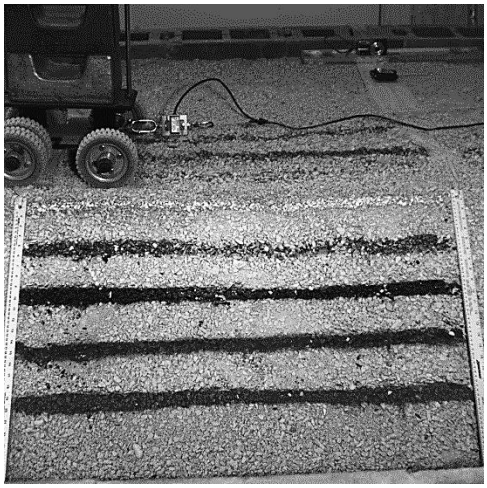

Figure 108: 15th second, test run 8

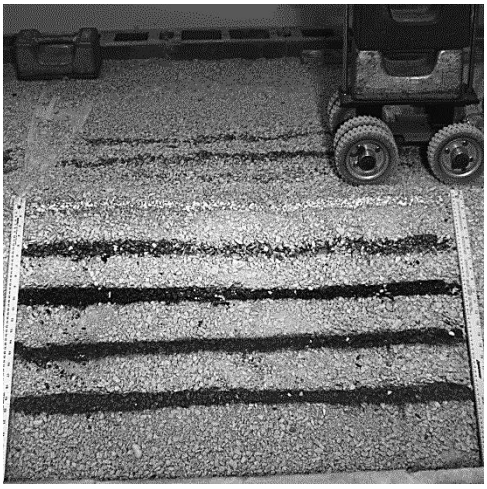

Figure 109: 60th second, test run 8

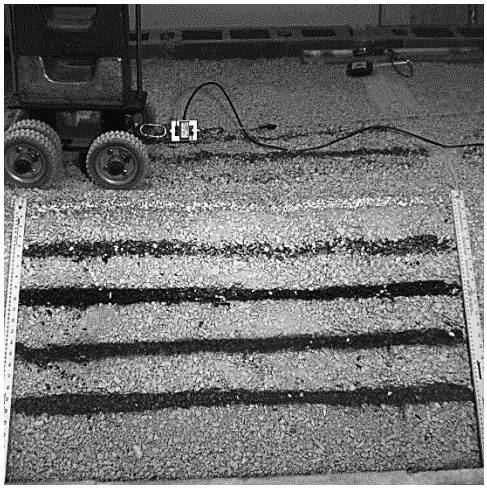

Figure 110: 15th second, test run 9

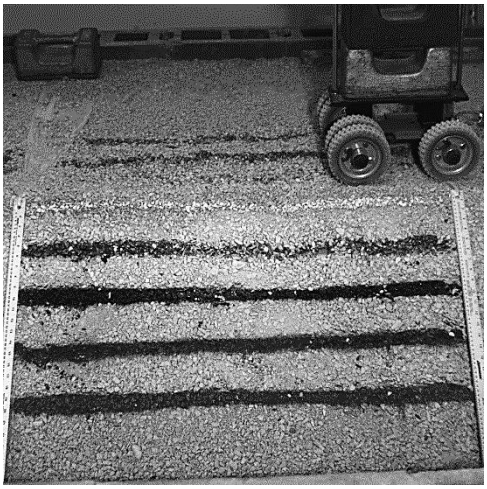

Figure 111: 60th second, test run 9

Test Run 10: Failure of broken limestone in the tenth test run commended after 25 seconds, 53.12 cm away from the first point of truck movement (Figure 114) which was measured as 1 cm down slope and continued for 34.4cm more and reached to 87.5 cm at 35 seconds (Figure 116). After the front right tire started to sink in to the ground and pushed broken limestone toward the crest, the top of the crest failed down by 5 cm down the slope (Figure 118, Figure 119).

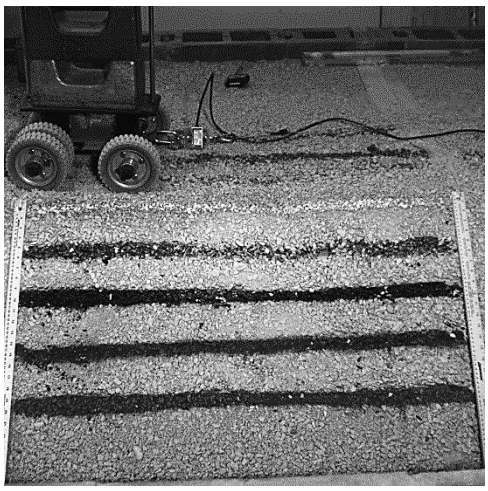

Figure 112: 15th second, test run 10

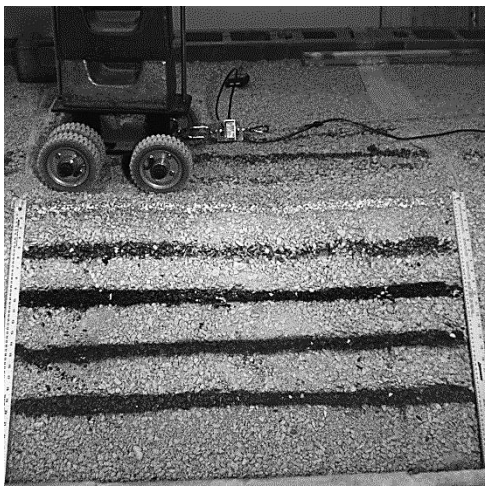

Figure 113: 20th second, test run 10

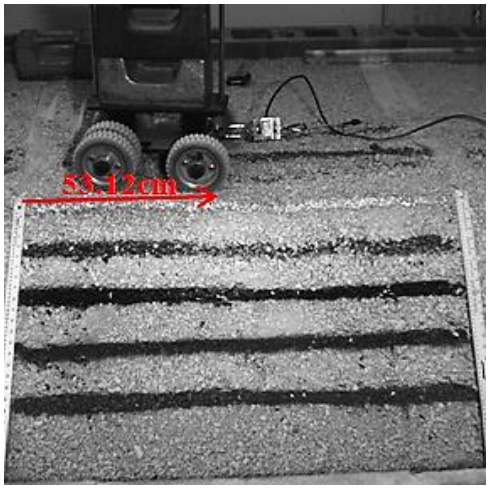

Figure 114: 25th second, test run 10

Figure 115: 30th second, test run 10

Figure 116: 35th second, test run 10

Figure 117: 40th second, test run 10

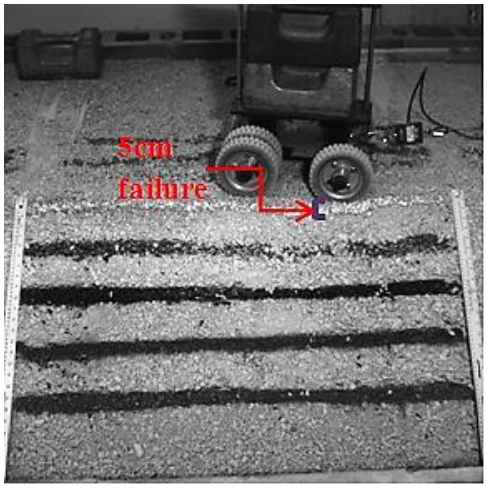

Figure 118: 45th second, test run 10

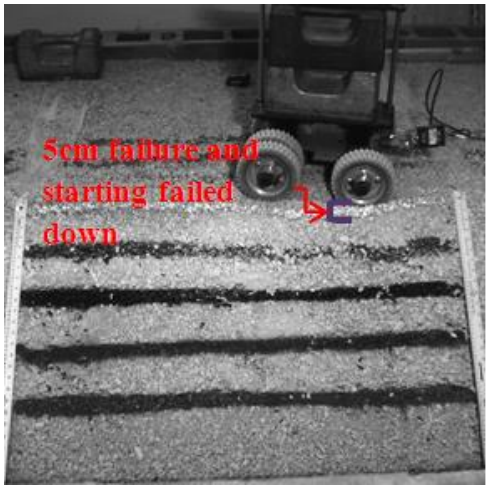

Figure 119: 50th second, test run 10

Test run 11: Failure in the eleventh test run occurred toward the end of the route; exact at the same place where the 5 cm failure in test run 10 occurred. The difference was that the failure extended for 2cm more than the first point of failure (Figure 121). In running the truck, circular arc failure and rolling of broken limestone down slope extended for 25.4 cm from the top of slope at 60 seconds (Figure 122); this behaviour was continued for the next five seconds with failure reach in 27.94 cm (Figure 123).

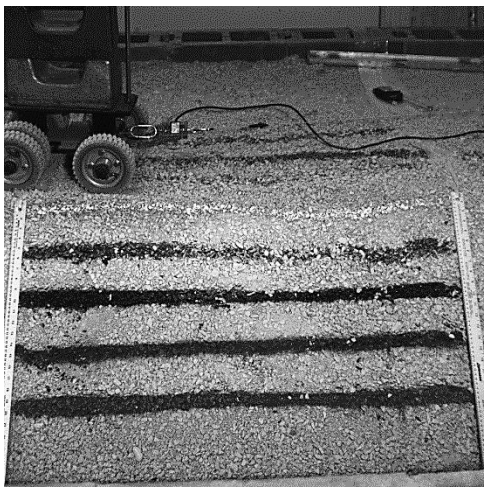

Figure 120: 20th second, test run 11

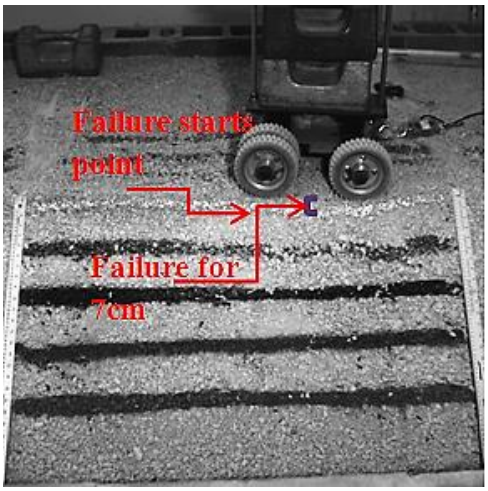

Figure 121: 55th second, test run 11

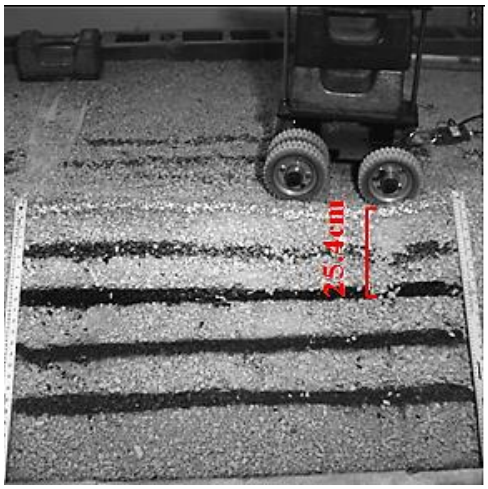

Figure 122: 60th second, test run 11

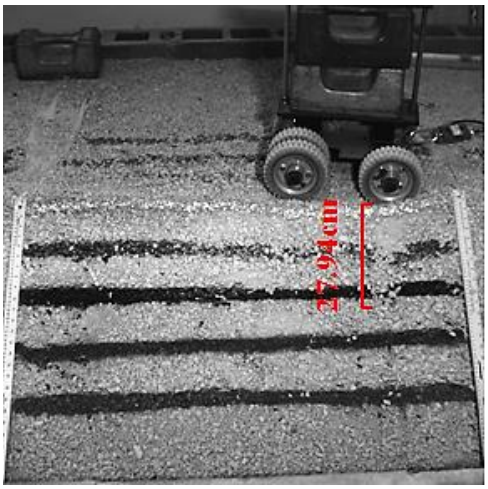

Figure 123: 65th second, test run 11

Test run 12: From start to failure in any of previous test run where nothing happened on a dump; but when the truck reached a specific zone, broken limestone moved down slope for another 1 cm in the top layer and some of crushed limestone rolled down (Figure 125). The horizontally length of the failure didn't change from 27.94 cm.

Test Run 13 to 15: In the next three test run nothing disturbed the slope, save a small quantity of rolling broken material down slope.

Figure 124: 55th second, test run 12

Figure 125: 65th second, test run 12

4-4-2-3. Post 22.6kg compaction and addition of a safety berm

This condition was the same as the test performed on the 17 cm away from the crest with a safety berm. The characteristics of the safety berm were dimensional only. Only the location of the truck was changed by 6 cm from the crest.

Photographs of the dump face were run at 0.2 Hz. By analyzes the photographs after each test run, it was recognised that truck movement has little to no effect on stability of the dump, where a berm is in place.

Figure 126: 40th second, test run 1

Figure 127: 65th second, test run 1

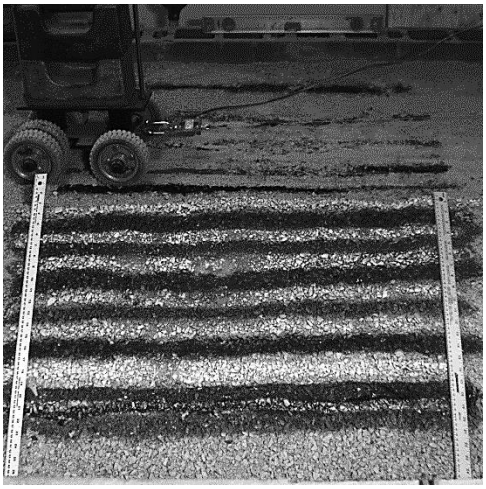

Figure 128: 20th second , test run 3

Figure 129: 65th second, test run 3

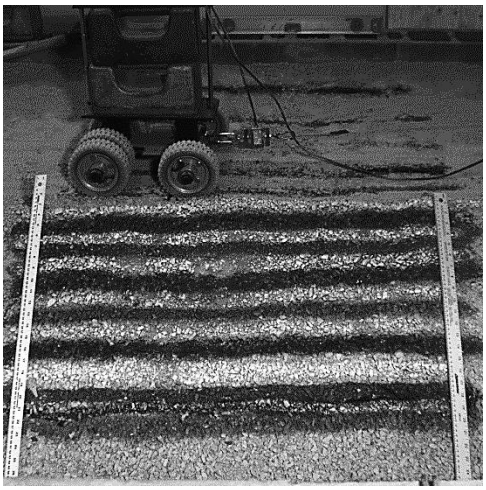

Figure 130: 20th second, test run 6

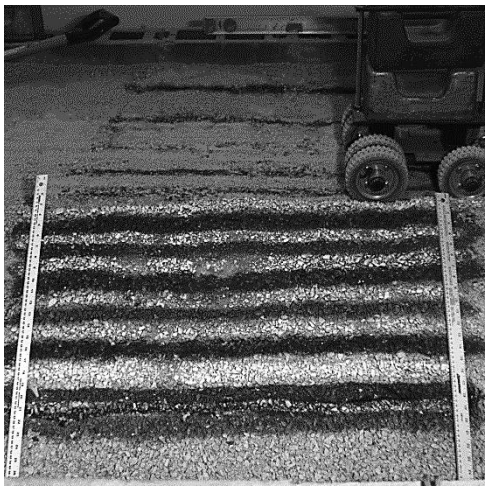

Figure 131: 55th second ,test run 6

4-4-2-4. Wet conditions

This test was performed under the same conditions described for wet conditions at 17 cm from the crest. Water was mixed with limestone at 6% by volume, and the test was command at 11 cm from the crest.

This test has been repeated for 20 test runs, where in each test run no failure or rolling crushed rock occurred down slope; shown in Figure 134 to Figure 139. Only the ground profile changed during the test runs was shown in Figure 132. The road beneath the tire deformed by 0.5 cm in the second test run and continued deforming to 2.5 cm on both sides of the truck in the 20th test run (Figure 133).

Figure 132: 0.5 cm settlement in to ground after second test run

Figure 133: 2.5cm settlement in to ground after 20 test run

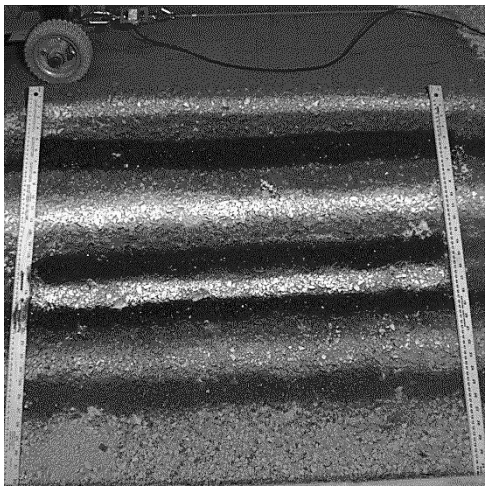

Figure 134: first second, test run 1

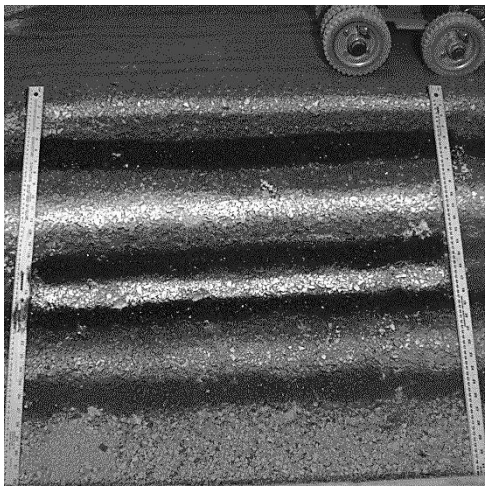

Figure 135: 65th second, test run 1

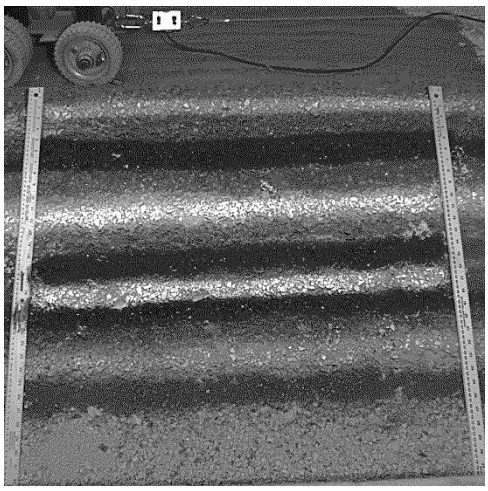

Figure 136: first second, test run 3

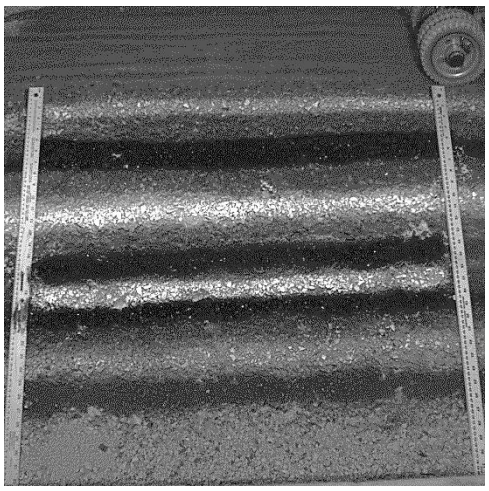

Figure 137: 65th second, test run3

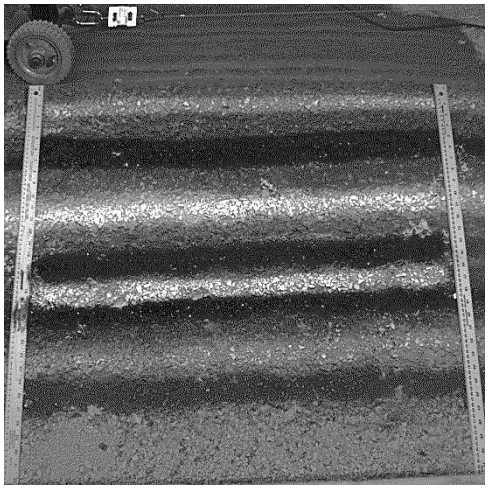

Figure 138: first second, test run 20

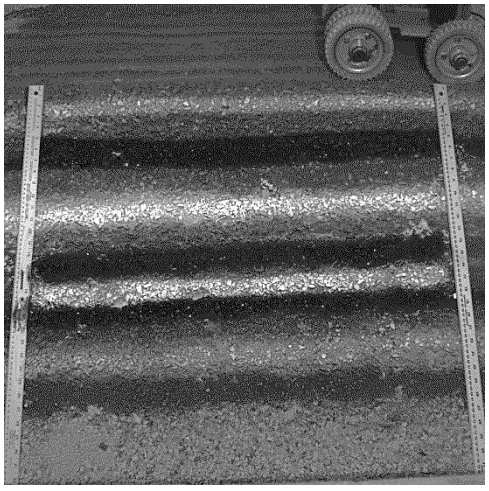

Figure 139: 65th second, test run 20

4-5. Rolling Resistance Test

During the truck movement on the dump, parameters other than waste dump stability and broken rock movement was considered such as the rolling resistance between the tire and the dump surface.

Rolling resistance is the resistance between the tire and the ground, which may be defined by recording pull force to move a truck over the surface. Recording pull

force was done via a load cell connected between the truck and a pull motor. All data was transferred to a computer, Data acquisition system from a load cell.

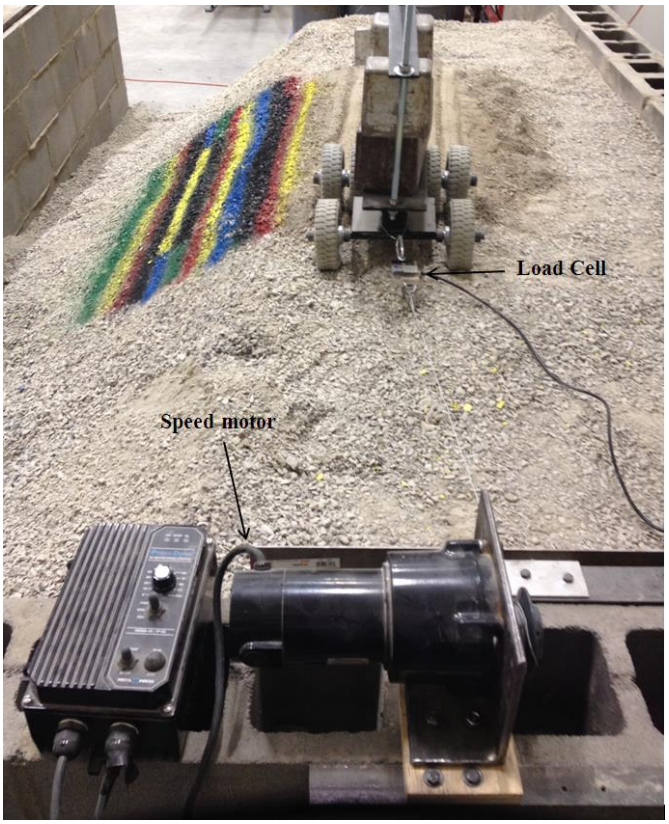

Figure 140: Picture of load cell connected to truck

By using rolling resistance relative to a calibrated 15.24 cm tire, all pull forces for different surface conditions are directly proportional to actual field rolling resistances at full scale for the actual tires and broken materials.

4-5-1. 17 cm from the crest (commensurate with 3.8 m field size)

4-5-1-1. The first lab condition tested was for truck at 17 cm (3.8 m) from the crest of the dump running on free dumped of limestone with no compaction. The test was completed in three test runs shown in Figure 141. The first test run yielded a maximum weighted mean rolling resistance, due to no compaction, but

with each successive test run the average rolling resistance dropped proportional to an increase in broken rock compaction.

Table 7: Weighted mean rolling reistance

	Run 1	Run 2	Run 3
Weighted mean Rolling Resistance	16.43%	8.37%	8.29%

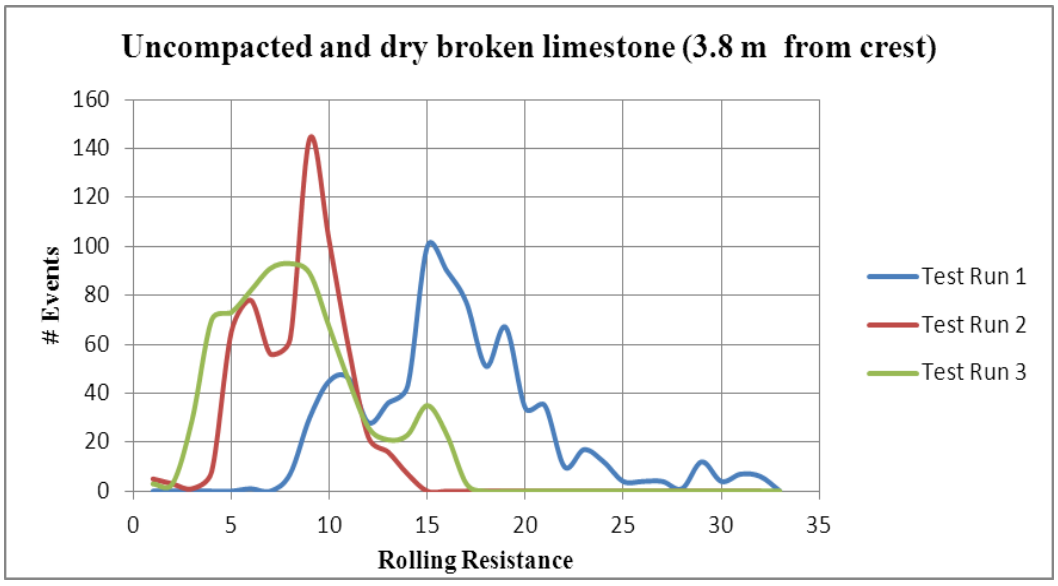

Figure 141: Rolling resistance in 17 cm (3.8 m) from crest, dry and uncompacted state

4-5-1-2. The second test condition evaluated in five test runs with the 22.6 kg compaction to be the same as the 158.58 kPa pressure applied by dozer, with a safety berm. The primary test runs had the higher rolling resistance, which with continuing tests, the rolling resistance decreased. The average of rolling resistance drop in comparison with dry and uncompacted condition.

Table 8: Weighted mean rolling resistance

	Run 1	Run 2	Run 3	Run 4	run 5
Weighted mean Rolling Resistance	5.55%	4.9%	5.2%	4.1%	4.1%

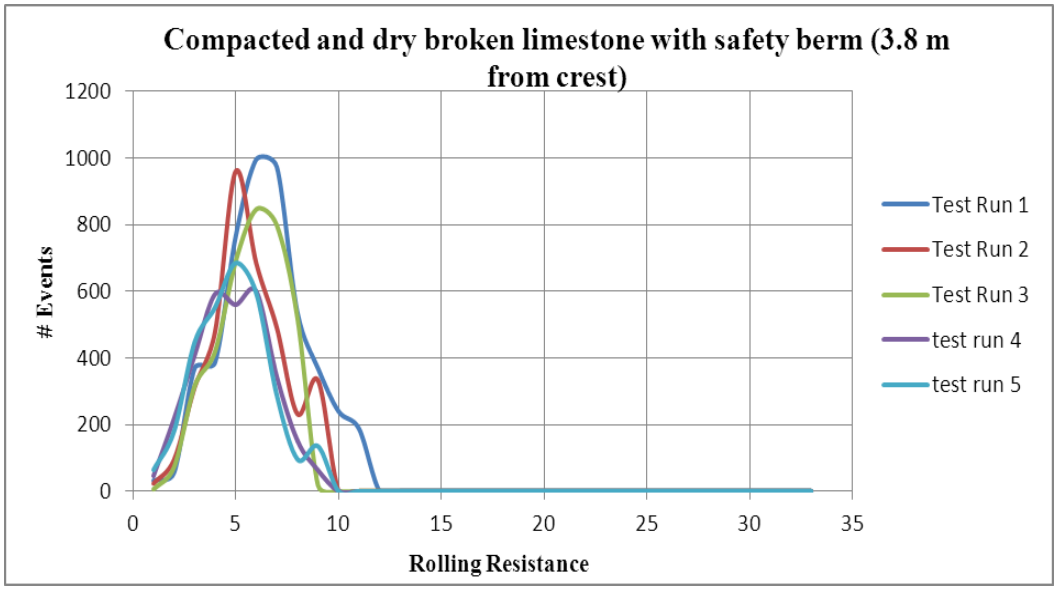

Figure 142: Rolling resistance in condition of safety berm and compaction

4-5-1-3. The last rolling resistance focus test was run at 17 cm from the crest with a wet wearing course when the broken limestone was mixed with water in 6% by volume. These tests were done in 10 test runs, but only the two first test runs and the last test run were used rolling resistance data, to represent the rolling resistance behavior. It was observed that the rolling resistance reduced from the first to last test runs commensurate with increasing compaction.

Table 9: Weighted mean rolling resistance

	Run 1	Run 2	Run 10
Weighted mean Rolling resistance	8.97%	6.39%	4.63%

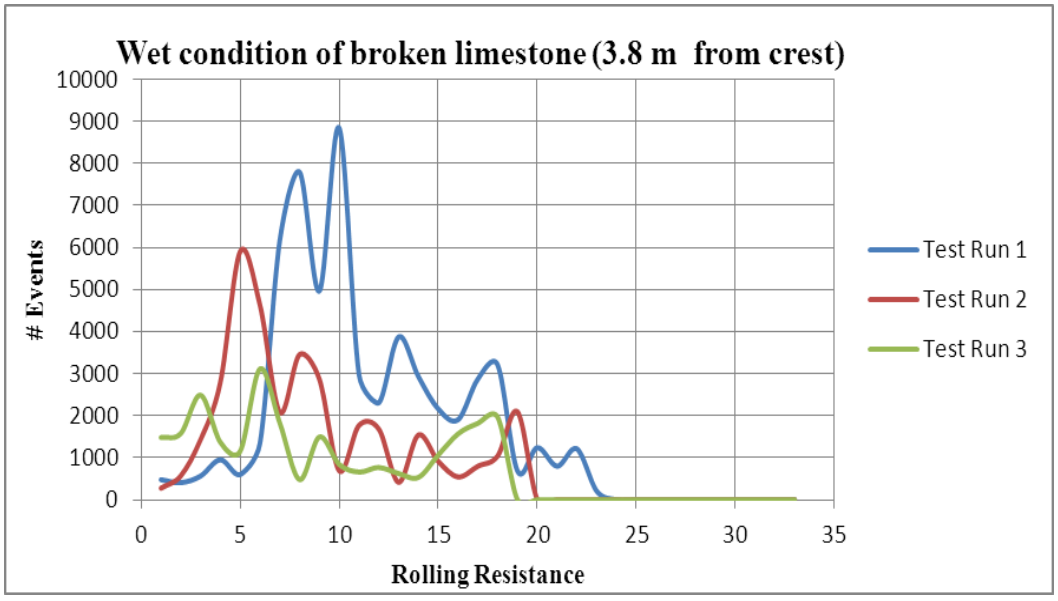

Figure 143: Rolling resistance in wet condition

4-5-2. Test on 11 cm from the crest (commensurate with 2.6 m field size)

4-5-2-1. The first tests were completed free dumped dry broken limestone with no compaction or safety berm. The first test run had the highest rolling resistance due to no compaction because no truck movement on crushed limestone had yet occurred. Also a bow wave of limestone created in front of the tires was observed increasing the effective resistance. Rolling resistance in the second test run dropped due to the limestone compaction from the previous run. In the third test run the mean rolling resistance increase in comparison with second test run, due to the changing direction of the front tires towards the crest and observed larger bow wave. The forth test run generated a circular arc failure in the slope, and the mean rolling resistance had a small decrease. In the fifth test run the rolling resistance decreased due to generate compaction in previous runs. In the sixth test runs (12 movement back and forth), from the onset truck movement, the tires penetrated the ground changing the run direction towards the

crest. In the first ten seconds of the test data of the pull forces were consistent but, after the tenth second, the truck failed down slope. During the initial ten second the rolling resistance increased with tire penetration in and pushing a bow wave of broken limestone.

Table 10: Weighted mean rolling resistance

Weighted mean Rolling resistance	Run 1	Run 2	Run3	Run 4	Run 5	Run 6
	25.19%	12.19%	17%	15.75%	12.69%	16.58%

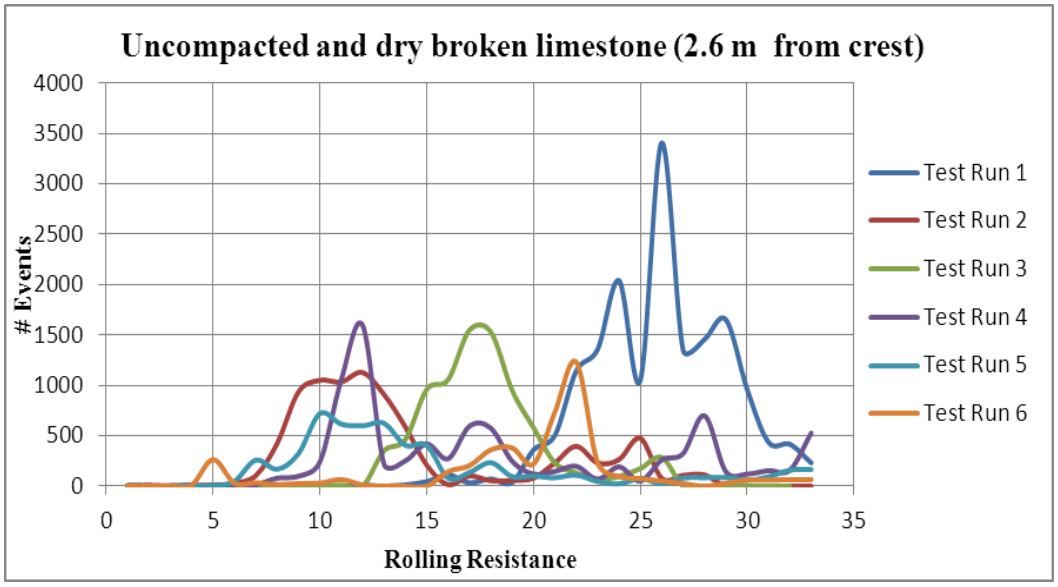

Figure 144: Rolling resistance in 11cm away, natural condition

4-5-2-2. In the second test for the truck spaced 11 cm from the crest with pre-compaction; the rolling resistance calculated for the four first test runs were approximately the same at 4.3% to 5%. There was an increase in rolling resistance in the fifth test due to tire penetration, changing direction and creating a bow wave of lime stone resisting truck movement (Figure 145, Table 11). In test runs 6

through 9, trucks ran generating rolling resistance similar to those calculated in initial runs (Table 12, Figure 146). Increasing rolling resistance in the tenth test run showed that the truck veered from the designated path where photographic evidence showed that the truck started to penetrate the ground after 40 seconds, causing dump failed. Tire-ground settlement made successive truck runs more difficult and increased rolling resistance. Mean rolling resistance decreased in tests 11 through 15 in comparison previous test run due to low compaction. However these values were higher than the initial test runs as the truck approached the failure zone, commensurate with sinking and formation of large bow wave ahead of the tires truck movement. In the two final test runs, with greater compaction and no change of direction, the rolling resistance decreased to that of the rolling resistance of the initial tests (Figure 147, Table 13).

Table 11: Weighted mean rolling resistance test run 1 through 5

	Run1	Run2	Run3	Run4	Run5
Weighted mean rolling resistance	4.8%	5%	4.3%	4.6%	8.6%

Table 12: Weighted mean rolling resistance test run 5 through 9

	Run5	Run6	Run7	Run8	Run9
Weighted mean rolling resistance	8.6%	4.3%	4%	3.77%	3.87%

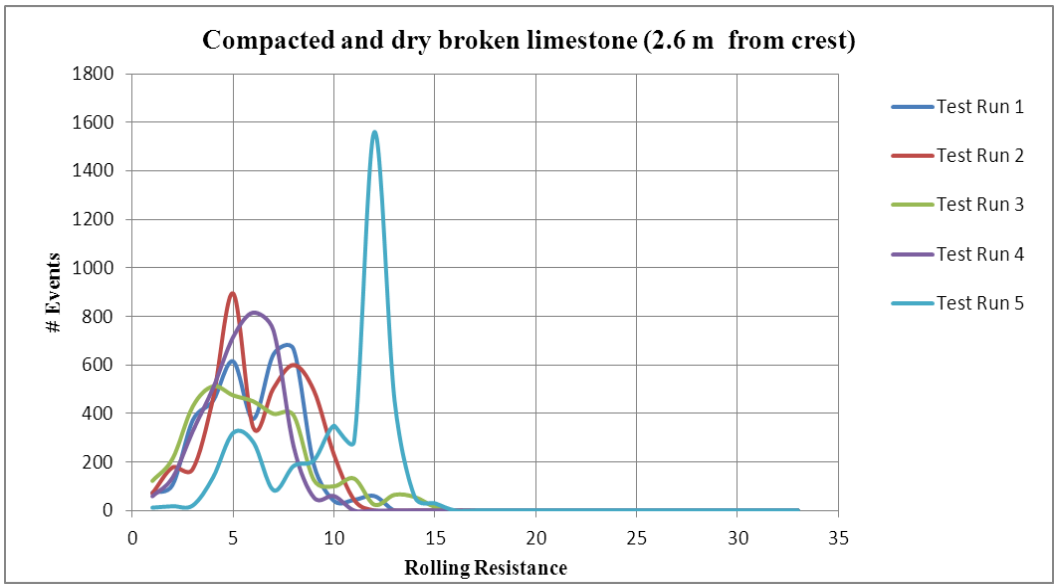

Figure 145: Rolling resistance of test run 1- 5 in 11 cm from crest and compaction

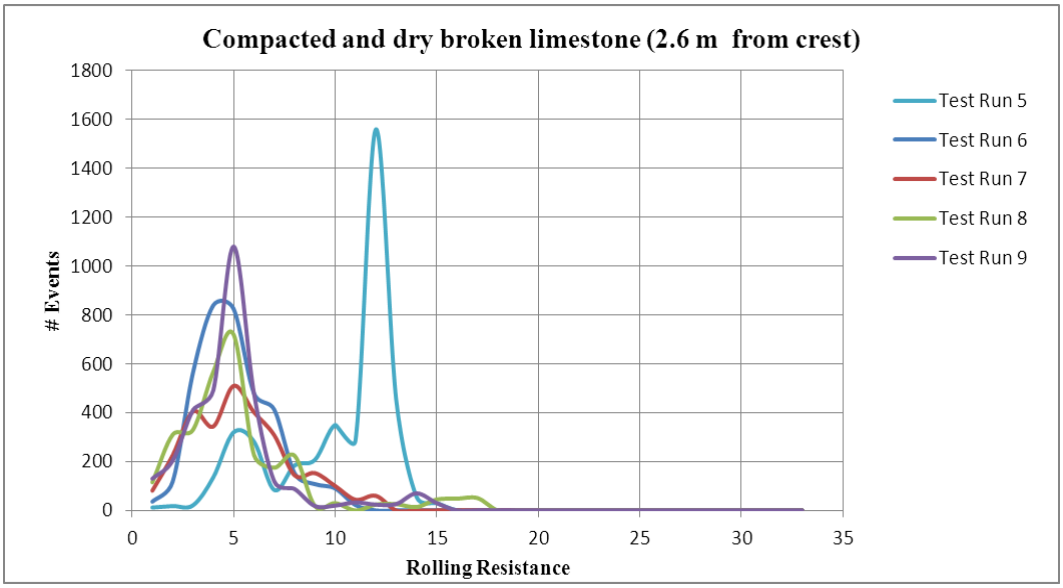

Figure 146: Rolling resistance of test run 5- 9 in 11 cm away, and compaction

Table 13: Weighted mean rolling resistance test run 9 through 15

	Run 9	Run10	Run11	Run12	Run13	Run14	Run15
Weighted mean rolling resistance	3.87%	8.2%	7%	6.7%	5.7%	4.7%	4.4%

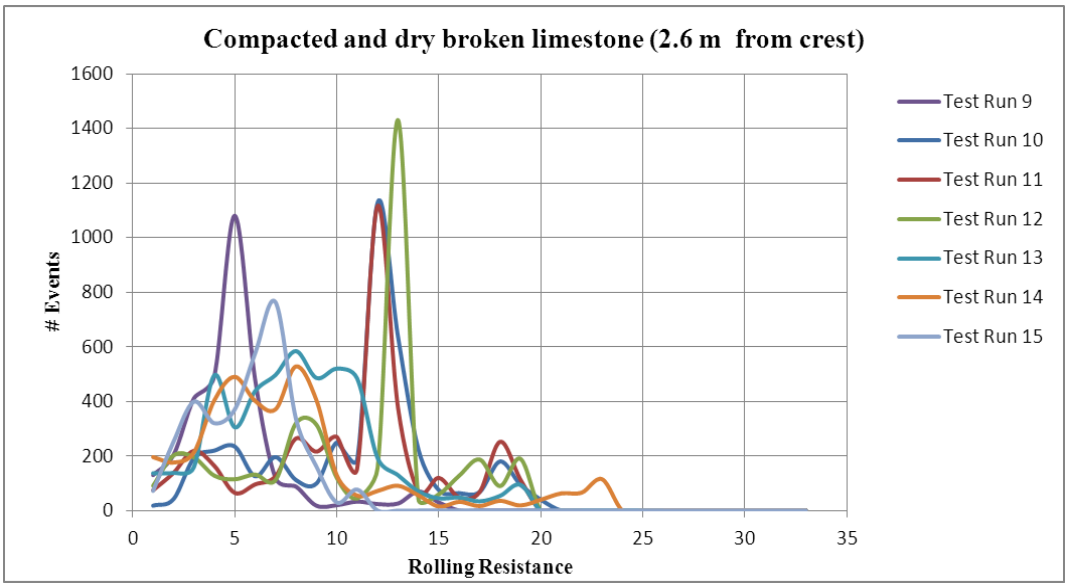

Figure 147: Rolling resistance of test run 9-15 in 11 cm away, and compaction

4-5-2-3. The third test configuration was addition of a safety berm and compaction. This condition was tested for 6 test runs where due to the degree of the compaction, the rolling resistance was lower, and since there was no slope failure perceived there was no huge variation between test runs.

Table 14: Weighted mean Rolling Resistance

	Run1	Run2	Run3	Run4	Run5	Run6
Weighted mean Rolling resistance	6.24%	4.99%	6.46%	5.41%	5.07%	5.11%

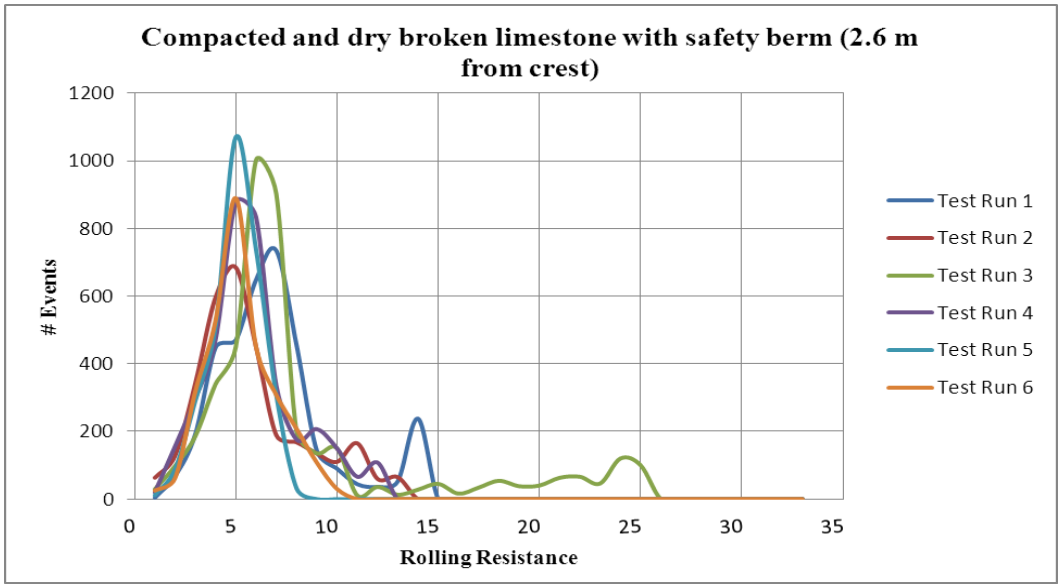

Figure 148: Rolling resistance in condition with safety berm and compaction

4-5-2-4. The final condition was tested a wet surface state (6% moisture by volume). In the first test run the rolling resistance was a little higher due to the sticky nature created by mixing broken limestone with water. After each test run, the overall rolling resistance dropped, stabilizing at 4.5% in the later test runs. The data shown in Figure 149 and Table 15 illustrated the four first test runs and the last test run.

Table 15: Weighted mean Rolling resistance

	Run 1	Run 2	Run 3	Run 4	Run20
Weighted mean Rolling Resistance	9.7%	5.9%	4.7%	4.2%	4.5%

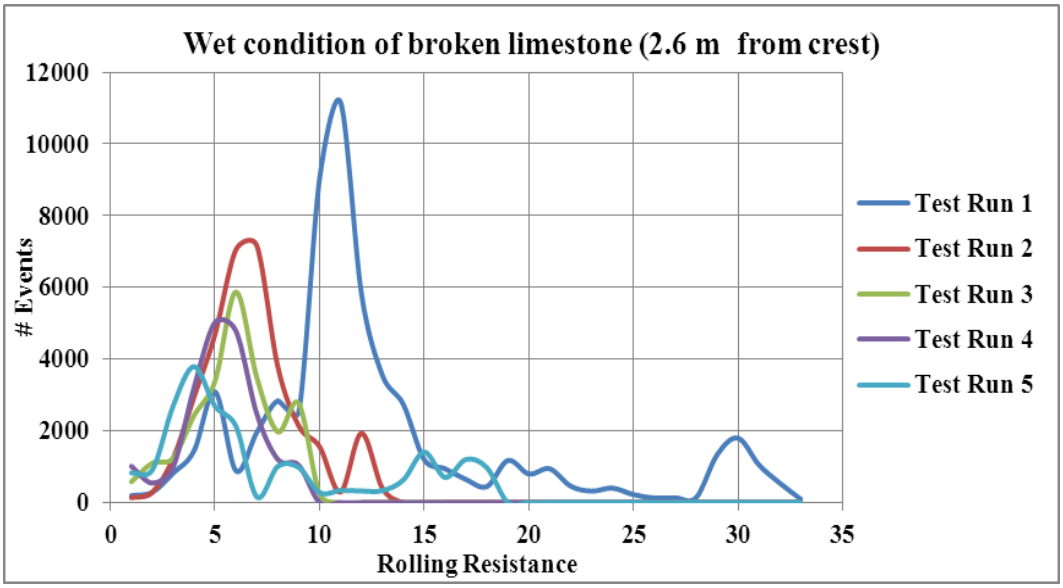

Figure 149: Rolling resistance in the wet condition

Chapter 5: Data Analysis

5-1. Analysis stability of waste dump during truck running on laboratory test

By comparing the results of tests which were done to study the stability of waste dumps during truck movement, it can be realized that there are a number of significant parameters related to truck and dump movement that can be used to improve the understanding of the failure condition and increase the stability of a dump.

These tests were done in two positions, first a half width of the truck from the crest and second at one third of truck width from the crest.

By comparing the total test experience performed in each of the truck positions, it was obvious that the truck runs at half of truck the width from the crest, didn't have any effect on dump failure, and provided a safe place for running trucks with no major concerns for truck or waste dump failure. The tests were done for different conditions; free dumped material, using a safety berm and also adding water to the mining surface. All approaches should be considered in dump design.

In some mines because of the limitation on dump space, building a large dump which can accommodate a haul road at half the width of a truck is unlikely, but the dimensions of any dump must at least span the minimum width to any crest at one third of truck width, as truck movement on a road less than this minimum to crest dimension would be impractical and dangerous for safe truck operation. The

second position tested for truck movement was set at one third of truck width from the crest.

In the first position, the truck ran on a free-dumped loses surface, which was obvious from the image record, indicated by set the onset progression of circular arc failure during truck move on the dump, with impending loss of truck.

The prime mode for stabilization of dump was the addition of compaction to the broken material surface. It was realized that, this improvement was insufficient for preventing failure in the dump and potential loss of the truck, because smaller failures progressed to layer, resulting in failure of truck and dump.

The second approach for stabilizing the dump was using a safety berm. Building of safety berms along with compaction on a dump are standard practices. Pictures taken during the test showed no circular arc failure occurred in the dump and the safety berm can reduce the effect of truck movement on a dump, at one third of the truck width from the crest.

Mixing the upper layer, surface course, with water by volume to 6%, causes the effective friction and cohesion of wet limestone to change the latter by 50% reduction, but increases the stability of the waste dump, reducing the effect of truck movement on waste dump failure. It was observed that the dump was stable during truck movement with increasing runs on the dump, and no circular failure occurred.

In conclusion, the physical modeling, shows that a half truck width from a crest is the safest position for truck movement and without need for enhanced road width

and dump dimensions. If dump construction dimensions are limited, constructing may be done at one third of truck width from the crest. This condition should be accompanied by some additional improvement such as wet condition only if material bonding is enhanced or constructing a safety berm.

5-2. Analysis of waste dump stability by limit equilibrium in a "Slide" software

5-2-1. Limit equilibrium method and Slide modeling software

The history of Limit equilibrium stability analysis via discretizing a potential sliding mass in slices goes back to the early 20th century. In 1916 Petterson (1955) analyzed the stability of a slope when circular failures are occurred in the Stigberg Quay in the Gothenberg, Sweden. This work was continued by Fellenius (1936) who established the Ordinary or Swedish Method of slices which was continued with improvements by Janbu (1954) and Bishop (1955) whose methods were widely used for over 50 years. New methods using more complicated mathematically formulas were developed by Morgenstern (1965) and Spencer (1967) paralleling the innovation of computers (Krahn, 2004).

Limit equilibrium approaches which was defined by these methods has become popular as the procedure of stability analysis that can be done faster than by hand calculation. The different between methods is based on interpretation of interslice shear and normal forces. Such slice discretization and forces are conceptually illustrated in Figure 150 (Krahn, 2004).

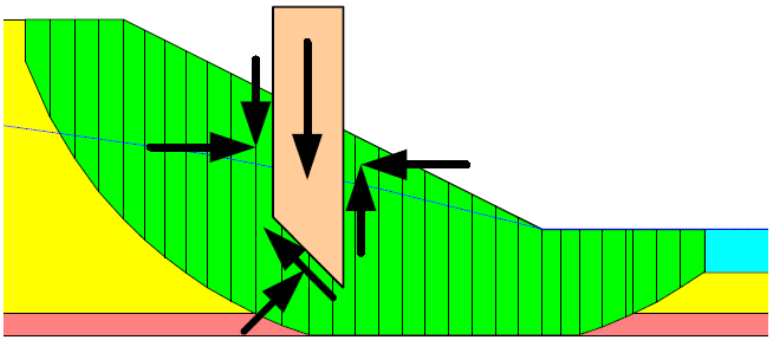

Figure 150: Slice discrezation and forces in mass sliding (Krahn, 2004)

Fellenius's, method was based on the elimination of interslice forces and is solely based on moment equilibra. Using this simplified assumption, a factor of safety can be easily calculated (Krahn, 2004).

Bishop's method (1955) presented a means of including interslice normal forces and eliminated interslice shear forces. Bishop simplified method included solely moment equilibra. The method analyzed and calculated a safety factor based on nonlinear equations (Krahn, 2004).

Janbu's method of slices is the same as Bishop's simplified but includes the interslice normal forces and ignores all interslice shear forces. The difference between these two methods is that Janbu's method just considers the horizontal force equilibria instead of the moment equilibria (Krahn, 2004).

Morgenstern (1965) and Spencer (1967) created a stability analysis using all components of interslice forces (Krahn, 2004).

Figure 151 shows a comparison of these methods for interslice normal and shear forces. The relationship between interslice forces is shown by λ, which and when equal to zero, means that there is no shear force between slices (Geoslope, 2004).

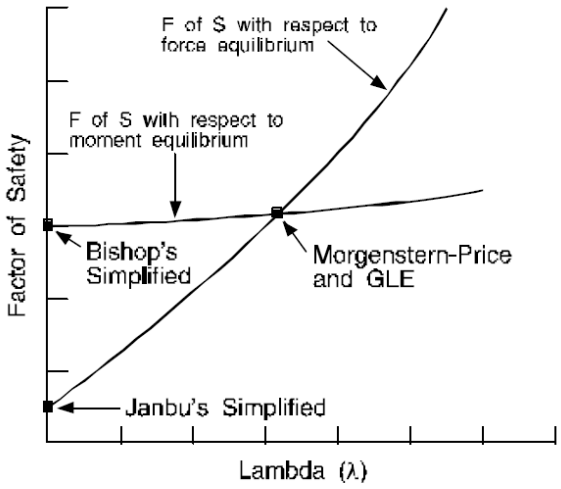

Figure 151: Factor safety- λ (Geoslope, 2004)

Based on the Figure 151 Janbu used normal forces and no shear forces with the respect to force equilibria, but Bishop included moment equilibria. Morgenestern-price and GLE (General Limit Equilibrium) use both shear and normal forces and respect to both forces and moment equilibria.

The General Limit Equilibrium is based on two factors of safety which include both interslice normal and shear forces. One equation is based on moment equilibria and the other with respect to horizontal force equilibria. This method was introduced by Spencer in 1967 (Krahn, 2004).

Based on these methods and using computers, software have been created to perform stability analyses for a variety of slip by accounting for all interslice forces, such as a "Slide", and "Slope/W". Analysing the stability of a waste dump made of broken limestone at actual field size was performed by modeling using Slide software.

“Slide” is a two dimensional slope stability analysis program that can be used to design and analyze natural slope and manmade cut, embankment and waste dump stability in mining or industrial sites. Slide calculates a safety factor, analyzing circular arc failure and non-circular failures via different limit equilibrium approaches. The program provides editing and graphical data input providing the user with tools for analyzing, studying, and viewing results (Rocscience, n.d.).

The failures made in waste dumps of broken rock such as limestone is circular are failures. Circular failure equilibria moments are independent of the interslice shear forces and are based on the horizontal normal forces. The independency of moment equilibria and shear forces is due to rotation of the sliding mass as a free body without slippage between slides. Independency of moment equilibria from interslice shear forces permits that interslice shear can be assumed to be zero when analyzing the stability of a dump. Thus, based on Bishop’s or Janbu’s simplified methods consideration are thus satisfied via overall horizontal force equilibrium, not moment equilibrium. Figure 152 shows an example of the free body and forces polygons of Janbu’s simplified (Krahn, 2004).

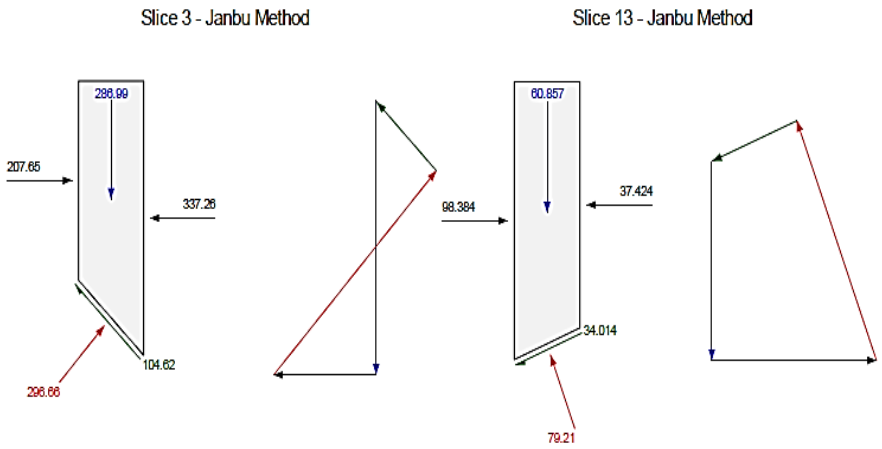

Figure 152: Free body of Slice and force polygon base on the Janbu way (Krahn, 2004)

Simulations were done mimicking both the conditions of the laboratory tests performed and for actual truck and dump relationship in the field, permitting comparing the results between physical and numerical modeling. The "Slide" program results show that a minimum safety factor for slope surface may be found and compared to stability of actual dumps for various loading and geometric conditions.

A safety factor is the parameter that defines a ratio of strength or resisting force to stress or disturbing force. A minimum safety factor that creates safe states must be >1. In road, bridge, and tunnel construction, the safety factor often selected is >1, and close to 2, as these are conservative public structures. A safety factor selected and assumed for mine waste dump is often set at 1.2, as all construction is mine has a finite life.

All minimum safety factors calculated from the "Slide" program will be compared with safety factors assumed for the waste mine dumps at 1.2.

To build a model in the “Slide” modeling software, dump dimensions and materials characteristics used dump design are necessary.

The parameters needed for material properties are density, friction angle and cohesion. The direct shear test was performed to determine the friction and cohesion of the broken, compacted broken and wet material states.

5-2-2. Direst Shear Test (ASTM D5321) (ASTMD5321, 2014)

The direct shear test was performed to determine the shear strength of the limestone model dump in various states. Shear strength is an important engineering property of soil and broken materials which are defined from two parameters; cohesion and friction angle. The direct shear tests are of the oldest strength tests for soil and broken materials. The direst shear box is used to discern shear strength of broken materials. From a plot of shear stress versus horizontal displacement the maximum shear strength for different normal loads can be determined. A plot of maximum shear stresses versus vertical normal stresses can be then determined generating a Mohr-Coulomb failure curve whereby the friction angle and cohesion of the materials can be determined (Sivakugan, Das, & Shukla, 2013).

Equation 16

$$\tau = c + \sigma \, tan\emptyset$$

Where:

τ : shear strength

c: cohesion(Si)

σ: normal stress $\emptyset$: is friction angle

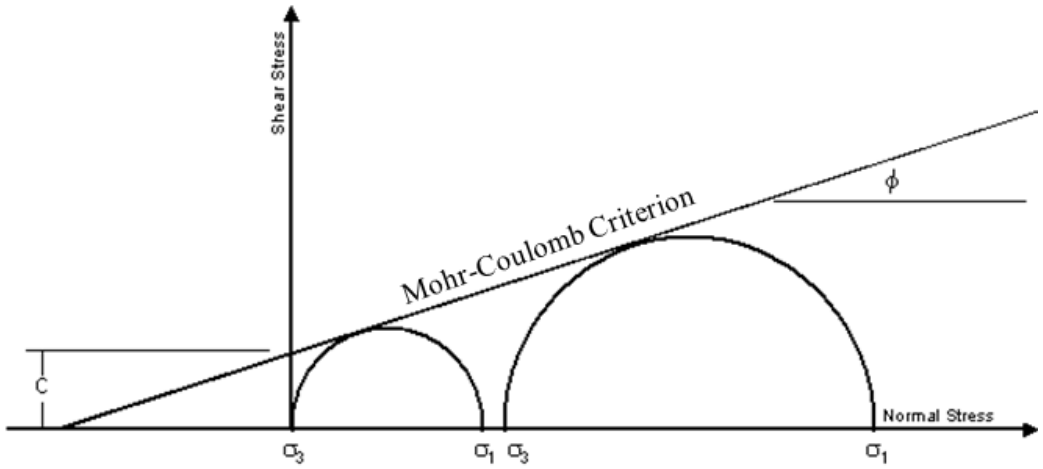

Figure 153: Mohr-Coulomb Failure criterion (Goodman 1980)

The direct shear test is an inexpensive and simple mode to measure strength of a soil in cohesive or non-cohesive state. A shear box test consists of a metal box in-to which broken material is placed, the box which is split in-to two halves. Shear forces are applied to one half of the box to move the box and create failure in the broken material, while normal forces are applied vertically through the metal plate. The schematic sketch of the shear box test is shown on Figure 154.

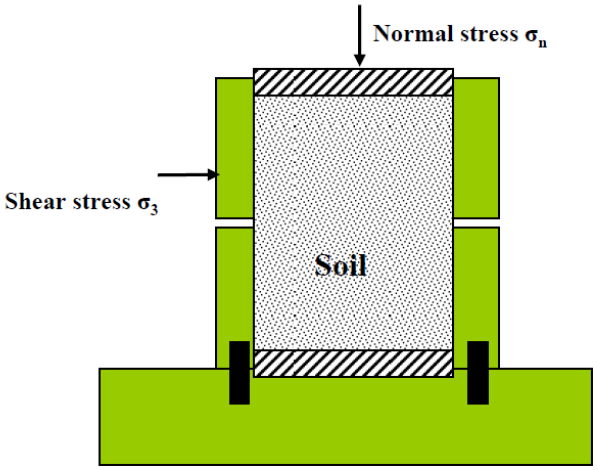

Figure 154: Schema of shear box test

A test commences by filling the metal box with the broken limestone and positioned in the shear machine. A normal load was applied, and shear forces then moved the upper box relative to the lower. All shear forces data, normal stress, held constant during the test and horizontal and vertical displacements were recorded via a data acquisition system. The test was performed for dry, dry compacted and wet limestone states. The shear stress versus horizontal displacement results for these three states for each normal stress applied are given in Figure 155, Figure 156, Figure 157. By increasing the shear force the interlocking friction angle between the broken particles increased until reaching a maximum value. Beyond this maximum stress, the friction angle was overcome creating a drop in shear stress.

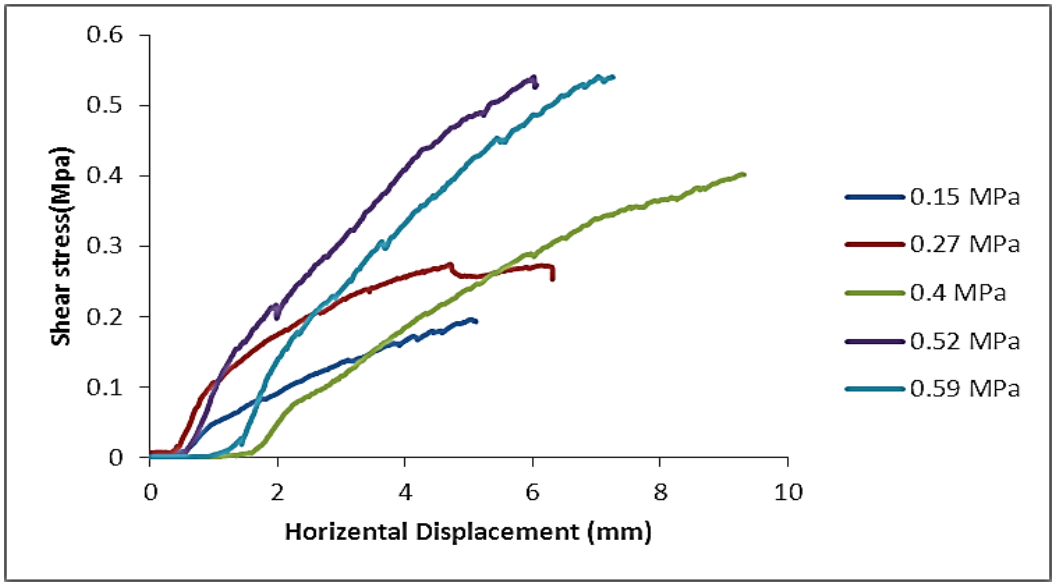

Figure 155: Shear stress vs. horizontal displacement for dry and uncompacted broken limestone state

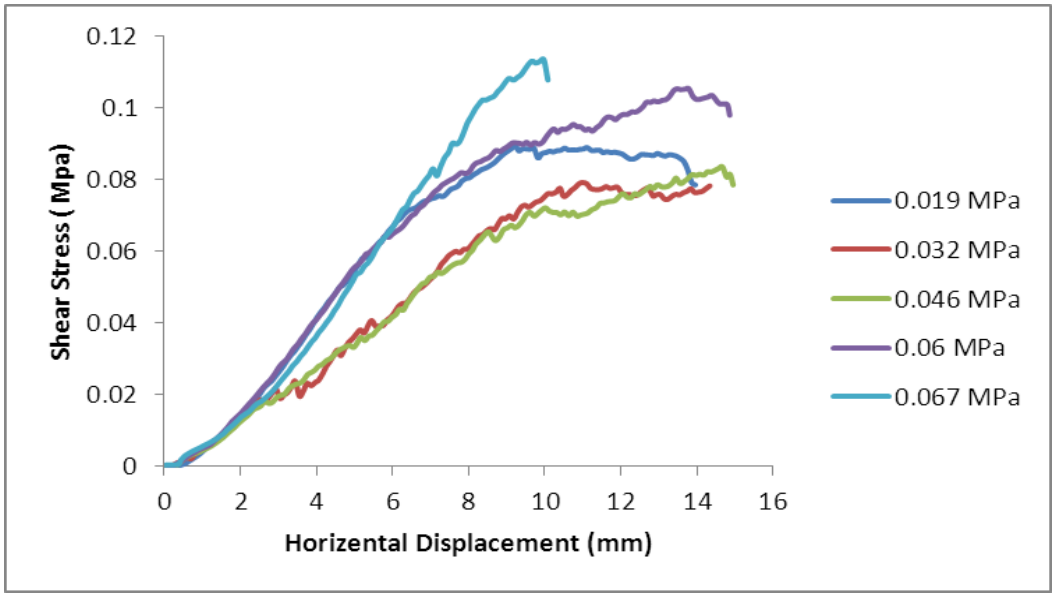

Figure 156: Shear stress vs. horizontal displacement for dry, compacted broken limestone state

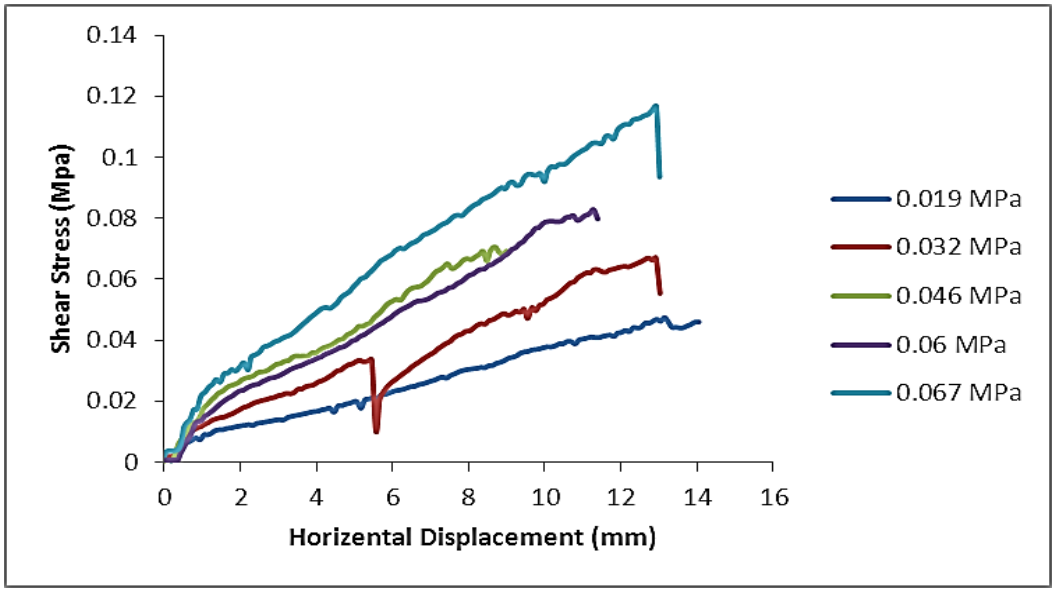

Figure 157: Shear stress vs. horizontal displacement for wet broken limestone state

Based on Figure 155, Figure 156, Figure 157 the maximum shear stress by normal stress was used to create Figure 158, Figure 159, Figure 160 creating the Mohr-Coulomb criteria, defining the friction angle and cohesion. The friction angle of

materials in each state is equal to the slope of the line of normal stress vs. shear stress. The results are shown in Table 16.

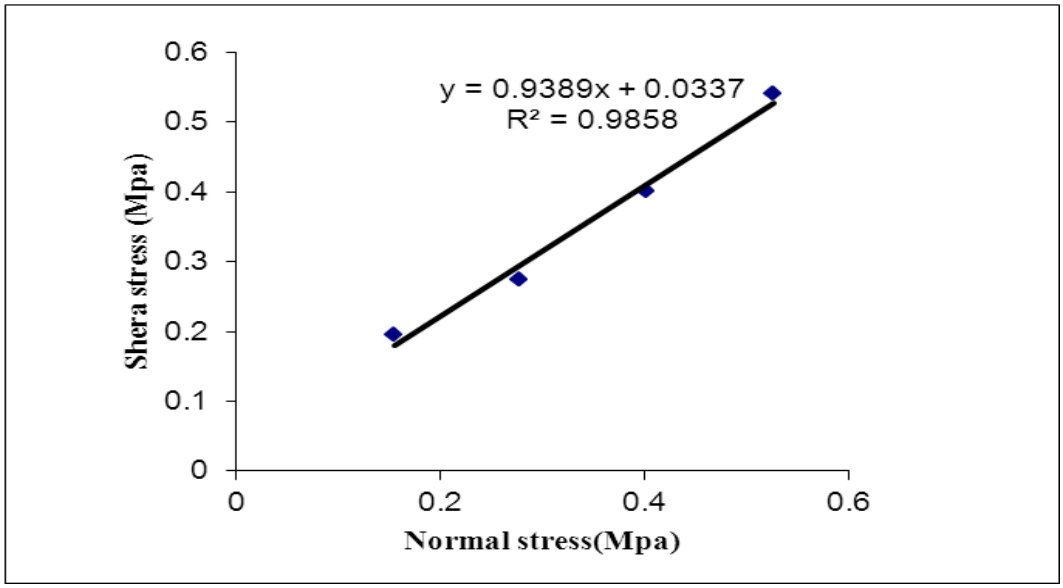

Figure 158: Normal Stress vs. Shear stress in dry and uncompacted state

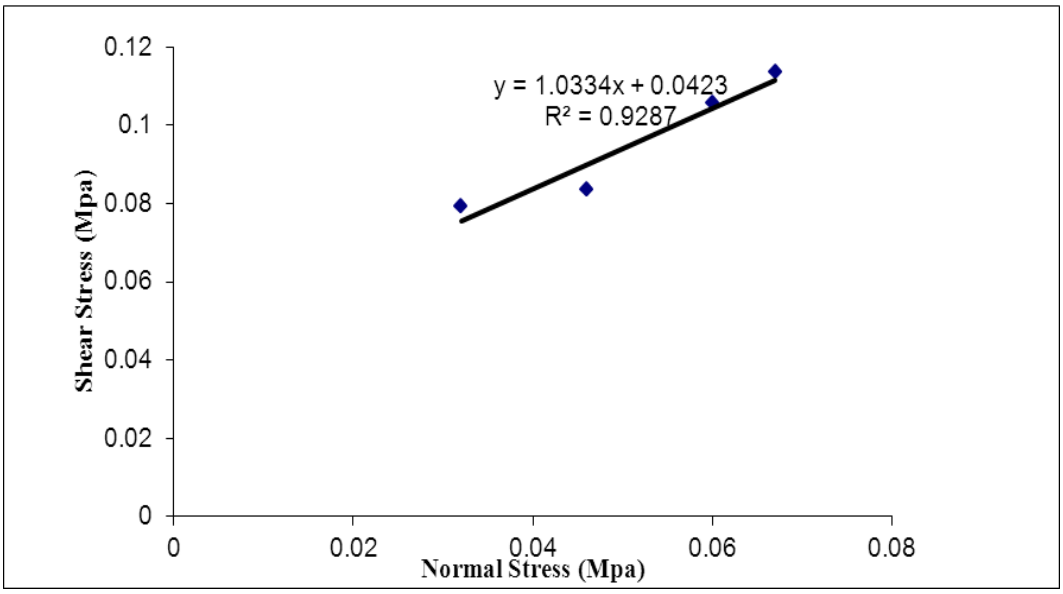

Figure 159: Normal Stress vs. Shear stress in dry and compacted state

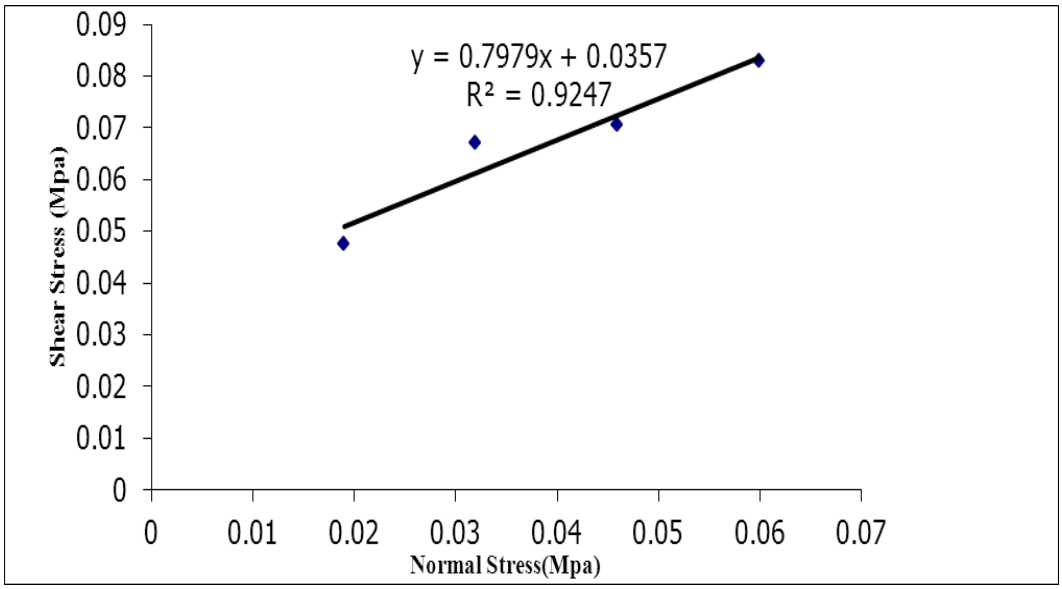

Figure 160: Normal Stress vs. Shear stress in wet state

Table 16: Comparison of different friction angle in various broken limestone condition

Broken limestone States	Correlation Coefficient (R^2)	Friction Angle (Degree)	Cohesion(kPa)
Dry & uncompacted	0.99	43.2	33.7
Dry & Compacted	0.93	45.9	42.4
Wet	0.93	38.5	35.7

The density of the each state was tested and calculated reflected in Table 17.

Table 17: Unite weight of broken limestone in various conditions

Broken limestone States	Unite weight (kN/m^3)
Dry & Uncompacted	15.24
Dry & Compacted	17.32
Wet	14.91

5-2-3. Result of a “Slide” modeling

Knowing the strength properties of limestone by state and given the geometry of the dump, a dump model can be built in “Slide”. By considering the truck-ground loading in two dimensions, it can be seen that the rear tires or front tires move from one specific location to another with time so, specific maximum forces that are modeled in Slide are associated with the forces applied by rear tires. A hauler truck has 6 tires, two in front and four at the back with a load distribution of 33% to front and 67% to rear, where each tire on the truck bears the one sixth of the total truck (GVW), weight during loaded activity. Here modeling forces on the dump surface was based on the rear tires which have the higher load although distributed over two tires each on the right and left hand side of the truck.

5-2-3-1.Dry and uncompacted state of broken limestone

The uncompacted dry condition was modeled for an actual truck size in two positions related to the crest for the truck movement on a dump; half and one third truck width away from the crest. The dump was modeled with the limestone material at a friction angle of 43.2º, 33.7 kPa cohesion and unites weight of 15.24 kN/m. Slide generated the minimum safety factor for slope and circular arc failure for both truck positions, which are illustrated in Figure 161 and Figure 162.

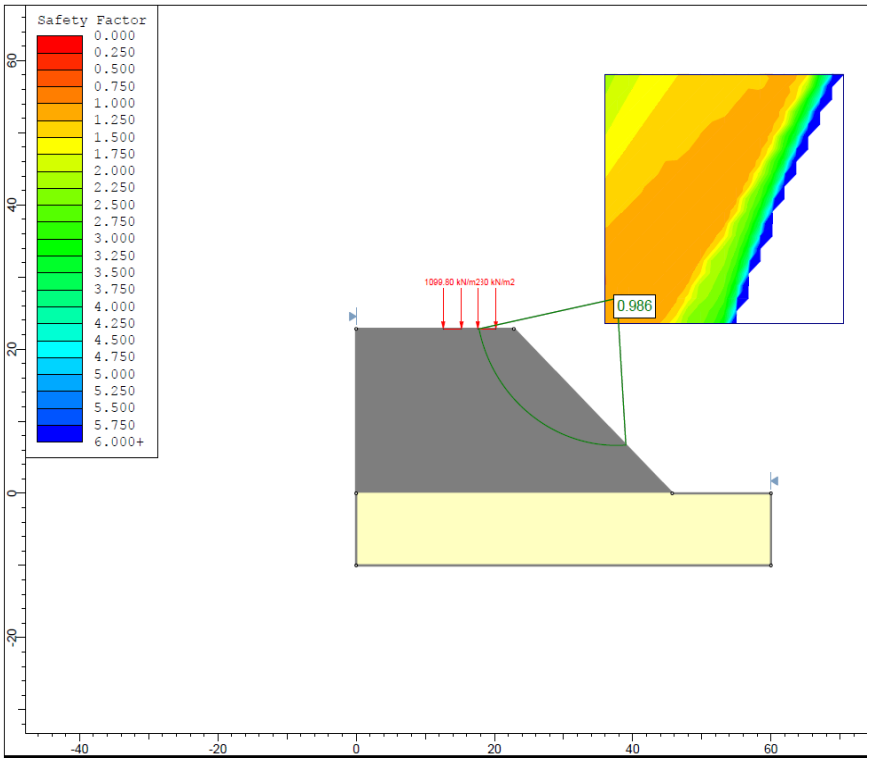

Figure 161: Minimum safety factor for uncompacted dry broken limeston in 1/3 truck width from crest

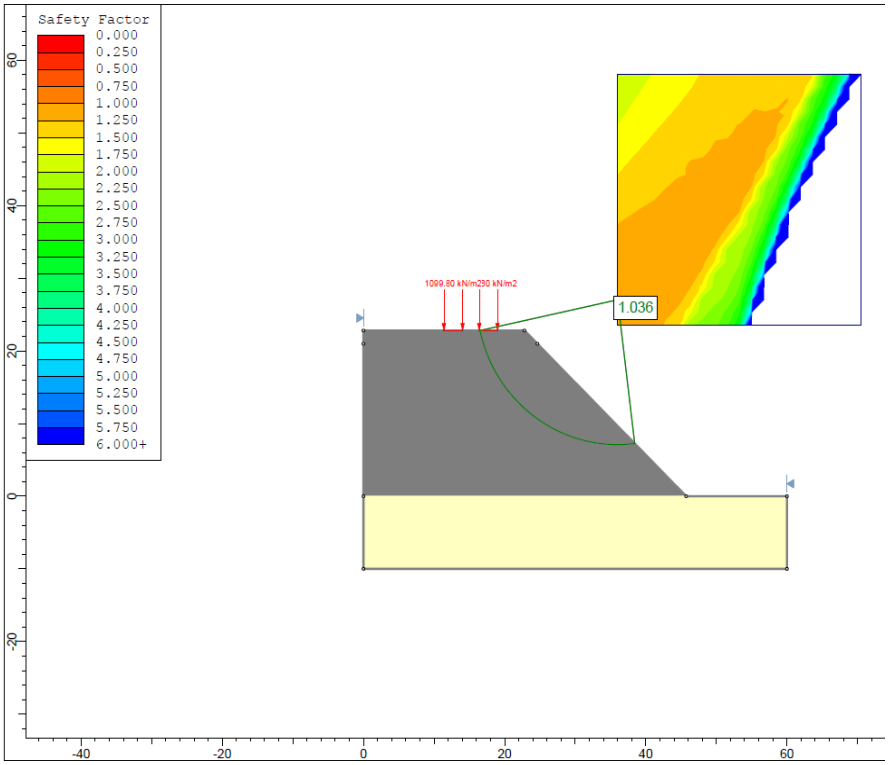

Figure 162: Minimum safety factor for uncompacted dry broken limestone in 1/2 truck width from crest

Comparing the safety factor at one third truck width from the crest at 0.99 to a base safety factor (1.2), showed an extensive failure matching the scale lab tests in that position.

The truck position set at half truck width from the crest generated a minimum safety factor of 1.04, compared to the base minimum safety factor at 1.2 with a small failure; suggested a decreased risk of failure. This result did not completely match the laboratory scale tests, which showed no failure. It is evident that there is no major difference between numerical and physical modeling as the safety factor in both cases was greater than 1, but to ensure the dump stability other qualitative evaluations may be prudent.

5-2-3-2. Compacted Broken limestone

With compaction, the dump was modeled similarly but with a unit weight of 17.31 kN/m, friction angle 45.9 and cohesion 42.4 kPa. The analysis for two truck positions, with two minimum safety factors, yielded minor failures.

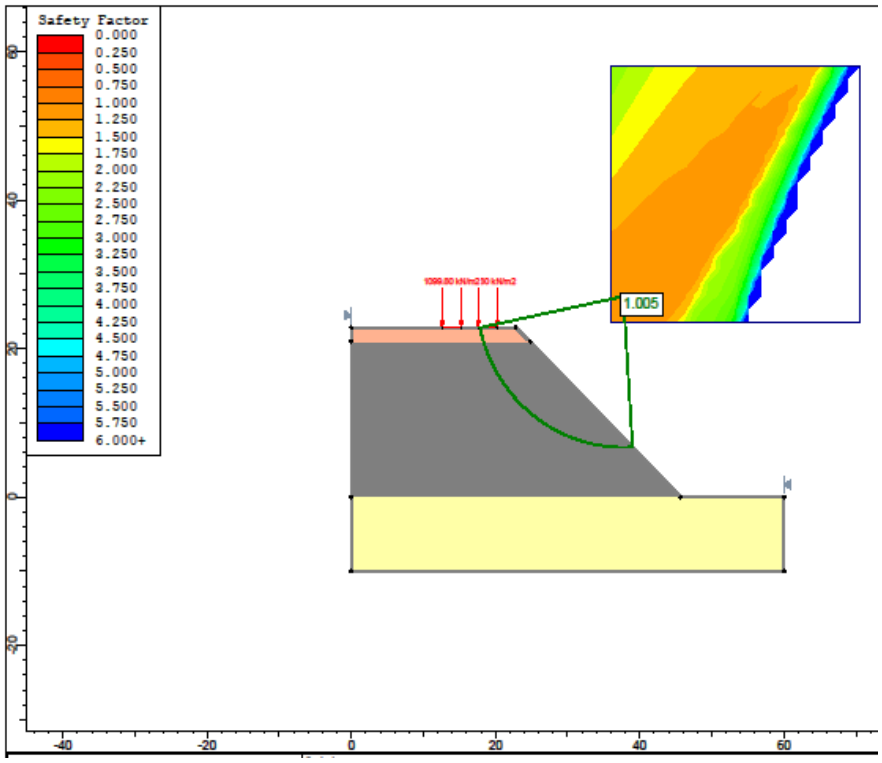

Figure 163: Minimum safety factor in compacted condition of broken limestone in 1/3 truck width from crest

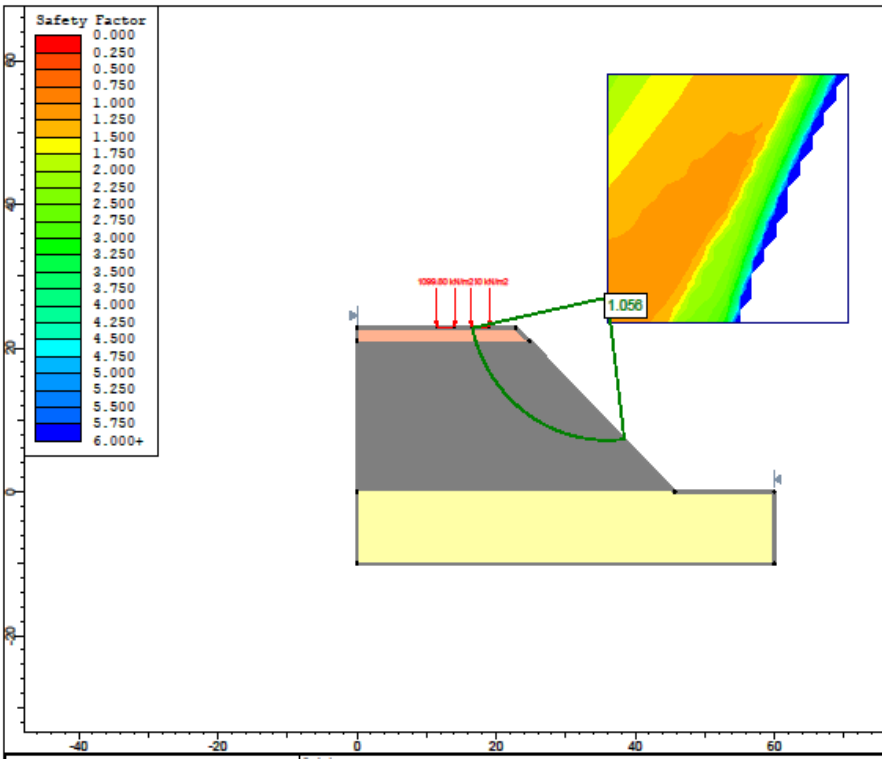

Figure 164: Minimum safety factor in compacted condition of broken limestone in 1/2 truck width from crest

The closet to the crest position, shown in Figure 163, a minimum safety factor was 1, with a failure relative to the safety factor of 1.2.

In the more distance position relative to the crest, at half truck width a minimum safety factor of 1.1 reflected a very small failure.

5-2-3-3. Compacted broken limestone with a safety berm added

This state yielded a high safety factor and safe state for both truck positions relative to the crest.

A minimum safety factor in the first position (Figure 165) was determined at 1.3, which suggested a safe set up matched to the results of the laboratory tests.

The second truck position (Figure 166) shows 1.3 as the minimum safety factor, suggesting a safe and greater stable condition for a truck and dump.

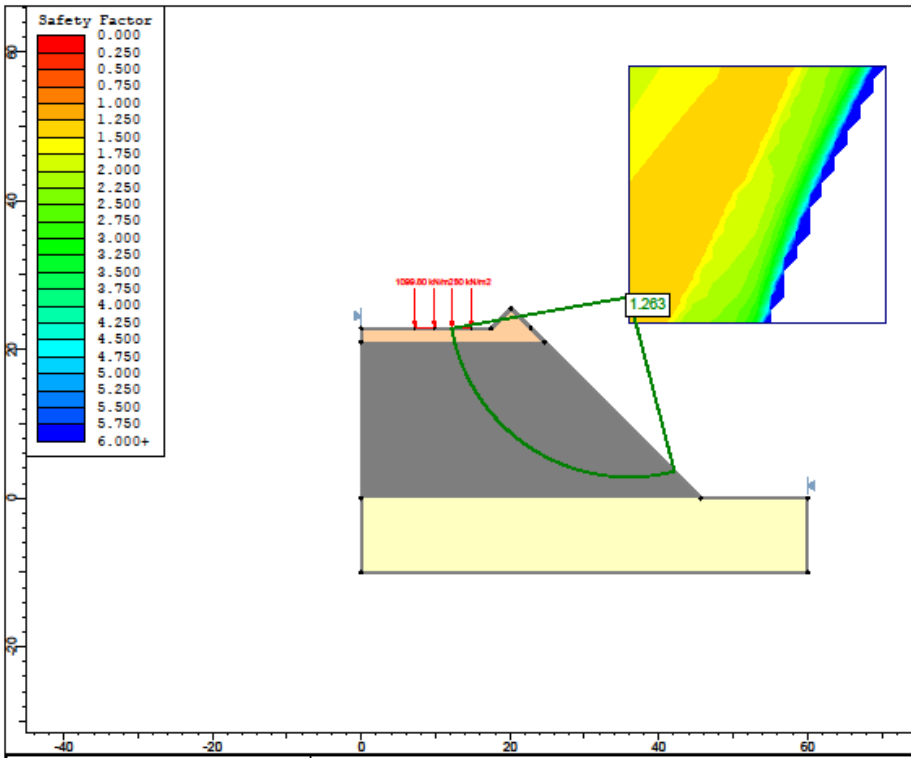

Figure 165: Minimum safety factor in compacted broken limestone and a safety berm in 1/3 truck width from crest

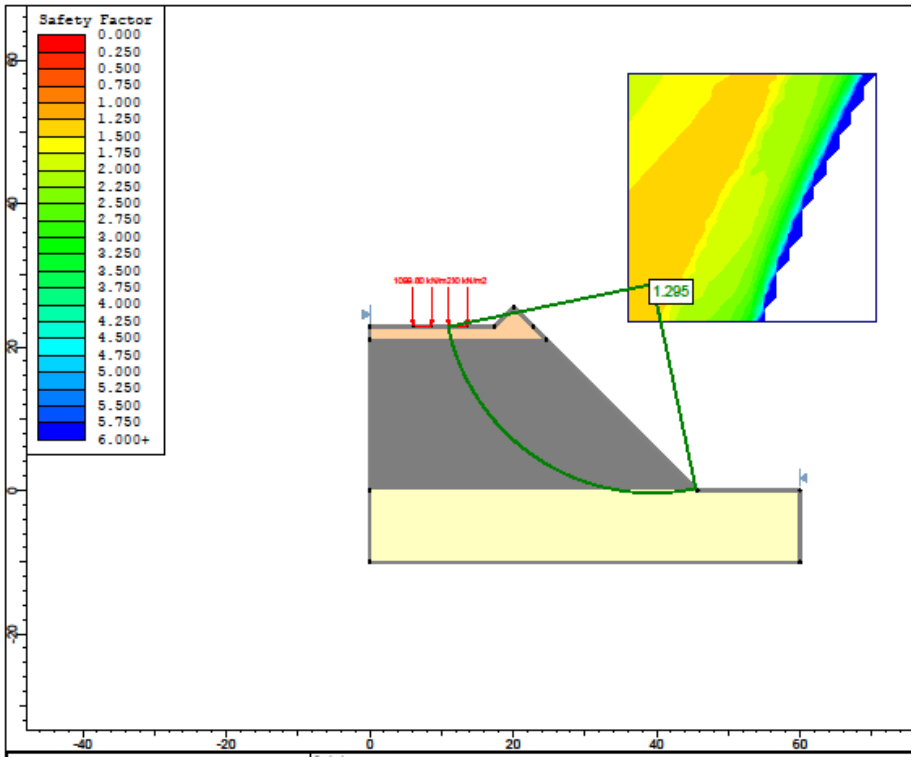

Figure 166: Minimum safety factor in compacted broken limestone and a safety berm in 1/2 truck width from crest

5-2-3-4. Wet condition of broken limestone

The first state recorded with mixing a specific depth of limestone on surface of the dump with water, where the mixture of water and broken limestone yielded a third set of material characteristics. The model in slide was built with adding a layer of wet limestone on top of the surface layer previously compacted with equipment runs. The wet layer was created with the unite weight of 14.19 kN/m, friction angle 38.5º, and cohesion 35.7 kPa.

A minimum safety factor was extracted from models in first truck position (1/3 of truck width from crest) at 0.99. A failure with respect to geotechnical safety factor (1.2), where lab tests showed no failure.

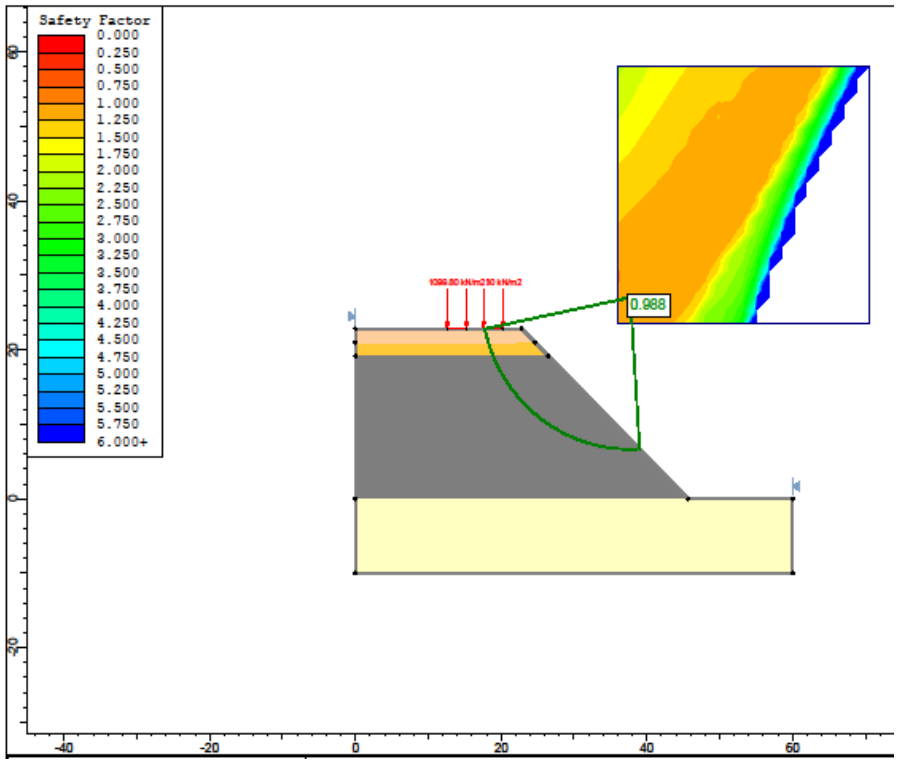

Figure 167: Minimum safety factor in wet condition of broken limestone in 1/3 truck width from crest

The Second truck position shows 1.04 as the minimum safety factor, with a small failure. An approximation of safety factor to the geotechnical safety factor (1.2) showed that the dump is stable in this state.

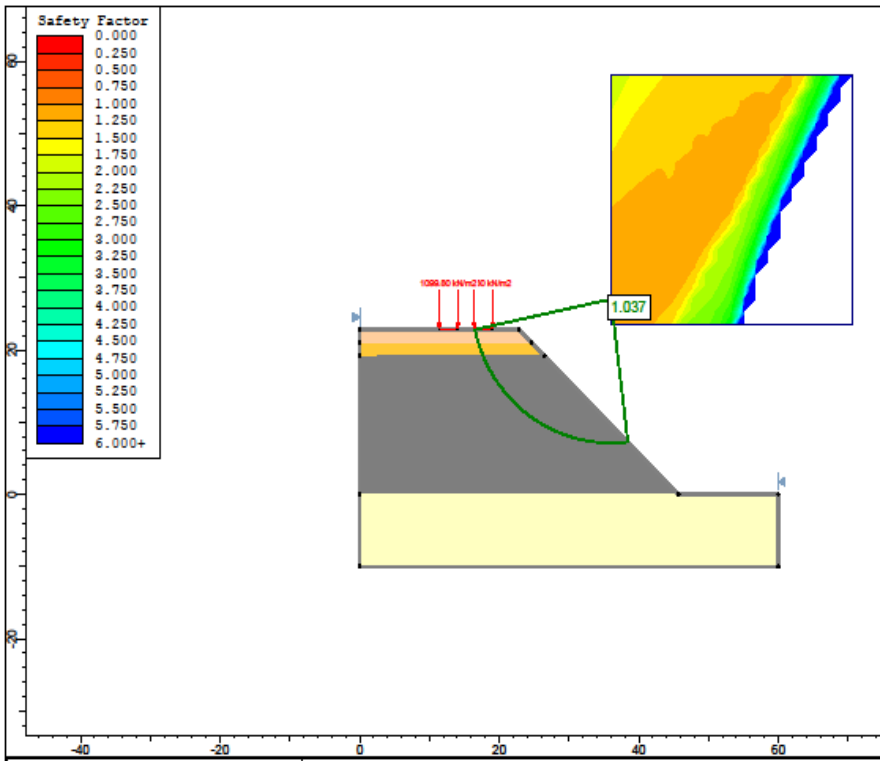

Figure 168: Minimum safety factor in wet condition of broken limestone in 1/2 truck width from crest

5-3. Linking safety factor to truck suspension data response

Hauler trucks are equipped with four suspension cylinders. Two cylinders at the back for four tires (each cylinder being assigned a dual pair) accommodate one third of GVW per cylinder. Two suspensions are at the front for two tires, with a larger diameter to accommodate one sixth of GVW per strut. This system of suspension provide equal load per each tire under static load on a level bearing surface (T.G. Joseph, 2001).

When a truck moves on undulated ground, any suspension strut may become extended or compressed, reflecting a decrease or increase in g-level gravity on the load share changing the suspension pressure response.

Data recorded from the truck suspension pressure is useful to understand loaded during truck motion, behavior of the truck in response to undulated ground, and also individual suspension response, described by the number of g's, reflected by: (T.G. Joseph, 2001).

Equation 17

$$\#g_{strut} = \frac{F_{Dynamic}}{F_{Static}}$$

F_{Static}, is calculated from the state, that truck contains load but is at rest, and the velocity is zero.

Equation 18

$$F_{Static} = g \sum_{1}^{4} M_i$$

M_i : Mass share at any strut

$F_{Dynamic}$, is introduced when a truck moves (v>0), whether the truck is empty or loaded, reflecting Newton's 2nd law applied to load.

Equation 19

$$F_{Dynamic} = \sum_{1}^{4} M_i(g + a_i)$$

a_i : is increment or decrement over g

A sample of data recorded from a 793D truck over 14 cycles. The purpose of this research section was to create a relationship between safety factor and g-levels range during the truck motion. Two dump cycles of this data were selected as a commensurate sample to study the relation between g-levels and safety factor.

The safety factor which was computed in Slide was associated to the 1g (static) ground bearing level. This was extended as revised modeling for a range of g-level, to determine a relationship between g-level and safety factor. Model analysis was performed for 0.5g, 1.5g, 1.67g, 2g for all truck dump states investigated.

In each state a graph of minimum safety factor versus g was plotted yielding a descending trend. By increasing the load on the tires the possibility of failure in the waste dump will be increased where this behavior was represented by g-level vs. safety factor. Figure 169 through Figure 176 indicate there are clear functions between g-level and safety factor permitting suspension recording to indicate safety factor for slope below running surfaces.

Plot of g-level vs. safety factor for various conditions shown as:

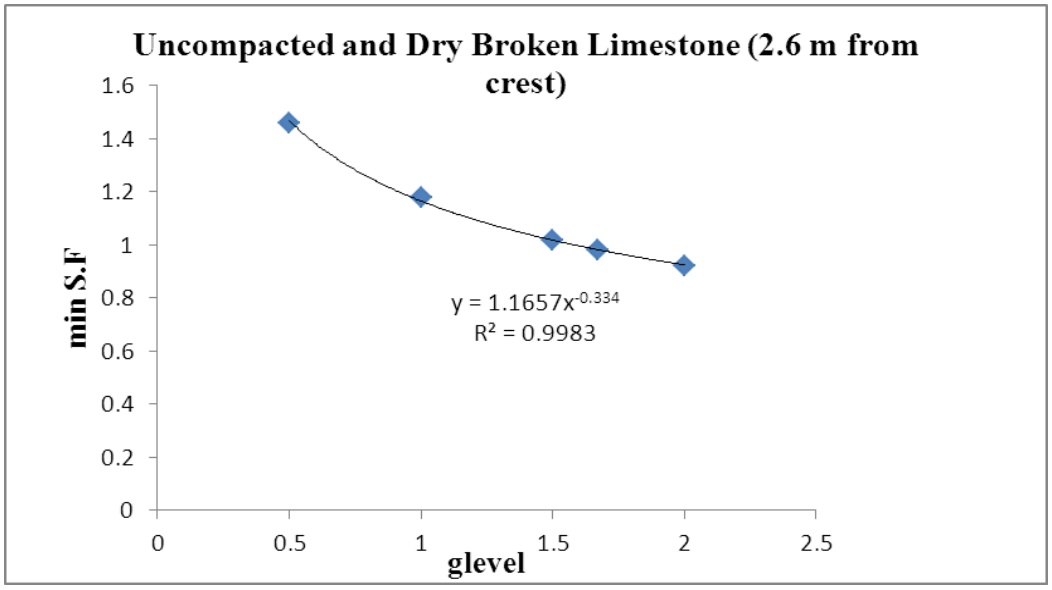

Figure 169: g-level vs. safety factor for uncompacted, dry limestone (1/3 truck width from crest)

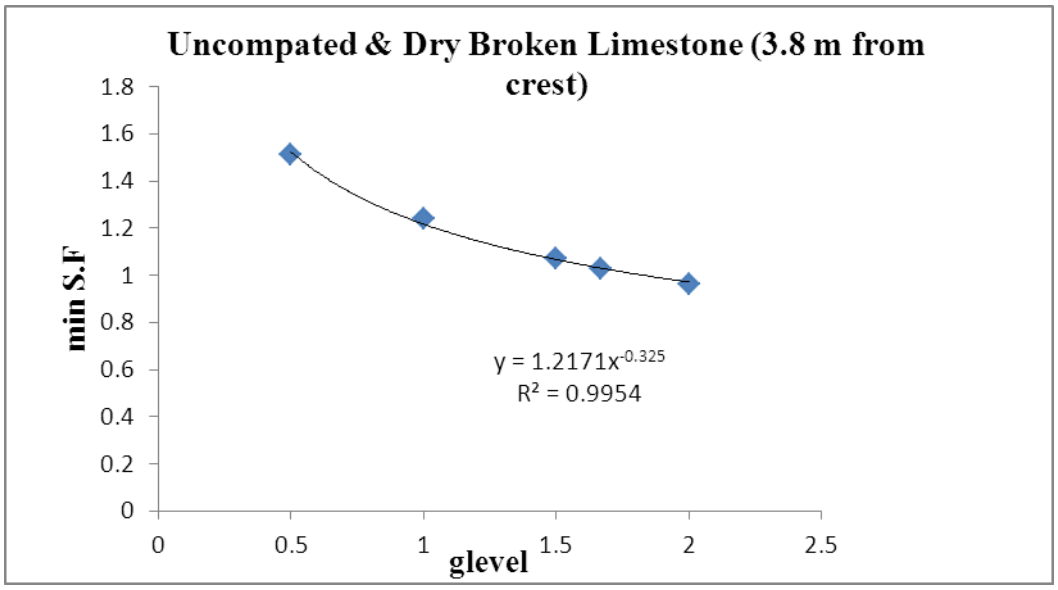

Figure 170: g-level vs. safety factor for uncompacted, dry limestone (1/2 truck width from crest)

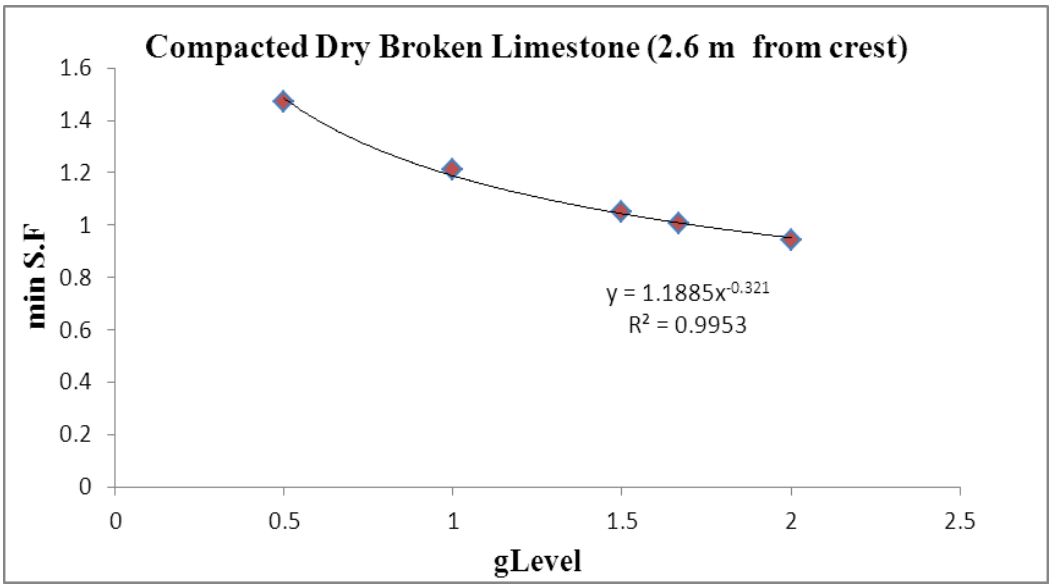

Figure 171: g-level vs. safety factor for compacted, dry limestone (1/3 truck width from crest)

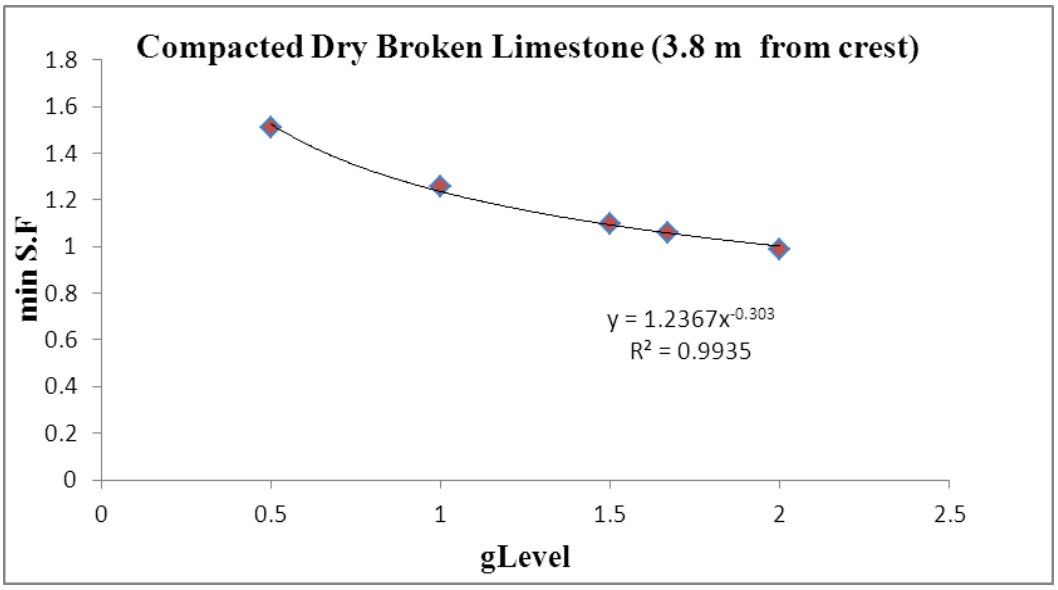

Figure 172: g-level vs. safety factor for compacted, dry limestone (1/2 truck width from crest)

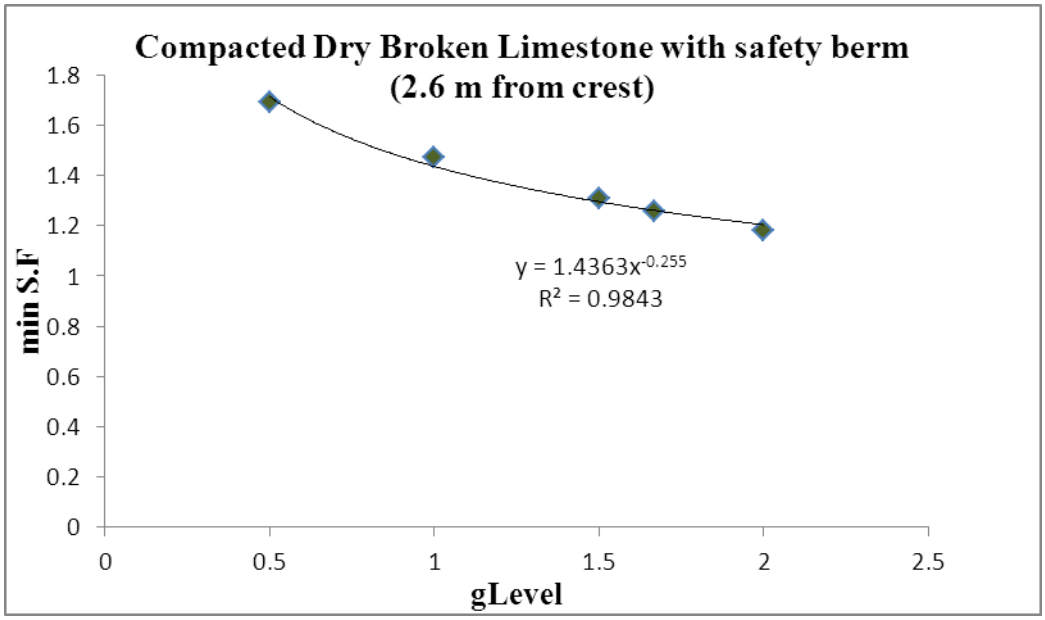

Figure 173: g-level vs. safety factor for compacted, dry limestone with safety berm (1/3 truck width from crest)

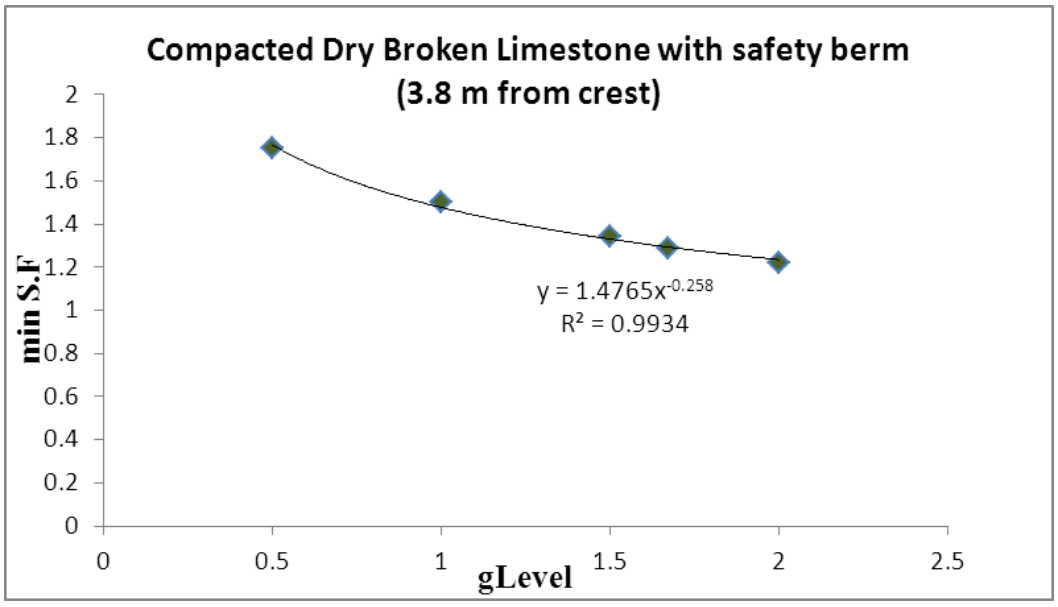

Figure 174: g-level vs. safety factor for compacted, dry limestone with safety berm (1/2 truck width from crest)

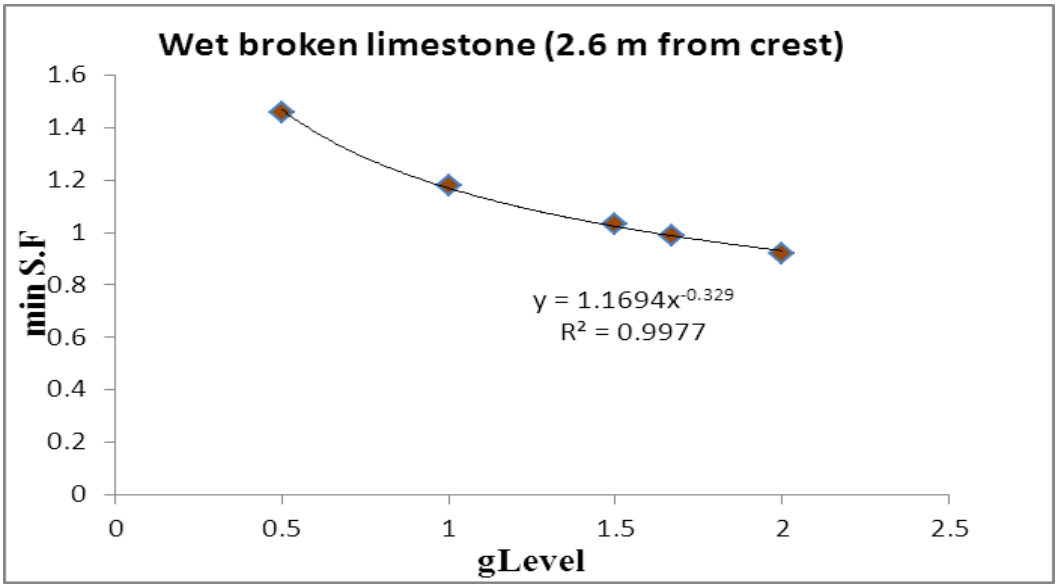

Figure 175: g-level vs. safety factor for wet limestone (1/3 truck width from crest)

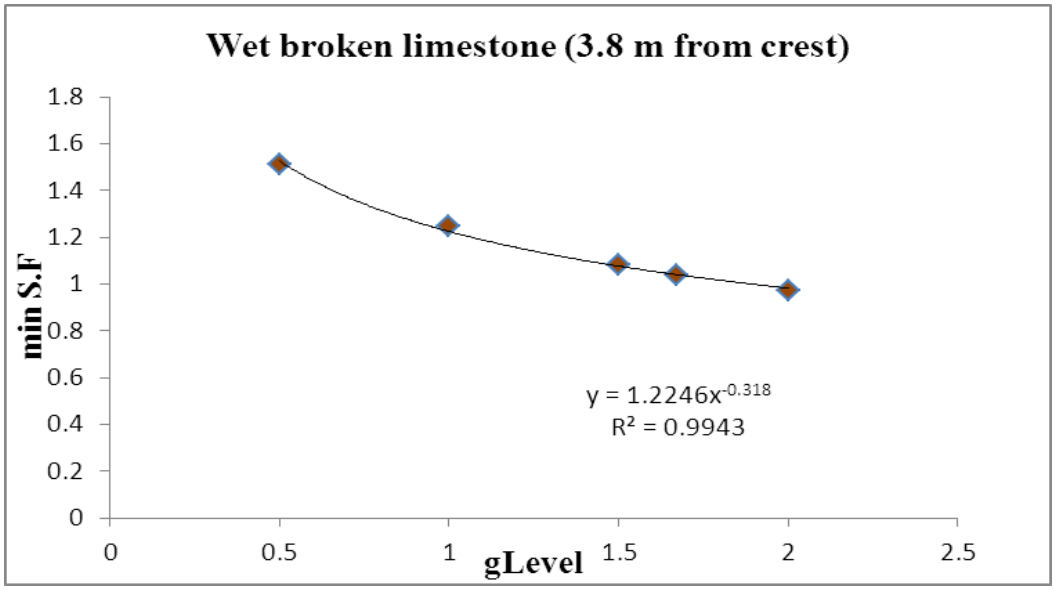

Figure 176: g-level vs. safety factor for wet limestone (1/2 truck width from crest)

Table 18: Summerise of g-level 2-dimentional for all numbers

Limestone slope state	2.6 m away from slope edge	3.8 m away from slope edge
Dry & uncompacted	S.F = $1.16g^{-0.33}$ R^2 =1	S.F = $1.22g^{-0.32}$ R^2 =1
Compacted & Dry	S.F = $1.19g^{-0.32}$ R^2 =1	S.F = $1.24g^{-0.30}$ R^2 =1
Compacted with Safety Berm	S.F = $1.44g^{-0.26}$ R^2 =1	S.F = $1.48g^{-0.26}$ R^2 =1
Wet	S.F = $1.17g^{-0.33}$ R^2 =1	S.F = $1.22g^{-0.32}$ R^2 =1

Dump data g-level for each suspension were converted to safety factor, using the functions from Table 18.

Figure 177 to Figure 192 show a weighted mean analysis of safety factor by loading event and unsafe conditions are shown by red shadow.

The weighted mean safety factor for each state provides a comprehensive understanding of the stability of a dump with a truck running on the surface.

Dry and uncompacted broken limestone shows a weighted mean around 1.18 for a range of g-level from 0.5 to 2 at one third of truck width from the crest, so encouraging the results of the experimental tests and showed that this state and truck location is not a safe place for truck running. At the half width truck from the slope crest the weighted mean safety factor, at 1.25 become well. The average safety factor in this state approached at 1.2. Overall a truck running in both

locations in an uncompacted state has a higher risk of stability, such that improvements should be incorporated to prevent dump failure and safety issues for operation of truck.

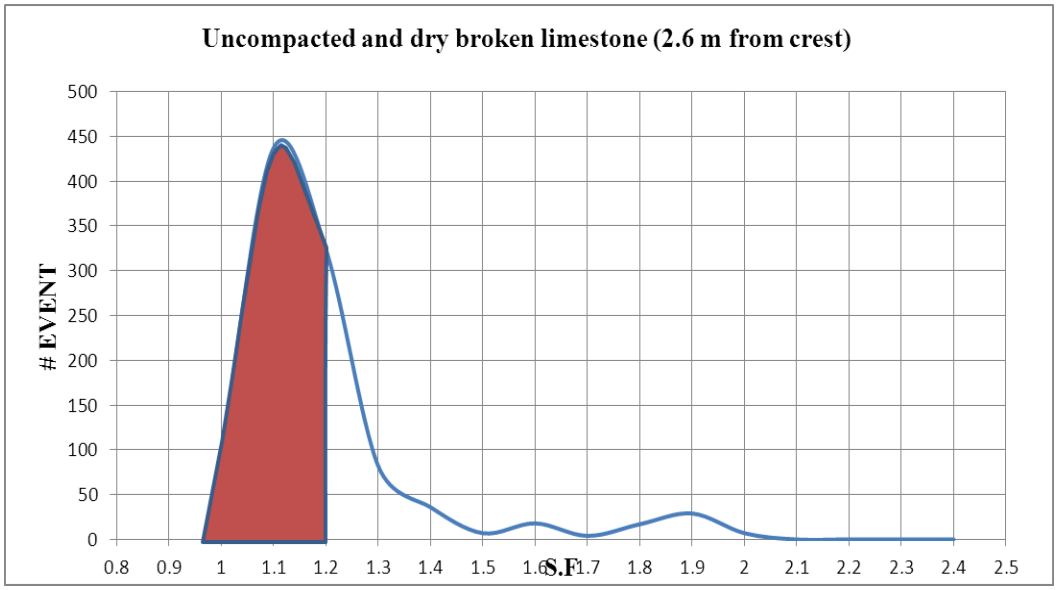

Figure 177: #event vs. S.F for uncompacted and dry state for rear tires, dump cycle 1 (2.6 m from slope crest)

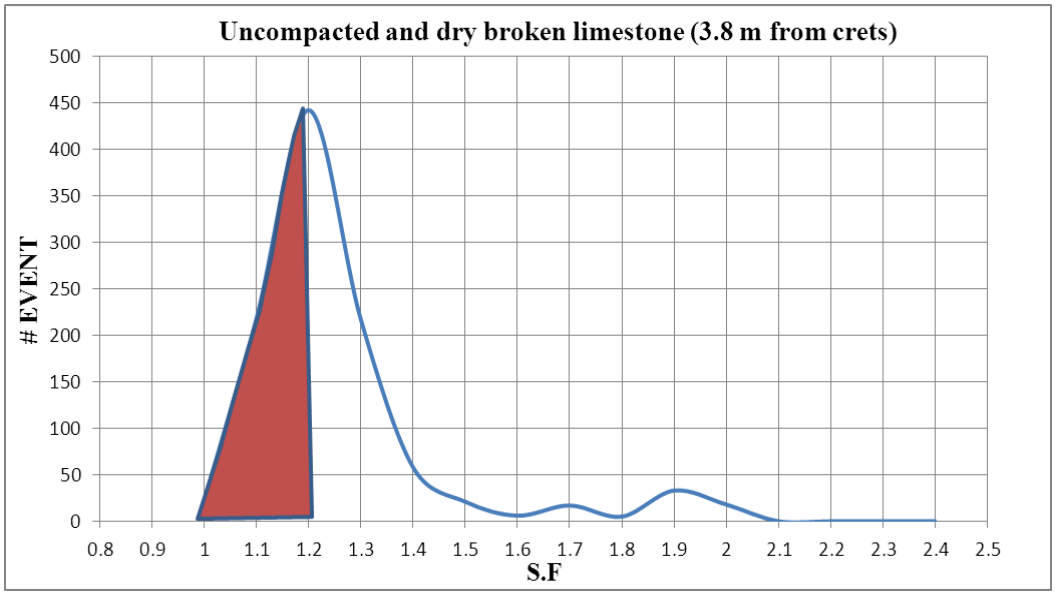

Figure 178: #event vs. S.F for uncompacted and dry state for rear tires, dump cycle 1 (3.8 m from slope crest)

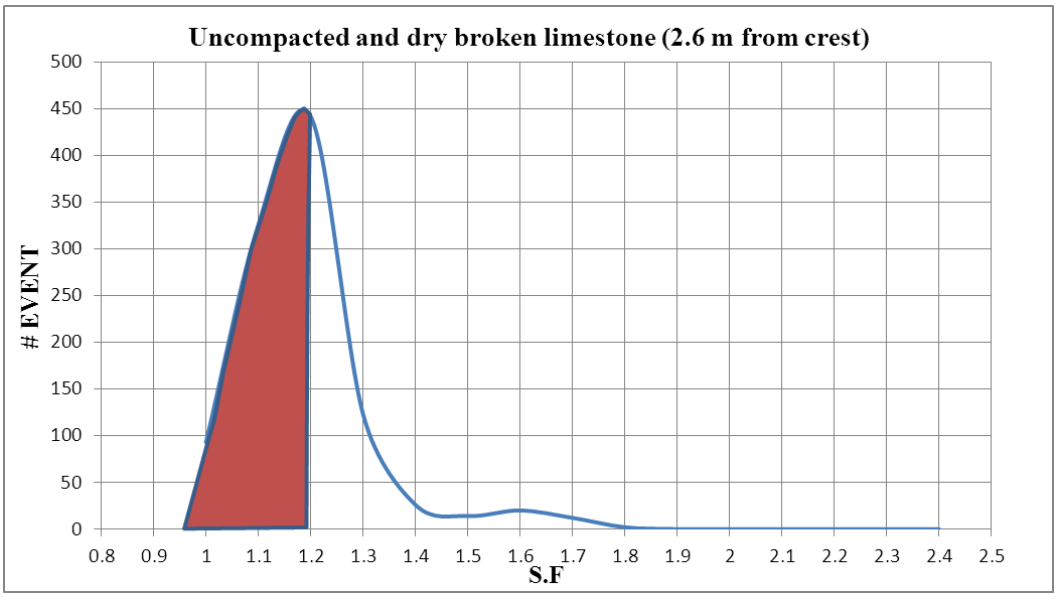

Figure 179: #event vs. S.F for uncomapcted and dry state for rear tires, dump cycle 12 (2.6 m from slope crest)

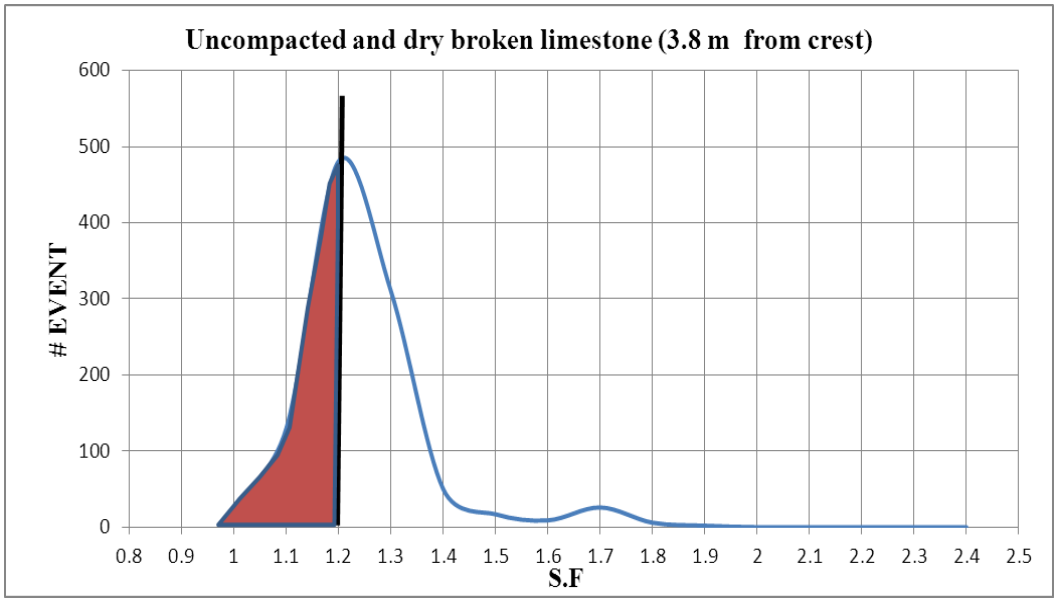

Figure 180: #event vs. S.F in natural and dry state for rear tires, dump cycle 12 (3.8 m from slope crest)

Table 19: weighted mean safety factor for uncompacted, dry state for cycle 1, 12

Truck Location	Weighted Mean Of Safety Factor
1/3 truck width from slope crest (cycle 1)	1.19
1/2 truck width from slope crest (cycle1)	1.26
1/3 truck width from slope crest (cycle 12)	1.18
1/2 truck width from slope crest (cycle12)	1.24

With compacted broken limestone to increase the stability of the waste dump, the weighted mean approached 1.25, which showed an improvement over the uncompacted state (unsafe zone shown in red shadow).

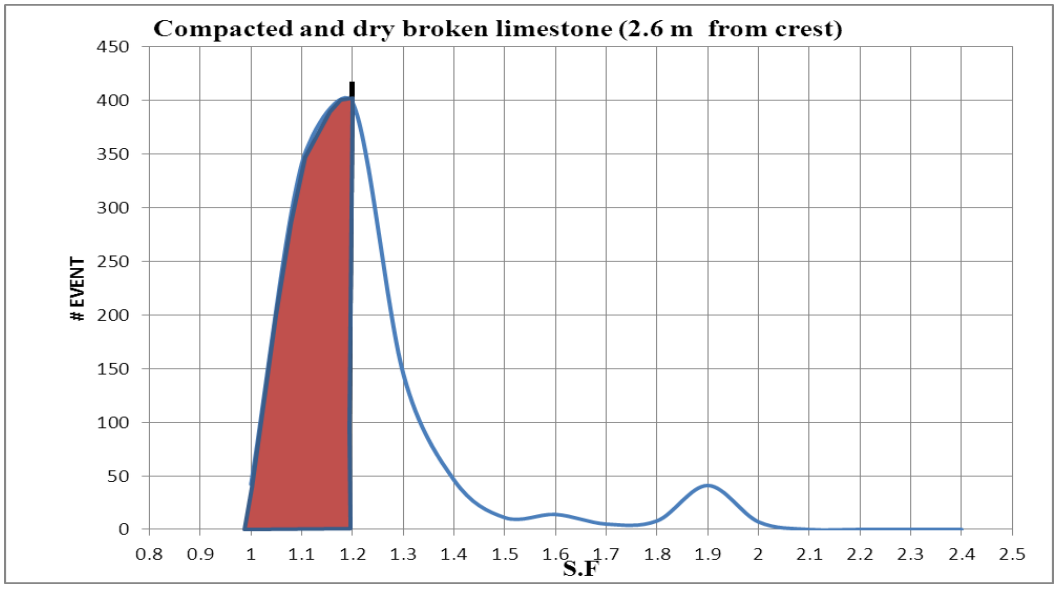

Figure 181: #event vs. S.F in compacted and dry state for rear tires, dump cycle 1 (2.6 m from slope crest)

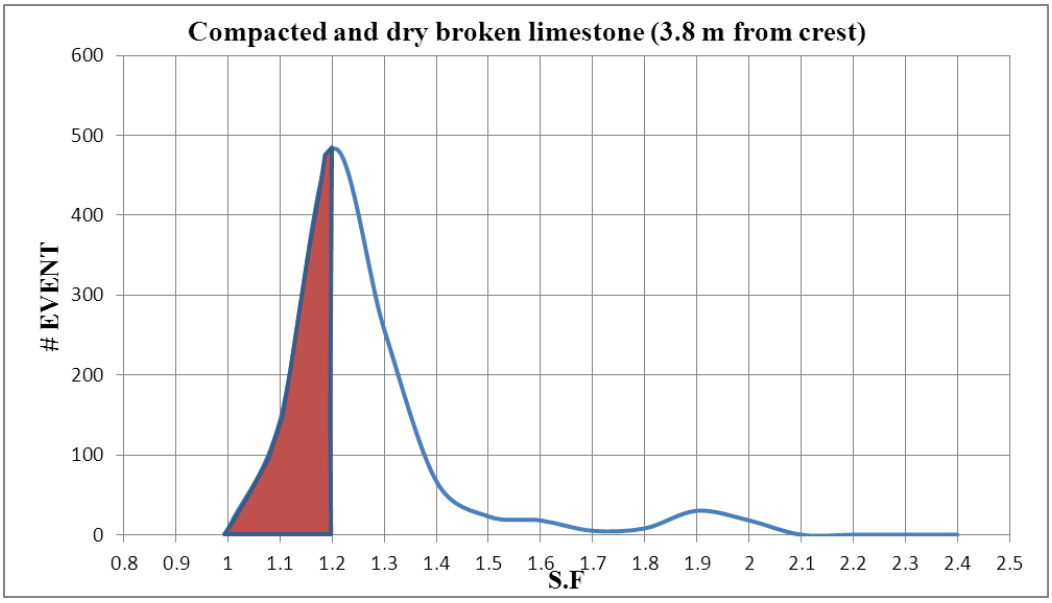

Figure 182: #event vs. S.F in compacted and dry state for rear tires, dump cycle 1 (3.8 m away from slope crest)

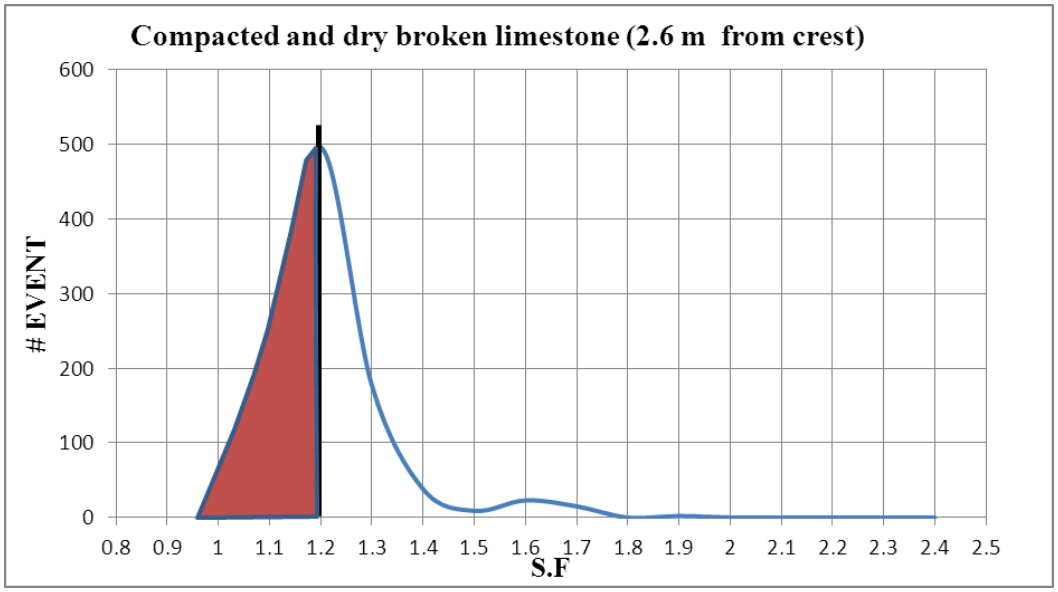

Figure 183: #event vs. S.F in compacted and dry state for rear tires, dump cycle 12 (2.6 m away from slope crest)

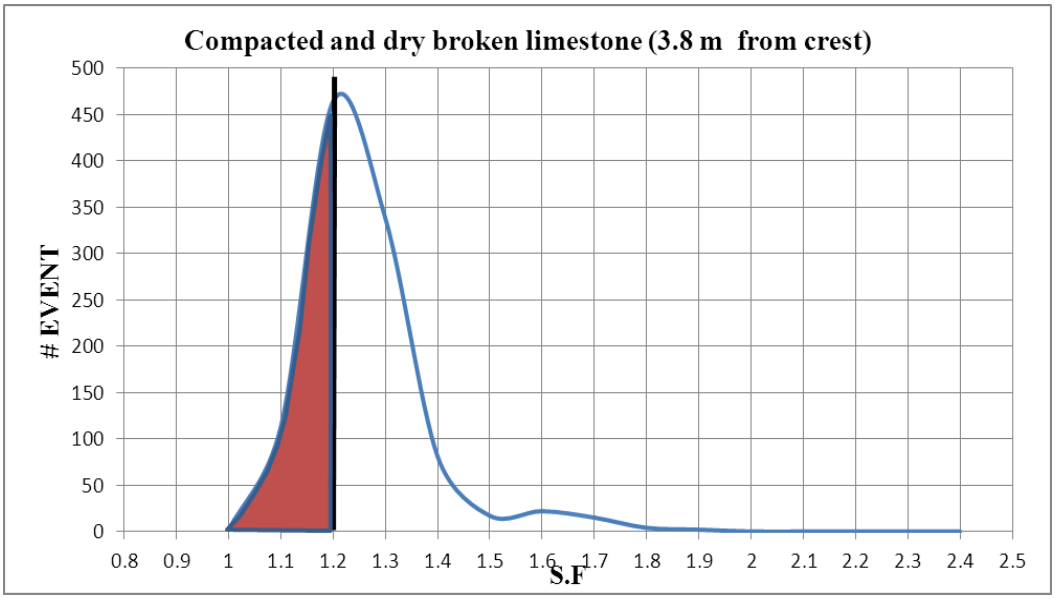

Figure 184: #event vs. S.F in compacted and dry state for rear tires, dump cycle 12 (3.8 m from slope edge)

Table 20: weighted mean safety factor in compacted and dry state, for cycle 1, 12

Truck Location	Weighted Mean Of Safety Factor
1/3 truck width from slope crest (cycle 1)	1.23
1/2 truck width from slope crest (cycle1)	1.27
1/3 truck width from slope crest (cycle 12)	1.21
1/2 truck width from slope crest (cycle12)	1.26

With the addition of a safety berm along the slope crest, a safe and stable condition for running trucks created in relative to a crest. A weighted mean safety factor at 1.5 was reviled.

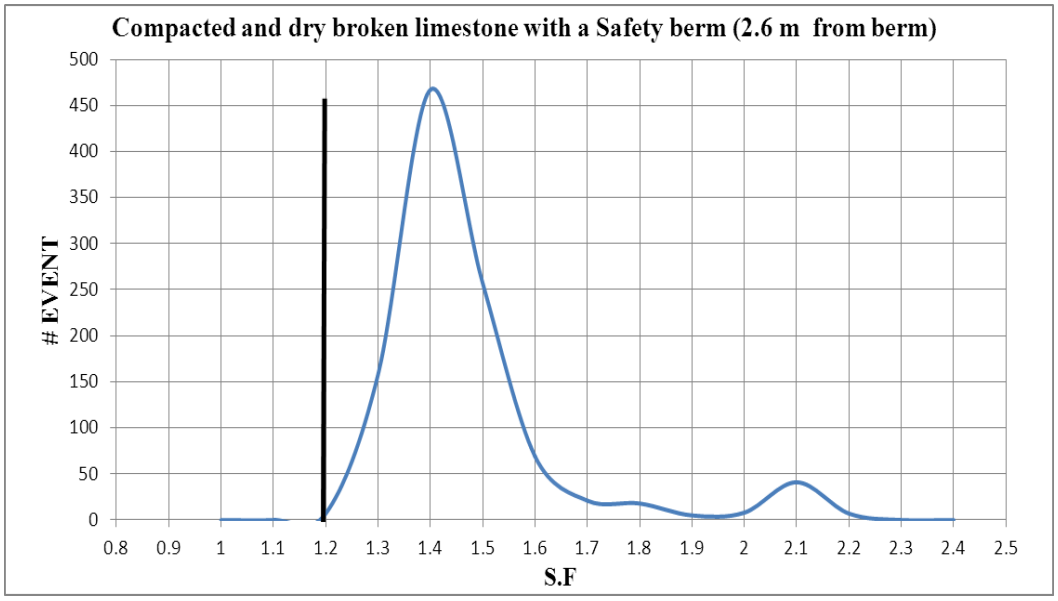

Figure 185: #event vs. S.F in compacted and dry state with safety berm for rear tires, dump cycle 1 (2.6 m from berm)

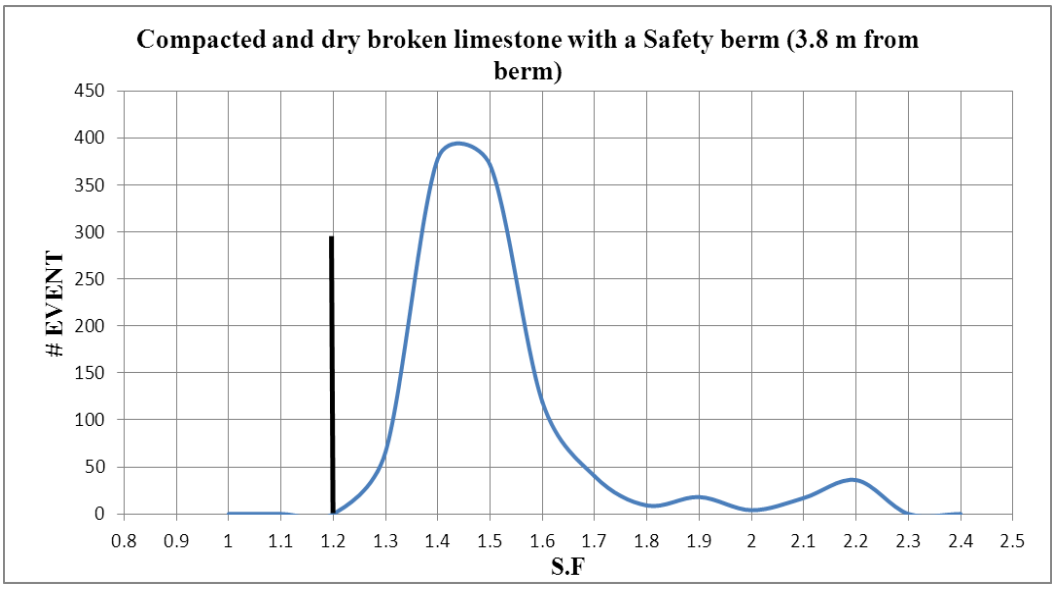

Figure 186: #event vs. S.F in compacted and dry state with safety berm for rear tires, dump cycle 1 (3.8 m from slope berm)

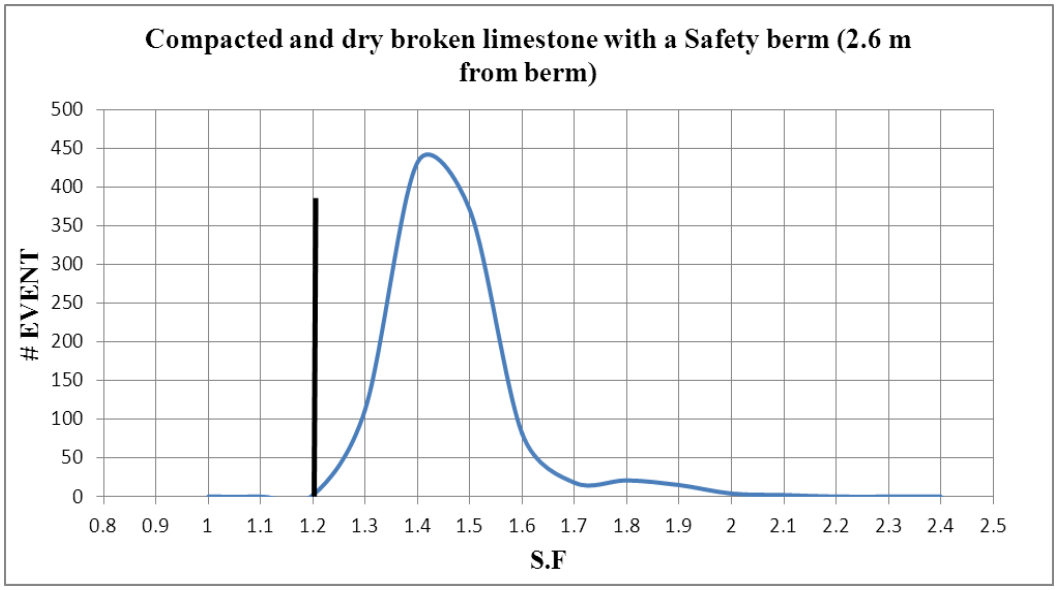

Figure 187: #event vs. S.F in compacted and dry state with safety berm for rear tires, dump cycle 12 (2.6 m from slope berm)

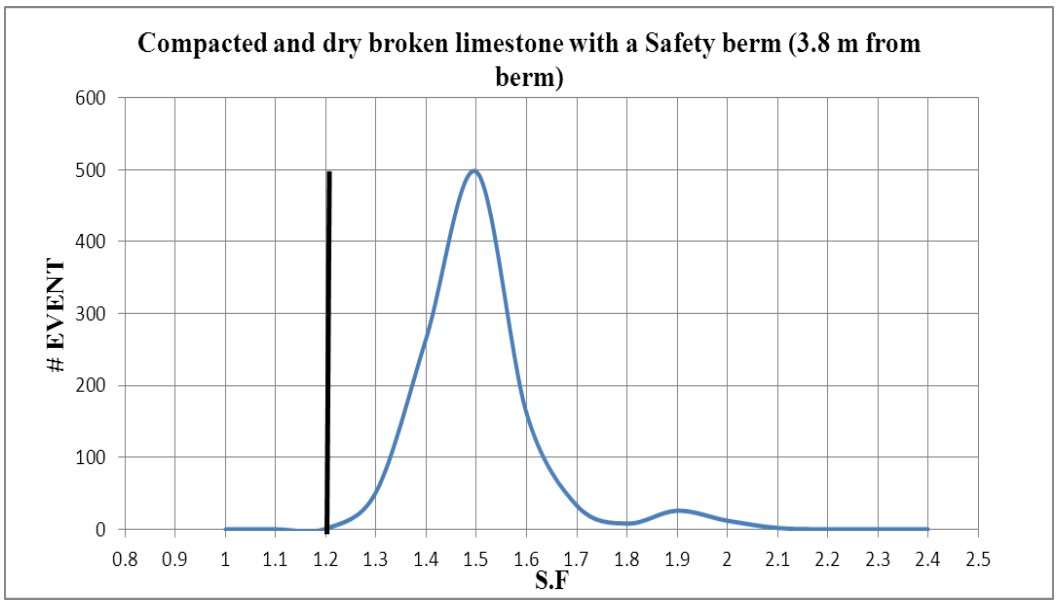

Figure 188: #event vs. S.F in compacted and dry state with safety berm for rear tires, dump cycle 12 (3.8 m from slope berm)

Table 21: weighted mean safety factor in compacted, dry state and safety berm, for cycle 1, 12

Truck Location	Weighted Mean Of Safety Factor
1/3 truck width from slope crest (cycle 1)	1.47
1/2 truck width from slope crest (cycle1)	1.51
1/3 truck width from slope crest (cycle 12)	1.46
1/2 truck width from slope crest (cycle12)	1.5

The final state evaluated was the impact of creating wet conditions for the surface course of the truck path. This situation improved and enhanced the weighted mean safety factor, at 1.23. This safety factor was seen to be an appropriate safety factor for waste dump stability, trucks running with no failures anticipated.

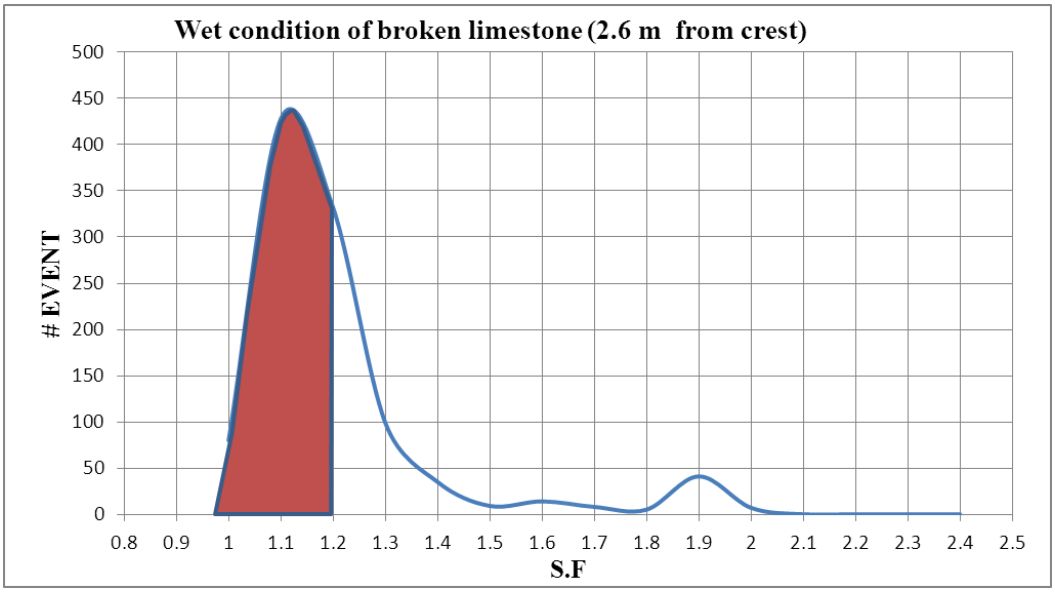

Figure 189: #event vs. S.F wet state for rear tires, dump cycle 1 (2.6 m from slope crest)

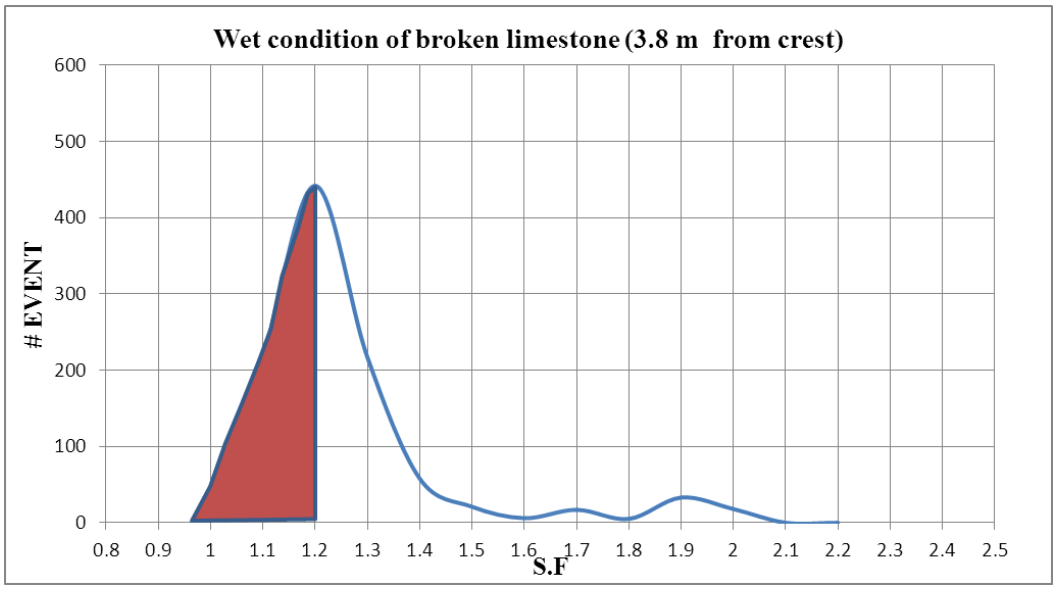

Figure 190: #event vs. S.F wet state for rear tires, dump cycle 1 (3.8 m from slope crest)

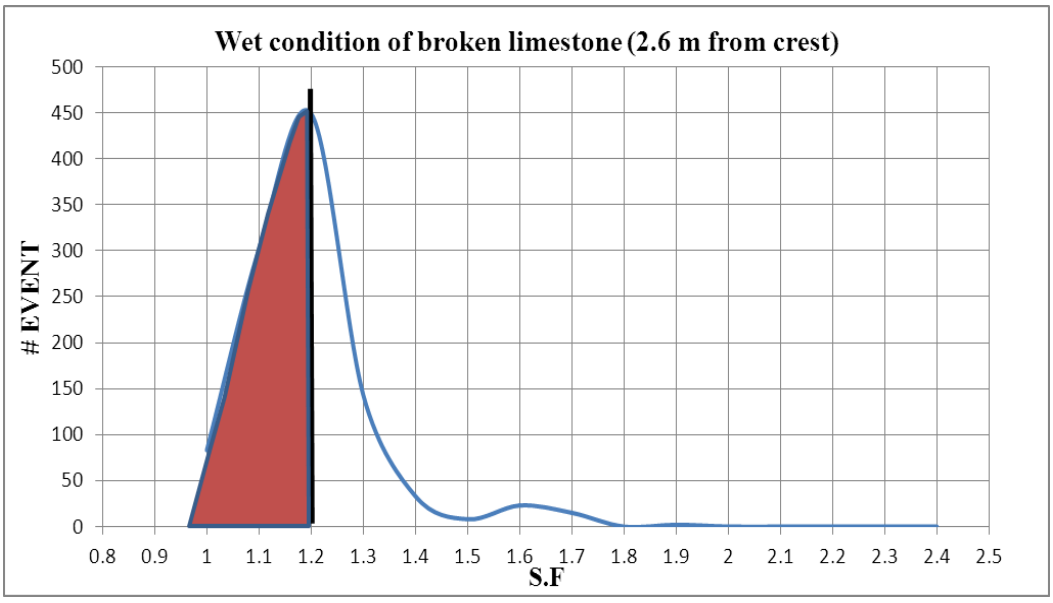

Figure 191: #event vs. S.F wet state for rear tires, dump cycle 12 (2.6 m from slope crest)

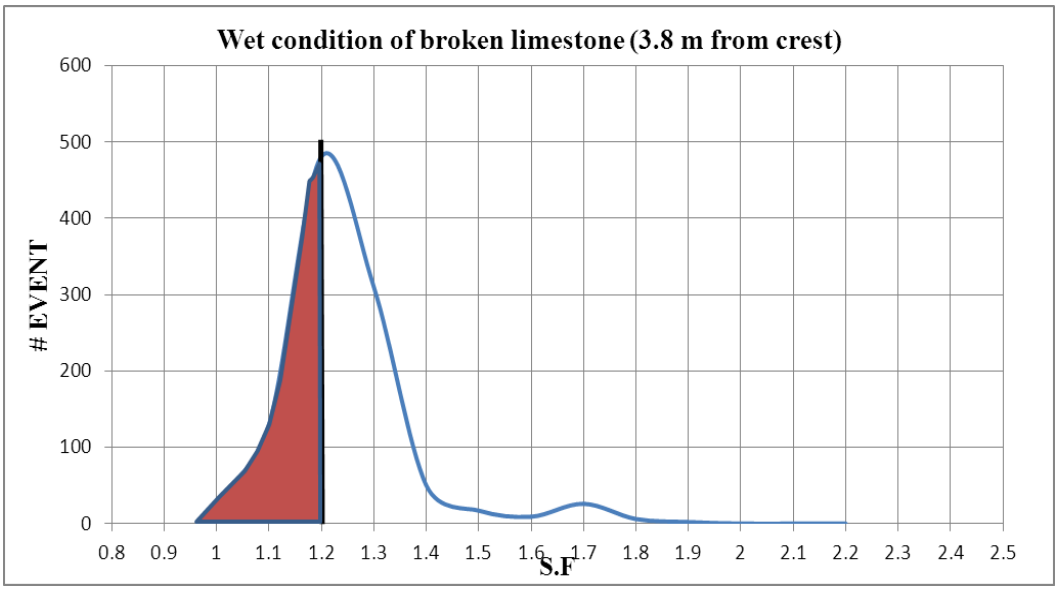

Figure 192: #event vs. S.F wet state for rear tires, dump cycle 12 (3.8 m from slope crest)

Table 22: weighted mean safety factor in wet state and safety berm, for cycle 1, 12

Truck Location	Weighted Mean Of Safety Factor
1/3 truck width from slope crest (cycle 1)	1.21
1/2 truck width from slope crest (cycle1)	1.26
1/3 truck width from slope crest (cycle 12)	1.19
1/2 truck width from slope crest (cycle12)	1.24

5-4. Rolling Resistance and emissions

In the previous chapter, rolling resistance by test run was compared for specific states of operation. Rolling resistance also impacts mining equipment fuel consumption, emissions and productivity.

Productivity decreases with increasing rolling resistance manifest as lost revenue and higher lost over a mine life (Tannant & Regensburg, 2001). Rolling resistance

has been shown to have a direct relation to fuel consumption emissions and cost (Tannant & Regensburg, 2001). Figure 193 illustrate that fuel consumption and cost increase with increasing rolling resistance.

The importance of fuel consumption and impacts on air quality through NOx and CO_2 emission has become a focus for using truck and shovel operations in mining operation (Singh, Rawlings, & Unrau, n.d.). Concern of fuel consumption and emissions has sparked studies on ways to reduce impacts.

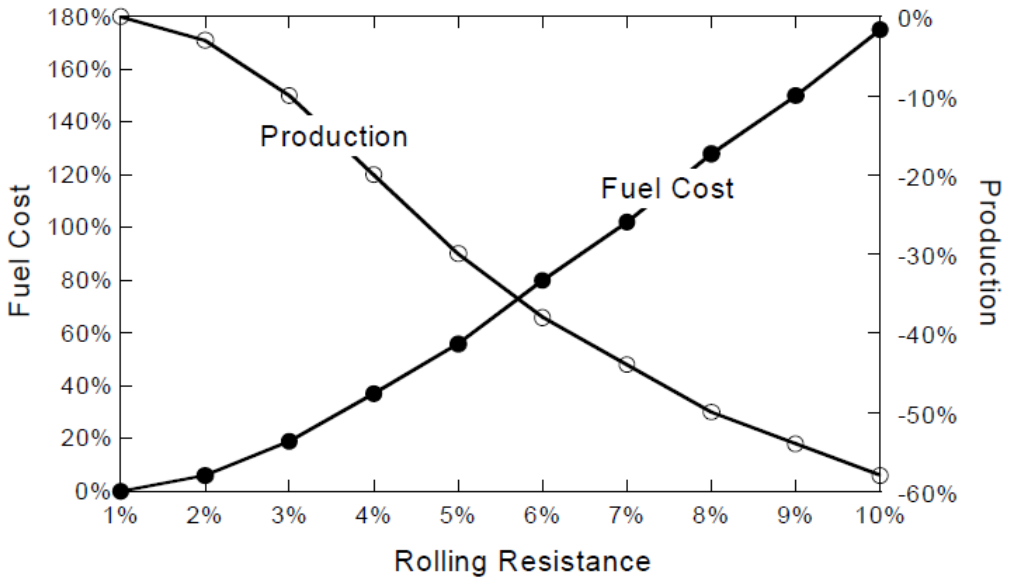

Figure 193: Rolling resistance vs. fuel cost and production (Tannant & Regensburg, 2001)

Reducing rolling resistance between tires and ground enhance this aim, and create situations to possibility lower fuel consumption and emissions.

For truck runs at one third of truck width from the crest, rolling resistance was pendulous, reacting to the uncompact limestone which allowed tires to easily

penetrate the waste dump surface. This state yielded a high weighted mean rolling resistance of 16.7%.

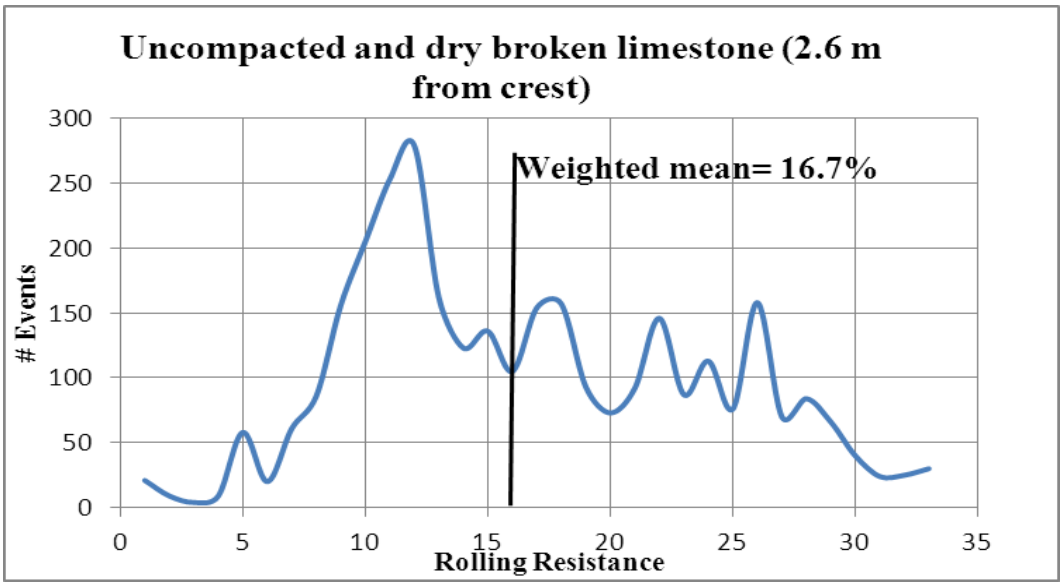

Figure 194: #event vs. rolling resistance for uncompacted and dry broken limestone (1/3 of truck width from the crest)

With compaction the broken limestone surface, rolling resistance reduced and the plot of rolling resistance, versus number of events became less erratic. The Weighted mean rolling resistance in this latter case had a value of 5.1% (Figure 195). Constructing safety berm at the crest caused narrowing of rolling resistance to 5 %.(Figure 196)

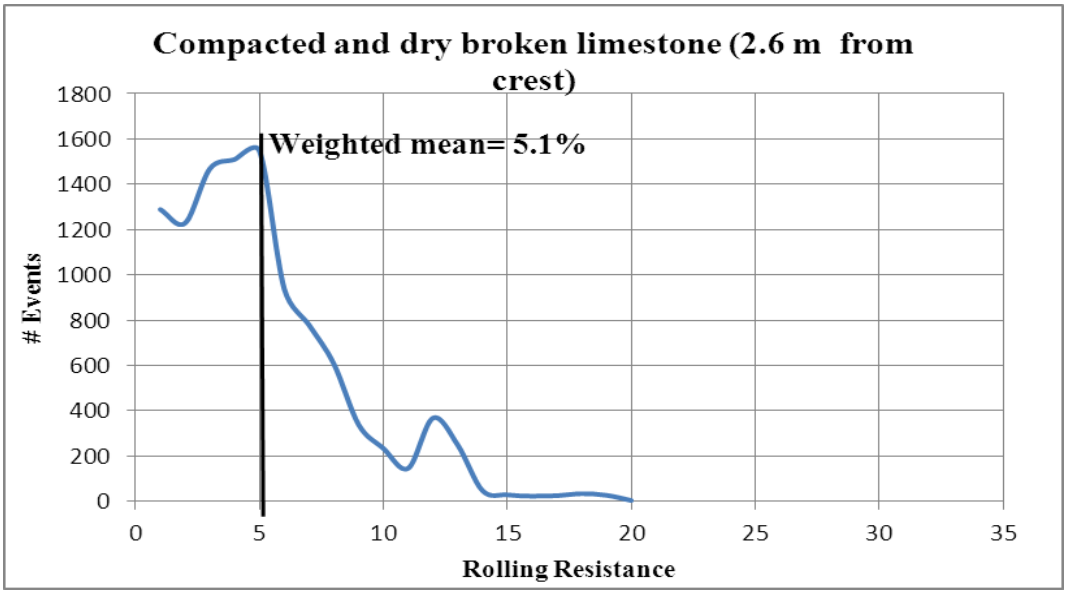

Figure 195: #event vs. rolling resistance in compacted, dry broken limestone (1/3 of truck width from crest)

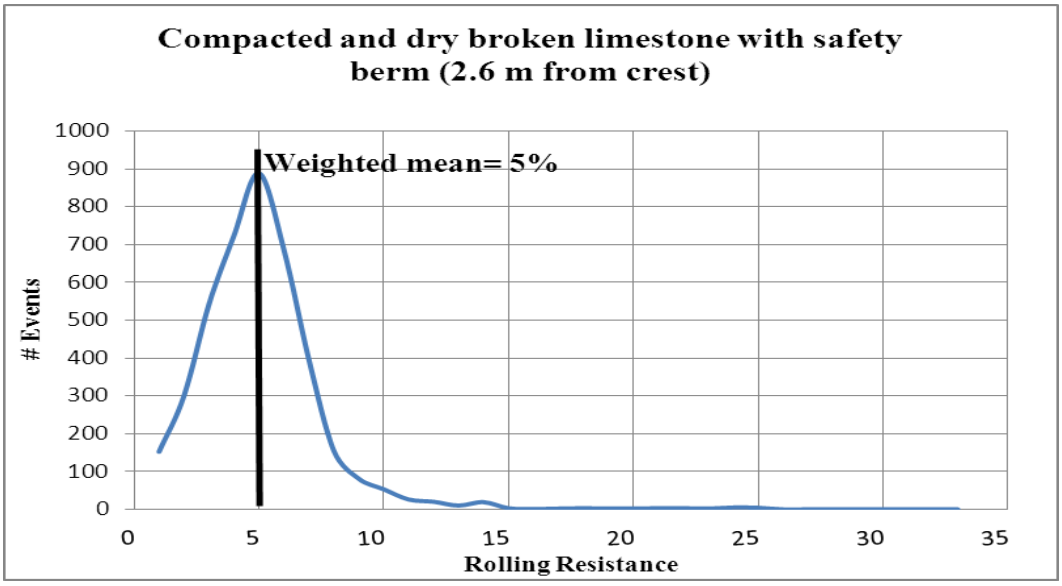

Figure 196: #event vs. rolling resistance in compacted, dry broken limestone with safety berm (1/3 of truck width from crest)

Adding of water created cohesion between the limestone particles, however adhesion developed between the tires and ground which caused an increase in

rolling resistance. The weighted mean rolling resistance showed higher values than the dry state, at 6% (Figure 197).

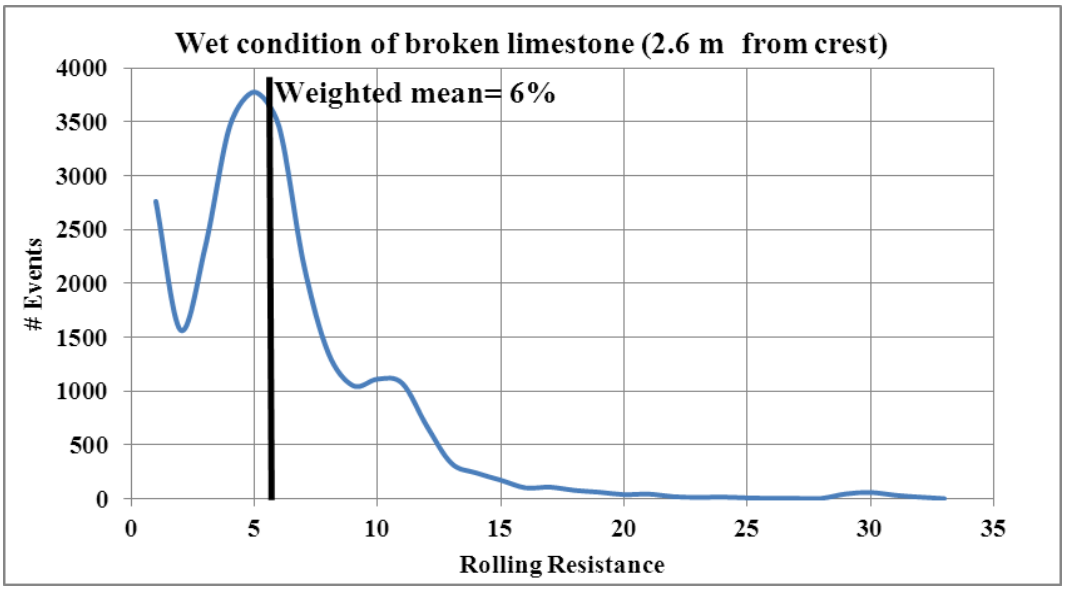

Figure 197: #event vs. rolling resistance in wet condition of broken limestone (1/3 of truck width from crest)

Comparing weighted mean rolling resistances, Table 23, showed using improvement methods for increasing safety and stability of waste dump developed improvements in the rolling resistance condition.

Table 23: Weighted mean rolling resistance in various broken limestone states (1/3 of truck width from crest)

States	Range of weighted mean rolling resistance
Uncompacted and Dry	3-33%
Compacted and Dry	1-14%
Compacted and Dry with Safety berm	1-12%
Wet	2-20%

By changing the location of truck relative to the crest, a descending trend reflecting an improved condition for broken limestone is maintained. The uncompacted state and proximity to the crest showed higher rolling resistance than farther the crest due to penetration impairing truck motion near a crest.

It is obvious from the summary Table 24 that rolling resistance decreased from uncompacted to compacted states. By water adding and creating cohesion between limestone particles, the rolling resistance decreased and reached to 6.8% in wet and 4.8% in compaction with addition a safety berm.

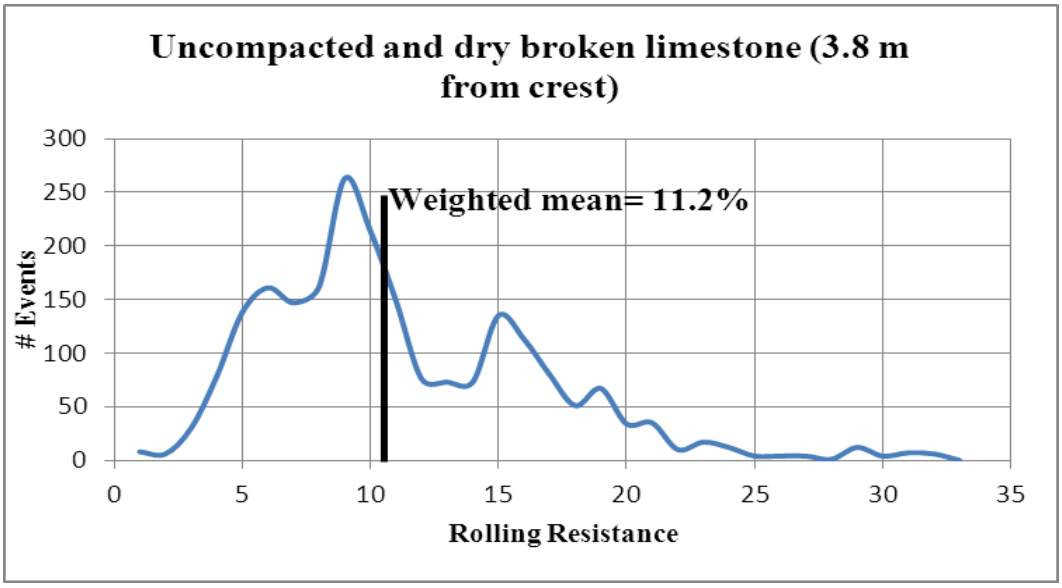

Figure 198: #event vs. rolling resistance in natural, dry broken limestone (1/2 of truck width from crest)

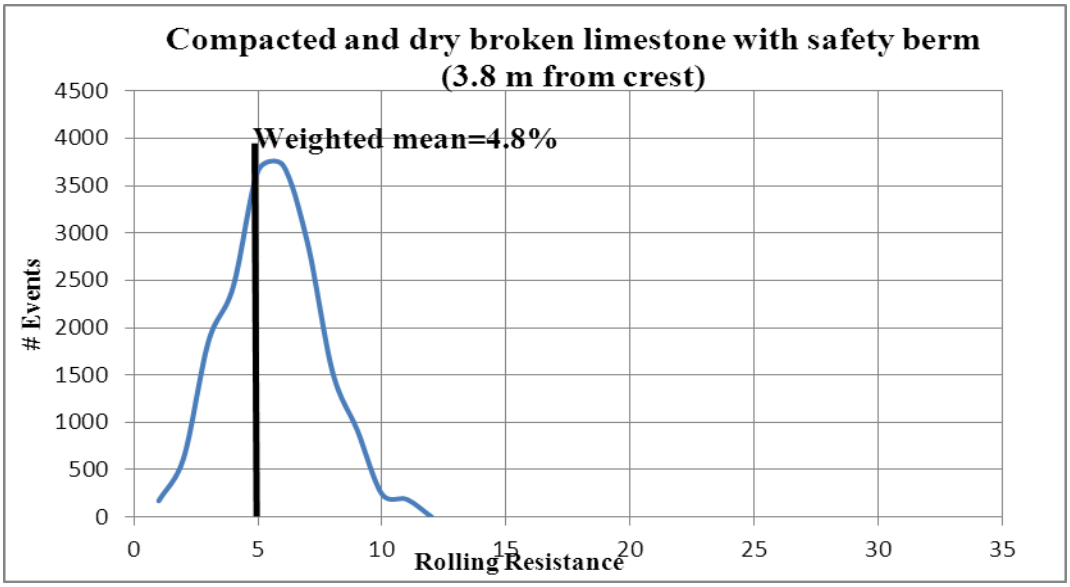

Figure 199: #event vs. rolling resistance in compacted, dry broken limestone (1/2 of truck width from crest)

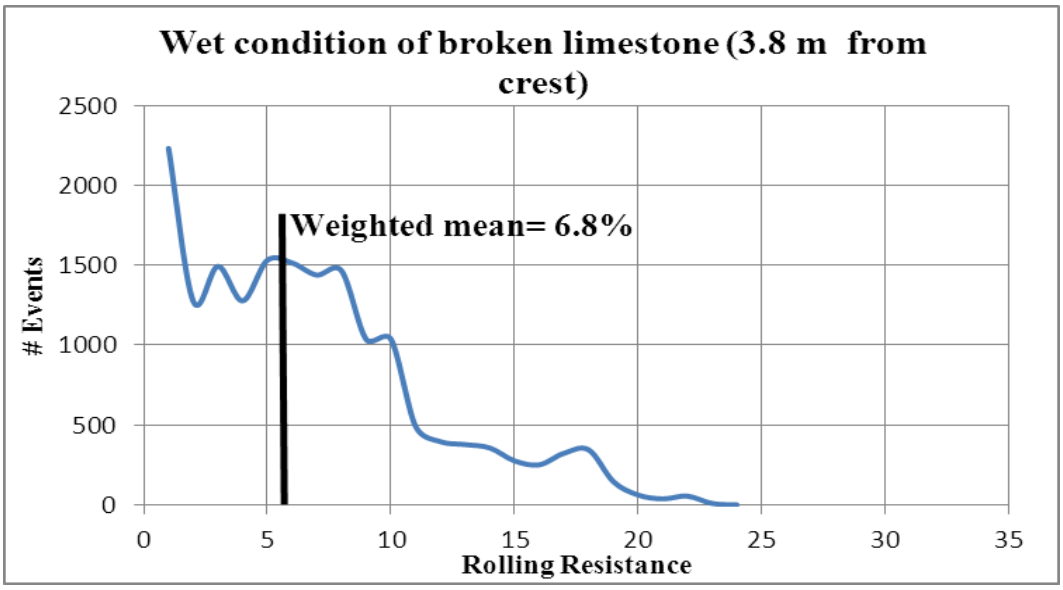

Figure 200: #event vs. rolling resistance in wet condition of broken limestone (1/2 of truck width from crest)

Table 24: Weighted mean rolling resistance in various broken limestone states (1/2 of truck width from crest)

States	Weighted mean of rolling resistance
Uncompacted and Dry	2-25%
Compacted and Safety berm	1-12%
Wet	2-24%

Chapter 6: Conclusion

A series of tests were performed on broken dolomitic limestone, representative of bed hard rock, to determine stability of the hard rock waste dump under mining haul truck motion, and also to evaluate effect of rolling resistance on stability. As it was beyond the capacity of the lab to test actual waste dump performance, scaled truck and waste dump were designed.

This test was designed to investigate state from dry uncompacted limestone to compacted, use of safety berms and wet surface conditions for broken rock.

A tire flexure test was performed to determine the scale load on the scale tire and the internal tire pressure required commensurate with an actual haul truck. The scale factor based on scale to actual diametric comparison was 22.83 such that all dimensions and components included in tests were scaled based on this factor.

Stability of the waste dump was studied easier by taking photographs of the surface of the waste dump. The surface of the slope collered in bands to create photographic movement interpretation. During the truck runs on the waste dump, in additional photographs that showed failure of the waste dump; data was associated with rolling resistance between the tire and ground was recorded via load cell and data acquisition system. Truck run at two locations, one third of a truck width from the crest and half a truck width from the crest were evaluated.

Physical modeling was compared with numerical modeling via “Slide” slope stability analysis software.

“Slide” modeling used the actual loads on a tire and actual waste dump dimensions. By applying the maximum load experienced on the rear tires, a model was created and evaluated for different states of broken limestone (uncompacted, compacted, wet).

By comparing different states of dolomitic limestone chip in the laboratory tests, it was realized that the optimum state for safe truck motion is constructing a safety berm in addition to surface compaction under truck and dozer motion. This state of the waste dump was constructed relative to location of the truck movement, creating a safe zone for truck operation. Another option which showed a safe scenario to run a truck was wet conditions for broken limestone in a surface course. This was move due to the cementation properties of dolomitic limestone crushed material.

“Slide” modeling of actual truck and dump showed an optimum safety factor for compacted limestone with actual constructed safety berm at the crest of the slope. Table 25 shows a comparison between physical and numerical modeling for different state of broken limestone.

Table 25: Comparison between physical and numerical modeling

States of broken limestone	Truck location	Result of failure form laboratory test	Safety factor from Slide modeling
Dry - uncompacted	Half truck width	No failure	1
	One third truck width	Big circular failure	0.98
Dry- compacted	One third truck width	Small Circular failure	1
Dry-compacted with adding safety berm	Half truck width	No failure	1.3
	One third truck width	No failure	1.26
Wet	Half truck width	No failure	1.04
	One third of truck width	No failure	0.99

"Slide" modeling was next extended to model truck runs at different g-levels to establish a function between safety factor and g-level. The g-level measured on board a truck suspension was then converted to an equivalent safety factor that

evaluated as a weighted mean safety factor for each run state. This also showed that the best condition for truck operation was the addition of a safety berm.

The actual water added to surface, created cemented cap layer. The cemented cap layer under the truck behaved as rough structure siting above the much more unstable surface.

In the wet condition, “Slide” Just showed the reduction of actual effective friction and cohesion that was measured using a direct shear box. “Slide” just molded the material with lower strength and could not show the cementation property which was created among the broken limestone. So the safety factor which Slide computed in this condition was low safety factor, but actually the performance goes higher due to cementing fact in broken limestone.

So the best condition for truck operation was the addition of safety berm or applying water to permit cementation of the surface.

Table 26: concluding on waste the best condition for waste dump stability and rolling resistance

Surface state	Safety Factor (1/2 truck width away from edge)	Safety Factor (1/3 truck width away from edge)	Rolling Resistance (1/2 truck width away from edge)	Rolling Resistance (1/3 truck width away from edge)
Compacted with Safety Berm	1.3	1.3	4.8%	5%
Wet	1	1	6.8%	6%

Bibliography

Anand, A. (2012). *Scaled test estimation of Rolling Resistance, Civil and Environmental Engineering*. University of Alberta.

ASTMD5321. (2014). *Standard Test Method for Determining the Shear Strength of Soil-Geosynthetic and Geosynthetic-Geosynthetic Interfaces by Direct Shear* (pp. 1–11).

Barton, N., & Kjaernsli, B. (1981). Shear strength of rockfill. *Journal of the Geotechnical Engineering, ASCE*, *107*(GT7), 873–891.

BSI (BSI PROPRIETARY INFORMATION). (2011). *FB-MultiPier Soil Parameter Table (US Customary Unit), Bridge Software Institute Department of Civil & Coastal Engineering College of Engineering University of Florida* (pp. 1–24).

CAT. (n.d.). *793D Mining Truck Cataloge* (pp. 1–32).

Das, G. (2011). *Analysis of slope stability for waste dumps in mine, Department of mining engineering, National institue of technology Rourkela*.

FLORA, C. S. (2009). *Evaluation of slope stability for waste rock dumps in amine, Department of Mining Engineering National Institute of Technology Rourkela*.

Geoslope. (2004). *Stability Modeling with SLOPE/W* (pp. 1–523).

Guo, M., Ge, X., & Wang, S. (2011). Slope stability analysis under seismic load by vector sum analysis method. *Joumal of Rock Mechanics and Geotechnical Engineering*, *3*(3), 282–288.

Hoek, E., & Bray, J. W. (1977). *Rock slope engineering, Inst. Min. Metallurg. : London, United Kingdom*. United Kingdom.

Joseph, T. ., & Sharif-Abadi, A. D. (2006). Cyclic loading of oil sand by large mobile mining equipment. In *Proceedings of the 1st Canada–US Rock Mechanics Symposium, Vancouver* (pp. 1665 – 1669).

Joseph, T. G. (2001). *Large mobile mining equipment operating on soft ground* (pp. 1–6).

Kainthola, A., Verma, D., Gupte, S. S., & N.Singh, T. (2011). A Coal Mine Dump Stability Analysis—A Case Study. *Geomaterials*, *01*(01), 1–13.

Komandi, G. (1999). An evaluation of the concept of rolling resistance. *Journal of Terramechanics*, *36*(3), 159–166.

Koner, R., & Chakravarty, D. (2010). Stability study of the mine overburden dumps slope: a micromechanical approach. *Studia Geotechnica et Mechanica,*, *XXXII*(1), 35–57.

Krahn, J. (2004). *Stability Modeling with SLOPE/W An Engineering Methodology* (pp. 1–408).

Omari, A., & Boddula, R. kumar. (2012). *Slope Stability Analysis of Industrial Solid Waste Landfills, Department of Civil, Environmental and Natural Resources Engineering, Lulea University of Technology*.

Orman, M., Peevers, R., & Sample, K. (n.d.). Waste Piles and Dumps. *SME Mining Engineering Handbook*, 667–680.

Perloff, W. H. (1975). Pressure distribution and settlement. *Foundation Engineering Handbook, H. F.Winterkorn and H. Y. Fang, Eds., Van Nostrand Reinhoil, New York,*, 148–196.

Piteau. (1991). *Mined rock and overburden piles, Investigation and design manual, British Columbia Mine Waste Rock Pile Research Committee* (pp. 1–177).

Pope, R. G. (1971). The effect of wheel speed on rollong resistance. *Journal of Terramechanics*, *8*(1), 51–58.

Robertson, A. M. (1970). *Mine waste disposal: An update on geotechnical and geohyrological aspects* (pp. 1–24).

Robertson, A. M. G., Robertson, S., & Kristen. (n.d.). Deformation and monitoring of waste dump slopes.

Rocscience. (n.d.). Slide (4.0), A synopsis of slope stability analysis with Slide.

Sankar, U. S. (n.d.). *Slope stability and dump stability, Project Planning Singareni Collieries Company Ltd* (pp. 1–51). Retrieved from www.slideshare.net/sankarsulimella

Sharif-Abadi, A. D., & Joseph, T. G. (2005). Soft ground reaction to cyclic loading by large mobile mining equipment. In *Proceedings of 19thInternational Mining Congress and Fair of Turkey, IMCET , Izmir, Turkey* (pp. 133–139).

Sharma, A. (2009). *Scale Tire-Oil Sand Interactions*. University of Alberta.

Singh, R., Rawlings, M., & Unrau, G. (n.d.). Assessment of Mobile Emissions in the Athabasca Oil Sands Region - High Resolution Nonroad Emission Factor Model. *2008*, 1–6.

Sivakugan, N., Das, B. M., & Shukla, S. K. (2013). Rock mechanics: an introduction / N. Sivakugan, S.K. Shukla, Braja M. Das., Boca Raton, FL : Taylor & Francis, 2013.

Srour, G. (2011). *Mine waste failure: an analysis of empirical and graphical runout prediction methods, THE FACULTY OF APPLIED SCIENCE, THE UNIVERSITY OF BRITISH COLUMBIA.*

Tannant, D. D., & Regensburg, B. (2001). *Guideline for mine haul forad design* (pp. 1–115).

Thompson, R. J. (1999). Design , Construction , and Maintenance of Haul Roads. *SME Mining Engineering Handbook*, 957–976.

U.S.E.P.A. (1995). *The design and operation of waste rock piles at noncoal mines, U.S. Environmental Protection Agency* (pp. 1–57).